# Data-driven Assessment and Control of Smart Power Distribution Systems

by

Pooya Bagheri

A thesis submitted in partial fulfillment of the requirements for the degree of

Doctor of Philosophy

In

Energy Systems

Department of Electrical and Computer Engineering
University of Alberta

# Abstract

Modern energy policies and emerging information technologies continuously encourage for innovative strategies in efficient and reliable operation of the energy grids. In electrical power systems, the existing forms of advanced control strategies depend heavily on computer simulations running based on circuit models. This becomes a challenge for operation of distribution feeders where accurate and complete circuit models are not easily attainable. This thesis introduces a data-driven approach in assessment and control of distribution grids. The key idea is to replace the conventional role played by circuit models with the statistical data-analytic techniques. Such innovation eliminates the difficulties and uncertainties generally associated with power system models at the distribution level.

A statistical framework is developed to realize model-free methods in operation and assessment of a distribution system. A comprehensive theoretical analysis is presented to support efficacy of this framework. The framework serves as a foundation to the proposed model-free Volt-Var Control (VVC) and Conservation Voltage Reduction (CVR) methods. The assessment and control schemes presented for VVC operates using the data from an Advanced Metering Infrastructure (AMI), while, the CVR one can perform with limited data from meters at the feeding substation, voltage regulators and critical buses of the system. The data-driven approach is also applied to power quality assessment of a distribution system in terms of voltage sag occurrence. Using statistical estimations, the present formulation of Voltage Sag State Estimation (VSSE) methods is generalized to cover both meshed and radial feeder configurations. This new perspective also allows for consideration of Distributed Energy Resource (DER) impact on the voltage sag profile.

Several simulation studies are presented to confirm feasibility and effectiveness of the proposed data-driven techniques. The results show that model-free VVC operates well even without synchro-phasor measurement or when the time resolution of data is as high as 15 minutes. Hence, it is consistent with existing technology of AMI systems. The simulations also confirm sufficiency of the measurement

requirement for a model-free CVR as specified by this thesis. The proposed VSSE methods are also demonstrated as effective even when only 25% of a system nodes are equipped with meters.

Indeed, the proposed concept can be considered as a tangible application for the available data from modern grid measurement technologies such as AMI systems. By taking advantage of technology advancements in communication and data-analytics, this research can act as a genuine support to ongoing transformation of energy grids toward the so-called Smart Grid vision.

# Preface

Some of the concepts and studies in Chapter 2 and Chapter 3 have been published as a journal article: P. Bagheri, and W. Xu, "Assessing Benefits of Volt-Var Control Schemes Using AMI Data Analytics," *IEEE Transactions on Smart Grid*, vol. 8, no. 3, pp. 1295-1304, May 2017.

Some of the concepts and studies in Chapter 2 and Chapter 4 have been published as a journal article: P. Bagheri, and W. Xu, "Model-free Volt-Var Control Based on Measurement Data Analytics," *IEEE Transactions on Power Systems,* Oct. 2018.

A version of Chapter 6 is submitted as a journal article *to IEEE Transactions on Power Delivery*.

# Dedication

To my Wife and my Mother,

and in Memory of my Father *whose praise for* REASON *is still alive as my ultimate guideline*…

# Acknowledgement

First and foremost, I would like to express my sincere gratitude and appreciation to Prof. Wilsun Xu. This research and dissertation would not have been possible without his guidance and great supervision. When it comes to profound knowledge and practical vision, his standing is rather unique in the power engineering field. I will be always proud to say I had the privilege of being his student for both my MSc. and PhD programs, and I hope to have learned enough from him to succeed in my future career.

Beside my supervisor, I would like to thank the rest of my thesis examination committee, Prof. Scott Dick, Prof. Qing Zhao, Dr. Hao Liang and Dr. Christine Chen for providing insightful comments to improve my thesis. I also need to thank Alberta Innovates Technology Future (AITF) and Natural Sciences and Engineering Research (NSERC) for their generous support in form of scholarships which allowed me to remain focused on my research.

Last and not the least, I thank my lovely wife, Elham, and my kind mother for encouraging and supporting me in so many different ways on my academic pursuit. This appreciation should also extend to my brother and sisters, and my dear parents-in-law whose kindness has been a source of motivation for m

# List of Tables

# List of Figures

# Contents

# List of Abbreviations

| | |
|---|---|
| AMI | Advanced Metering Infrastructure |
| CVR | Conservation Voltageg Reduction |
| DER | Distributed Energy Resources |
| KNN | K-Nearest Neighbour |
| LLS | Linear Least Squares |
| LDC | Line Drop Compensation |
| LG | single-phase-to-ground fault |
| LLG | double-phase-to-ground fault |
| LLLG | three-phase-to-ground fault |
| LVRT | Low Voltage Ride-Through |
| MVD | Mean of Voltage Deviation |
| NLLS | Nonlinear Least Square |
| PCA | Principal Component Analysis |
| PQ | Power Quality |
| SLTC | Substation's Load Tap-Changer |
| SSE | Sum Square of Errors |
| VR | Voltage Regulator |
| VSSE | Voltage Sag State Estimation |
| VVC | Volt-Var Control |

# List of Symbols

General Note: matrices and vectors are denoted by bolded alphabets (e.g. $\mathbf{X}$) and arrows (e.g. $\vec{x}$), respectively.

| | |
|---|---|
| $\vec{a}$ | vector of tap ratios for all tap-changing equipment (i.e. VRs and SLTCs) |
| $a_i$ | tap ratio of $i^{th}$ tap changing device (i.e. $i^{th}$ element of $\vec{a}$) |
| $BW_{CVR}$ | bandwidth for voltage control in CVR (see the definition in section 5.3 of chapter 5) |
| $\vec{\beta}$ | vector of unknown variables for a parameteric regression analysis (such as LLS) |
| $\vec{C}$ | vector of switching states for all system capacitors |
| $C_i$ | switching state of $i^{th}$ capacitor (i.e. $i^{th}$ element of $\vec{C}$) |
| $CSI$ | identifier number describing switching states of all system capacitors |
| $\Delta X$ | the change in $X$ (e.g. due to capacitor switching) |
| $E[]$ | expected value of a probablistic variable |
| $\vec{e}$ | vector of measurement errors |
| $e_i$ | measurement error of $i^{th}$ meter (i.e. $i^{th}$ element of $\vec{e}$) |
| $f_x, f, g, h$ | generic function terms used for illustrating different statistical estimation processes |
| $H_P$ | function relating power loss changes (due to capacitor switching) to modified voltage vector before switching |
| $h_P$ | function relating power loss changes to the capacitor state changes (due to switching) and voltage vector and tap ratios before switching |
| $H_V$ | function relating power loss changes (due to capacitor switching) to modified voltage vector before switching |
| $h_V$ | function relating voltage changes to the capacitor state changes (due to switching) and voltage vector and tap ratios before switching |
| $\mathbf{H}$ | voltage transfer matrix (for VSSE) |
| $[]^H$ | conjugated transpose of a vector/matrix |
| $\hat{h}$ | estimated value of function $h$ |
| $h_i(\vec{x})$ | the function relating a measurement to the state vector (for VSSE) |
| $\vec{I}$ | vector of current injection at every system nodes (excluding voltage source(s) nodes, for VSSE) |
| $\overrightarrow{I_{DER}}$ | vector of current injection from a DER (for VSSE) |
| $\overrightarrow{I_f}$ | an equivalent current vector representing the effect of a fault (for VSSE) |

| | |
|---|---|
| $I_{f,i}$ | $i^{th}$ elements of $\overrightarrow{I_f}$ |
| $\mathrm{Im}\{x\}$ | imaginary part of the complex number/vector $x$ |
| $k$ | $k$ parameter in KNN method |
| $l$ | identifier number of the faulted line (for VSSE) |
| $m_i$ | measurement of $i^{th}$ meter used for state estimation (for VSSE) |
| $M$ | number of smart meters |
| $M_V, M_a$ | functions related to definition of modified voltage vector (see the definition in section 2.4 of Chapter 2) |
| $MVD$ | mean of voltage deviation |
| $N$ | number of recorded measurement instants |
| $N_m$ | number of voltage sag meters (for VSSE) |
| $N_S$ | number of phases for system voltage source(s) |
| $Nph_l$ | number of phases of the $l^{th}$ line (for VSSE) |
| $N_C$ | number of capacitors |
| $N_{nodes}$ | number of system nodes (excluding substation ones) |
| $n_i^M$ | identifier number for the node of $i^{th}$ meter (for VSSE) |
| $n_{l,j}$ | identifier number for $j^{th}$ node of $l^{th}$ line (for VSSE) |
| $P_{Loss}$ | system total power loss |
| $P_k^{Load}$ | active power consumption of $k^{th}$ load |
| $P_m^{SM}$ | power measured by $m^{th}$ smart meter |
| $\overrightarrow{P_o}$ | vector of nominal active power load at all system nodes |
| $P_{o,i}$ | $i^{th}$ elements of $\overrightarrow{P_o}$ |
| $P_{Sub}$ | total power measured by substation meter |
| $Phase(n)$ | index that shows phase of $n^{th}$ node (see the definition in section 2.4 of Chapter 2) |
| $\overrightarrow{Q_C}$ | vector of capacitors sizes (kvar) |
| $Q_{C_i}$ | size of $i^{th}$ capacitor (i.e. $i^{th}$ element of $\overrightarrow{Q_C}$) |
| $\overrightarrow{Q_o}$ | vector of nominal reactive power load at all system nodes |
| $Q_{o,i}$ | $i^{th}$ elements of $\overrightarrow{Q_o}$ |
| $\mathrm{Re}\{x\}$ | real part of the complex number/vector $x$ |
| S | number of data sample points |
| $SSE$ | sum square of errors |

| | |
|---|---|
| $STD_V$ | standard deviation of system voltages |
| $STD_{VZ,i}$ | standard deviation of voltages in the $i^{th}$ VR zone |
| $Sum\left(\vec{x}\right)$ | algebric summation of $x$ entities |
| $t$ | time |
| $[]^T$ | transpose of a vector/matrix |
| $U$ | matrix defined for linear least squares |
| $\vec{V}$ | system's voltage vector (excluding substation source nodes) |
| $\vec{V'}$ | modified voltage vector (see the definition in section 2.4 of Chapter 2) |
| $V_i$ | voltage of $i^{th}$ system's node (i.e. $i^{th}$ element of $\vec{V}$ ) |
| $V_i^M$ | voltage recorded by $i^{th}$ meter during a sag event (for VSSE) |
| $V_{Min,Lim}$, $V_{Max,Lim}$ | minimum and maximum regulatory voltage limits |
| $V_m^{SM}$ | voltage measured by $m^{th}$ smart meter (in AMI) |
| $V_{min,z}$ | minimum voltage in the $z^{th}$ VR zone |
| $V_{Nom,C_i}$ | nominal voltage of $i^{th}$ capacitor |
| $V_{Nom,Load_i}$ | nominal voltage of $i^{th}$ load |
| $V_{ref}$ | reference voltage |
| $\vec{V_S}$ | voltage source vector |
| $V_{S,j}$ | $j^{th}$ element of the voltage source vector |
| $\vec{x}$ | *In Chapter 6:* state vector<br>*In other Chapters:* generic vector for different illustrations |
| $\vec{x_i}, \vec{y_i}$ | generic input and output vectors for a function |
| $\mathrm{X}[f]$ | data sample set for regression on function $f$ (input) |
| $\mathrm{Y}[f]$ | data sample set for regression on function $f$ (output) |
| $\mathbf{Y}$ | addmittance matrix (excluding substation nodes) |
| $\mathbf{Y_{all}}$ | complete addmittance matrix (including every system nodes) |
| $\mathbf{Y_S}$ | addmittance matrix (the part relating current injections to substation voltages) |
| $\mathbf{Z}$ | impedance transfer matrix (for VSSE) |
| $\Pi$ | mathematical production symbol |
| $\wedge$ | logical conjunction (AND) |
| $\Gamma[\ ]$ | vector operator (see the definition in section 2.3 of Chapter 2) |

$\Phi[\ ]$ vector operator (see the definition in section 3.3.2 of Chapter 3)

$\odot$ vector operator (see the definition in section 2.3 of Chapter 2)

# Chapter 1

# Introduction

Modern energy needs, global warming concerns, advancement of communication and information technologies are all gradually shaping a prevailing vision for electrical power systems. Well-known as 'Smart Grid', this vision encourages for more reliable and energy efficient operation of power systems. Generous integration of renewable energy sources is also a key feature of this inspired transformation. Distribution systems are usually responsible for a significant portion of energy losses in today power grids. Moreover, they are the most welcoming section of grids to adopt different types of renewable energy sources such as wind farms, solar cells and etc. Therefore, it is not surprising that distribution systems are currently attracting special research attention due to such on-going transformation of energy grids [1]-[3].

The characteristics of modern grids present both of opportunities and challenges to the distribution system owners. It is undeniable that advancement in communication and control technologies contribute to more reliable and efficient operation of distribution systems. Wider area visibility in modern grids also allows for easier implementation of conservative energy policies and demand response programs. On the other hand, emergence of Distributed Energy Resources (DER) raises the risk of overvoltage and overloading [43]. The traditional operation methods might be no longer effective for the feeders with widespread DER penetration. The energy saving initiatives are also continuously raising the bar for performance and efficiency of the power grids. As an important aspect of Smart Grid vision, the distribution systems are expected to be equipped with new control features to face these new expectations and challenges. Revolutionized operation strategies appear as an inevitable destiny for modern power delivery.

In recent years, distribution systems have benefited from significant advancements in measurement and communication technologies [4]. Advanced Metering Infrastructure (AMI) is a bold example of such advancements which can potentially provide tremendous data including voltage and power measurement across a feeder [5]-[7]. Although the original purpose of AMI was collecting the customer energy-usage data for billing purposes, research has identified novel applications for the AMI outcome. Commonly known as 'AMI data-analytics', analysis of tremendous data available from AMI can substantially benefit various control strategies and study tasks. AMI data-analytics can serve to improve accuracy of feeder models [8]-[9]. It can be also employed in Demand Response programs [6]. Such advancements in measurement and data-management technologies provide a unique opportunity to realize enhanced operation techniques on modern distribution grids.

This thesis intends to introduce and examine feasibility of a novel data-driven approach which can considerably support the ongoing advancements in distribution grids. The proposed methods allow to maximize utilizing the emerging data access opportunities such as AMI in the modern systems. The rest of this chapter will present a brief background on key elements of the present situation which leads to a promising ground for the concepts presented in this thesis. Sections 1.1 and 1.2 provide some background information on typical assessment and control strategies in distribution grids. The advantage of data-driven method and a brief introduction to statistical estimation techniques are presented in section 1.3 and 1.4. At the end of this chapter, section 1.5 portrays the scope of this thesis, as well as giving an overview of topics studied in each of the next chapters.

## 1.1 Control Methods in Distribution Systems

Advanced control and automation is an essential feature for any distribution grid evolving toward Smart Grid vision. Voltage regulation and power loss reduction are among the primary objectives in feeder automation plans. Utilities need to ensure that voltage levels for every customers fall within the regulatory standard ranges. On the other hand, lowering the power losses along the power lines and equipment is the key to efficient energy delivery.

Capacitor and Voltage Regulator (VR) are the two main feeder component that allow for control of system voltage and losses. During peak load hours, capacitors provide local supply of reactive power to the loads, thus, reducing the burden on feeder main trunk. VRs can compensate for overvoltage during light load hours or high DER generation. They can also eliminate the undervoltage resulting from heavy load conditions. However, control of capacitors and VRs are necessary to guarantee their positive effect. For example, capacitors usually need to be switched OFF during light load times, otherwise, they can cause extra losses or overvoltage due to a reactive power surplus [38].

In general, automatic control of capacitors and voltage regulators inside a feeder is called Volt-Var Control (VVC)[1] [10]. As depicted in Figure 1.1, a VVC scheme determines and send the appropriate switching commands and tap positions to each respective capacitor and VR inside the system. The settings by VVC are selected in a way to ensure minimal feeder losses and well-regulated system voltages. From a mathematical standpoint, VVC is an optimization problem with a couple of inequality constraints. For example, a basic VVC can be formulated as follows (for the operation instant of *t*):

$$\begin{aligned} &\{\overrightarrow{a(t)}, \overrightarrow{C(t)}\} = \arg\min P_{loss}(t) \\ &\text{subject to } V_{\max}(t) \le V_{Max,Lim} \text{ and } V_{\min}(t) \ge V_{Min,Lim} \end{aligned} \tag{1.1}$$

[1] VVC is also referred to as Voltage-Var Optimization (VVO) in some references.

As apparent from the above expression, feeder total power loss ($P_{loss}(t)$), system's maximum voltage ($V_{max}(t)$) , system's minimum voltage ($V_{min}(t)$) are the main indices of interest for a basic VVC operation. Each of such indices can be themselves a sophisticated function of different system parameters, e.g. $P_{loss}(t)$ is essentially a function of the following variables:

- Capacitor(s) switching states at time $t$ ($\overrightarrow{C(t)}$)
- VR tap ratios at time $t$ ($\overrightarrow{a(t)}$)[2]
- Power generation of DERs at time $t$
- Dependency of load powers on their voltage at time $t$
- Power consumption of the loads at time $t$
- Topology of feeder
- Power-line impedances
- Size of capacitors

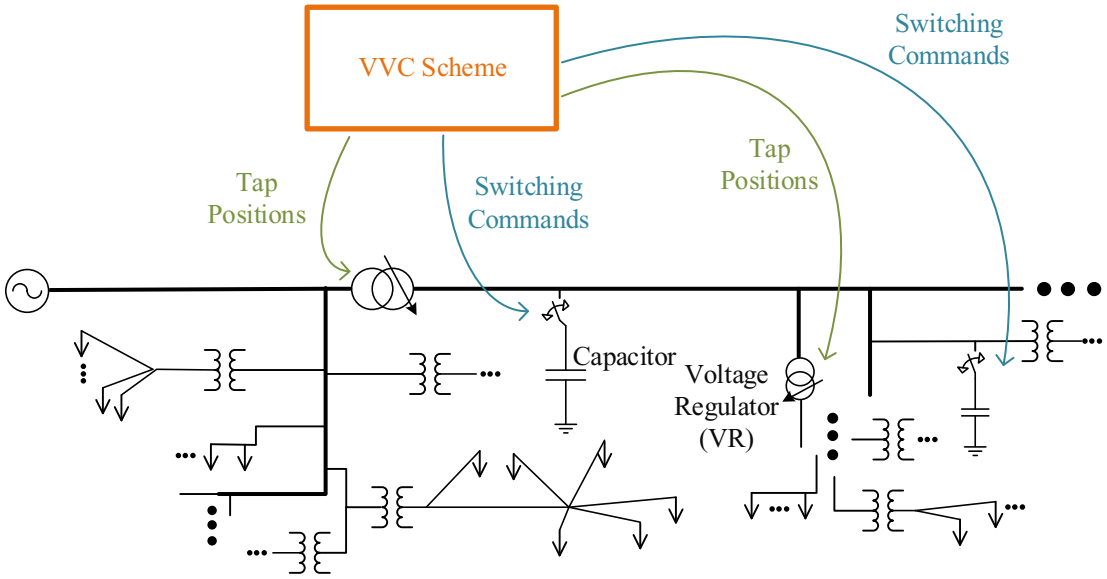


Figure 1.1 Example of a VVC scheme in a distribution feeder

A central scheme can be also aimed with alternative objectives instead of total loss minimization. Conservation Voltage Reduction (CVR) is a common example of such application. CVR targets to reduce the costumers consumption by means of decreasing their supply voltages. In order to achieve this, the feeder voltages are adjusted to the lower band of permissible regulatory voltage range. This action leads to an overall lower energy usage since many of system loads are voltage dependent [11]. In advanced automation

[2] It shall be noted that '*t*' in this thesis stands for time, not tap ratio.

schemes, the CVR and VVC objectives might be also combined within one central control unit [11]. A basic CVR can be formulated as follows:

$$\{\overrightarrow{a(t)}, \overrightarrow{C(t)}\} = \arg\min \sum_{k} P_k^{Load}(t)$$
$$\text{subject to } V_{\max}(t) \le V_{\text{Max,Lim}} \text{ and } V_{\min}(t) \ge V_{\text{Min,Lim}} \tag{1.2}$$

## 1.2 Assessment Methods in Distribution Systems

The assessment methods for distribution systems are important from two perspectives. One perspective is concerned with evaluating the performance of existing control strategies in a system. Are the installed controllers meeting their expected objective? Is the improved performance by an installed VVC scheme justifying its costs? The second question is especially important since implementation of control schemes such as VVC is usually costly. Hence, utilities are always interested to assess true benefits of such schemes in operation of a distribution feeder. Such information are crucial for proper decision making in planning studies for future systems or in upgrades of existing feeders. This need has driven a separate research stream devoted to methods for benefit assessment of different control strategies rather than developing the control schemes themselves [13]. More information about VVC assessment methods will be presented in chapter 3.

The other assessment perspective is concerned with Power Quality (PQ) condition of a system. The assessment may involve harmonic pollution, voltage sag performance or the extent of voltage unbalance/ fluctuation in the feeder. Among different PQ assessment techniques, Voltage Sag State Estimation (VSSE) is considered as subject of some studies in this thesis. Voltage sag is defined as a temporary[3] voltage reduction below the acceptable standard level. Temporary short-circuit faults are the most common source of this PQ phenomenon. The aim of VSSE is to evaluate performance of the system in terms of voltage sag occurrence by using the measurement record of a limited number of meters. More information regarding different voltage sag assessment methods will be given in chapter 6.

## 1.3 Model versus Data

A common class of control schemes for distribution grids is realized by model-based optimization techniques. Indeed, most of recent literature in this area is devoted to study and development of sophisticated VVC/CVR control schemes using advanced optimization algorithms. In these methods,

[3] Usually less than 1 minute

computer simulations based on circuit-models provide the basis for control decisions. For example, both scenarios of a capacitor switched ON and OFF can be simulated for each time of operation. Then, the switching state leading to most optimal condition (e.g. minimal power loss) is selected accordingly. Figure 1.2 shows a generic schematic for an optimization-based control strategy. Since there is usually more than a single capacitor and VR equipment are also present, the search space for optimal control decision can become huge, making the use of an optimization algorithm necessary. The so-called Hybrid schemes might also benefit from metering data to enhance load models inside the simulations.

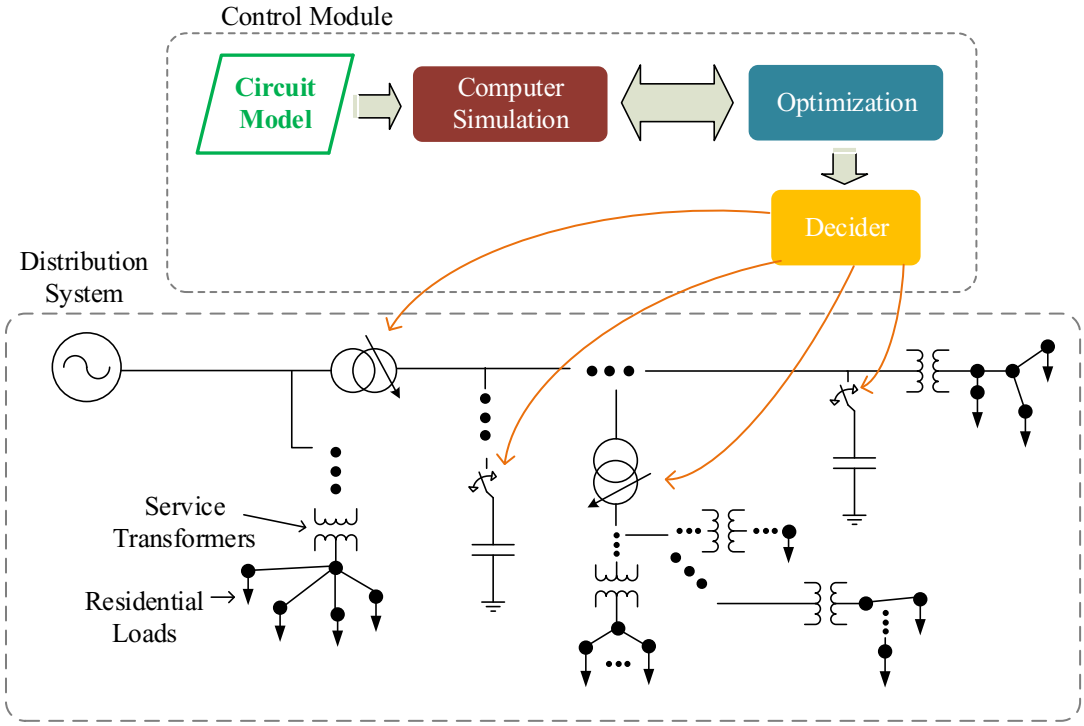


Figure 1.2 General schematic of a model-based optimization control strategy

Although optimization methods have significantly progressed, heavy reliance on circuit models remains as a key challenge to their actual implementation. One of the main obstacles is due to the fact that complete and accurate set of models are not easily attainable at distribution level. The following reasons can be listed as the root of difficulties in distribution system modeling [9],[13],[34][4]:

- Almost every loads are, to some degree, voltage-dependent. However, it is quite difficult to accurately determine relationship of power and voltage for every various loads served by a distribution feeder[5]. It is worth to note that voltage-dependency of loads has a significant effect on performance of many control schemes. For one reason, many common control indices of interest

[4] [37] is one example of the challenging route toward complete build-up of a comprehensive and accurate network model for a distribution feeder

[5] This issue becomes even further complicated considering the random and time-varying nature of most of the loads.

such as total feeder loss is directly related to the amount of load powers. As another reason, many control devices such as VRs change the system voltages, and thus, the way they affect system power flows is directly determined by voltage-dependency of system loads. Indeed, the prediction of a control decision's impact is reliable only if voltage-dependency characteristics of loads are taken into account.

- There are typically several feeder sections of both single-phase or multi-phase types, service transformers and service conductors in a distribution grid. Collecting accurate and up-to-date information of every equipment is very difficult. In most cases, utilities do not even invest any effort to collect information of secondary circuits (i.e. information pertaining to downstream of service transformers such as service conductors, house connections, etc.)
- Most of distribution loads (especially residential) are unbalanced and behave in a random nature. Assignment of accurate models or daily profiles to the system loads is thus a challenging task.
- With transformation of systems toward Smart Grids, customers are becoming more influential. Any customer might be in possession of grid-connected DER or energy storage units which their exact specifications or operating conditions might be unknown to the network operator.

The above shortcoming in optimization methods has made model-free control a common choice in present industry practice. With a model-free[6] approach, the distribution network operator does not have to collect circuit information and build individual models for each feeder. Besides, results of a model-free scheme are never negatively affected by low accuracy or deficiency of circuit or load models. Traditionally, model-free methods usually operate by adopting simplified rules for controlling different equipment. In a rule-based scheme, each equipment is controlled by means of local measurement and a set of rules. A common example is a capacitor that is switched ON and OFF based on voltage measured at the connection point of capacitor bank. The rule in this example consists of maximum and minimum voltage thresholds. Once the voltage drops below the minimum threshold, the capacitor is switched ON. Alternatively, exceeding the maximum threshold switches the capacitor OFF the grid. Another example is the normal voltage control mode in commercial VRs, where the tap position is continuously adjusted based on measuring regulator secondary voltage [38]. Figure 1.3 shows a generic schematic of rule-based control schemes. In more advanced forms of rule-based schemes, the main settings in control rules are updated based on operation experience and measurement record by communication to a central unit [41].

[6] In this thesis, the term model refers to circuit models only. It shall not be confused with the models used in statistical methods.

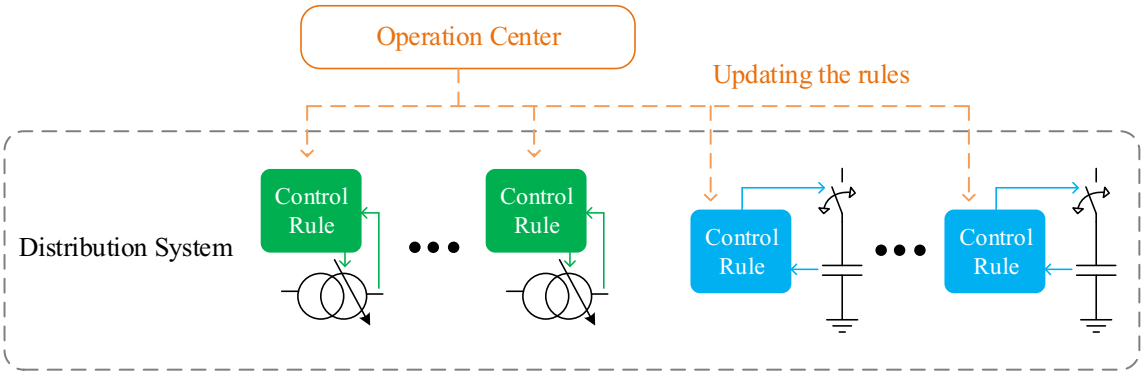


Figure 1.3 General schematic of a rule-based control strategy

Rule-based methods are generally easy to implement and mostly reliable to meet voltage regulation constraints. However, relying only on experience and judgement, they are not usually suitable for optimizing system operation, especially when loss reduction is a concern. In addition, widespread growth of DERs across modern grids has further jeopardized the effectiveness of such schemes. Several studies have demonstrated the vulnerability of conventional rule-based schemes in presence of DERs [42]-[44].

The above discussion highlights the importance of an enhanced model-free approach in development of different control schemes for the modern grids. One of the objectives of this thesis is to use statistical techniques to develop rigorous data-driven and model-free control techniques for distribution feeders. As the example on Figure 1.4 shows, statistical estimations are expected to replace the role of circuit models in such data-driven approach.

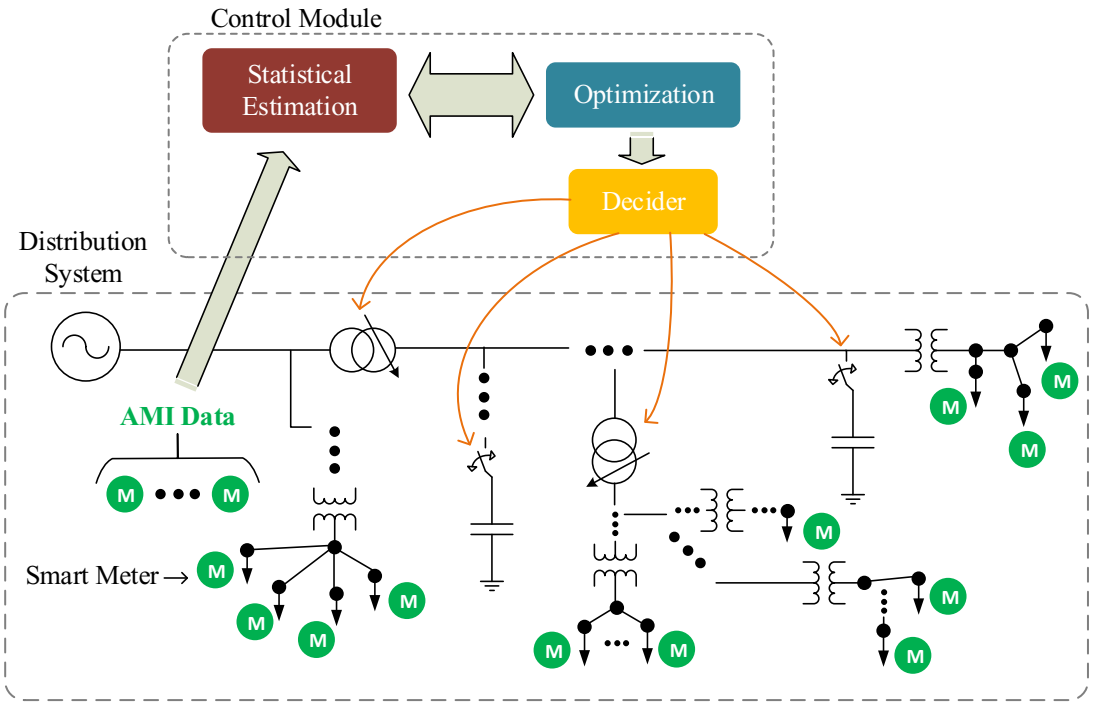


Figure 1.4 Example schematic of a data-driven model-free control strategy

The described uncertainty in models of distribution grid also affect the efficacy and validity of the methods offered to assess benefits of an existing control scheme such as VVC or CVR. Most of the advanced assessment techniques in this area rely on computer simulations based on circuit models. However, a model-dependent procedure cannot be logically considered as a suitable framework for assessing the benefits of an automation scheme, where the scheme is itself founded on the same system models [13]. As will follow in section 1.5, one of this thesis goals is to address this concern by developing data-driven assessment methods.

## 1.4 Statistical Estimation

The main challenge in any data-driven methodology is that the measurement data can be only recorded for a single status of the system equipment at each time. However, most control schemes and assessment studies require information for every different equipment status. In the other words, a piece of equipment can be, say, ON for a period. This implies that the case of equipment OFF during the same period is not available within measurement data. A control scheme or assessment method requires the impact of the equipment ON versus OFF, while, it cannot be determined directly from a data-driven approach. Since the system conditions such as loads or DER generations might be always changing, it is neither acceptable to use measured values of one time as the reference versus the other times [13].

This issue is illustrated by an example for data-driven assessment of VVC schemes in Figure 1.5, where a single capacitor is controlled in the system. In this example, VVC switches the capacitor ON and OFF as shown in Figure 1.5 (a). Recorded system loss is also plotted in Figure 1.5 (a). Now, one is unable to measure true power loss reduction benefit of this VVC, unless, the reference curves as shown in Figure 1.5 (b) become available (for the same test period). However, such reference curves can be never directly derived from measurement data, since the capacitor can be either in an ON or OFF state at each time of the test and not at the both. Therefore, the crucial step within a data-driven approach is developing methods to estimate the variables for system states which are not directly measured. Hence, statistical estimations will be used as the core engine of the proposed data-driven methods in this thesis.

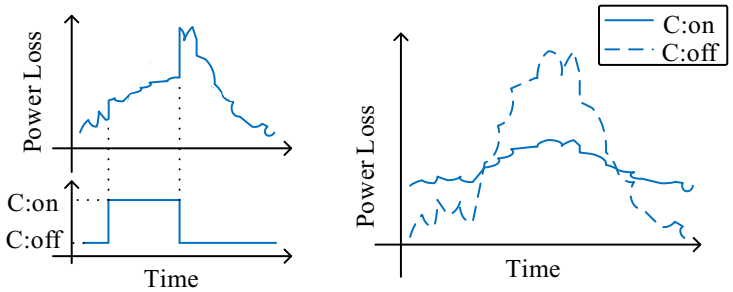


(a) Measured power loss and capacitor state

(b) Reference curves required for VVC assessment

Figure 1.5 Example of VVC on a single-capacitor system ('C' stands for capacitor in the figure) [13].

Statistical estimation methods constitute the building foundation for most of Machine Learning algorithms. Indeed, they have already become a crucial aspect of several practical applications such as intelligent robotics, auto-pilot vehicles and medical diagnosis [15]. The key method in statistical estimation of continuous variables is usually referred to as 'Regression Analysis' [15]. Almost all of the data-driven methods presented in this thesis benefit from regression analysis. The idea of regression is to estimate output of an unknown function for a new input based on the historical data of inputs and the output samples collected for the same function. Suppose $x$ and $y$ are two measurable parameters for a system (both $x$ and $y$ could be vectors), and these two parameters are related through an unknown function $f$: $y=f(x)$. Now, we can label the sample data derived from measurement on that particular system as pairs of these two parameters: $(x_1,y_1)$, $(x_2,y_2)$, $(x_3,y_3)$, … , $(x_n,y_n)$. For each sample, a measurement error ($e_i$) might be also present, thus, each pair is subject to the following expression:

$$y_i = f(x_i) + e_i \tag{1.3}$$

For this example, a successful regression method is expected to estimate value of $y$ parameter for any new $x$. Such estimation is labelled as $\hat{f}(x)$ or $\hat{y}$ in this thesis.

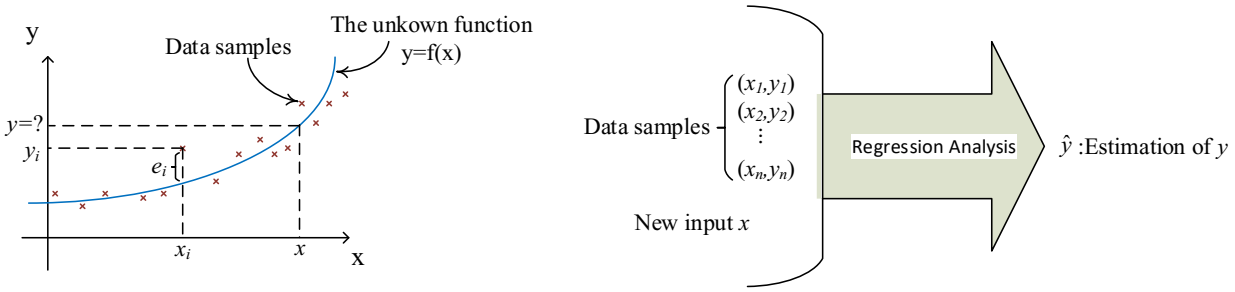


Figure 1.6 Illustrating the sample data and expected outcome for a typical regression analysis

A large number of regression methods approach this problem by presupposing a general model with some unknown parameters to describe the relationship of $x$ and $y$. We can formulate the assumed model with the function $h$ and the unknown parameters in a vector labelled as $\beta$:

$$y = h(x, \vec{\beta}) \tag{1.4}$$

Consequently, the task of regression will become to estimate the $\beta$ parameters. Estimated value of $y$ for a known $x$ will be then:

$$\hat{y} = h(x, \hat{\vec{\beta}}) \tag{1.5}$$

A popular example of such approach is the Linear Least Square (LLS) method where a linear model is assumed to describe the relationship of regression parameters. For example, $h$ is defined as follows:

$$h(x, \vec{\beta}) = \beta_1 x + \beta_2 \tag{1.6}$$

Obviously, accuracy of these regression techniques highly depend on the choice of pre-assigned model to the system. For example, LLS methods only perform well when there is an actual linear relationship between the regression parameters[7]. Another class of regression methods, known as Non-parametric, perform the estimations without assuming a general model for the system. Non-parametric methods directly employ the sample data to derive the estimated value. For example, they might offer a universal function $H$ which gives the estimation based on the sample data as follows:

$$\hat{y} = H(x, x_1, y_1, x_2, y_2, x_3, y_3, \cdots, x_n, y_n) \tag{1.7}$$

The right choice of regression method depends on characteristics of the specific data-driven application. As we will see in the next chapters, non-parametric methods are a suitable choice for VVC and CVR applications, while the parametric approach better suits the VSSE problems.

[7] Or at least, the function approximately shows a linear behavior around the data samples and the point where estimation is conducted.

## 1.5 Thesis Scope and Outline

The discussions of this chapter has clarified the essence of rigorous data-driven and model-free approach for the future of modern grids. The scope of this thesis to develop data-driven methods for assessment and control of power distribution systems. By engaging statistical techniques, the available measurement data in modern grids can be processed and elevated to an adequate level to replace the role conventionally occupied by circuit models. Thus, the main objective is to develop control strategies and evaluation studies that can be fully conducted independent of system models[8]. Not only this strategy eliminates the modelling difficulties, but it also provides an opportunity to engage the emerging metering and communication technologies more effectively. Overall, the proposed approach will be beneficial from the following perspectives:

- This strategy eliminates the efforts and difficulties in constructing circuit models for each individual feeder. In the other words, through an analogy to software engineering, it can be claimed that model-free methods benefit from a 'Plug and Play' feature.
- Model-free methods are not negatively affected by low accuracy or deficiency of system model[9].
- True benefit assessment of an automated scheme is only sound if conducted based on data and independent of models used to construct the scheme itself [13].

Since this pure data-driven and model-free approach is relatively new in this field, there are obviously many questions and challenges that need to be addressed. Some of the key questions that this thesis is aimed to answer are:

- Which type of control schemes in a distribution system can be operated independent of models? What type of measurement data is available in existing systems that can be used for model-free methods?
- Is it possible to estimate every indices for a control scheme only using data? If not, how a control method can be simplified in order to allow for model-free approach?
- How to employ statistical regression techniques in data-driven applications for distribution feeders? Is there a theoretical guarantee that these statistical techniques give accurate and reliable estimation for control and assessment purposes?

[8] There is an exception with VSSE methods discussed in chapter 6. A VSSE method cannot be considered model-free since it still requires system topology and line impedance data. However, as we will see in chapter 6, VSSE methods are mainly fed by measurement data, and rely much less on system models compared to their stochastic counterparts. Therefore, they still benefit from most advantages of data-driven approach.

[9] As aforementioned in section 1.3, the information on secondary network, and voltage-dependency characteristic of loads are almost always missing in the models.

- Does the model-free approach need to presuppose some assumptions on the system they are applied for? If yes, do such assumptions undermine the reliability of these methods for practical applications?
- How will the data-driven approach respond to deficiencies in the measurement data? How issues such as measurement noise, meter failure, lack of synchro-phasor measurement affect the efficacy and accuracy of the proposed model-free methods?
- How can a data-driven approach benefit the PQ assessment methods in present distribution grids?

This thesis introduces several new methodologies and conducts different analytical and simulation studies to address the research needs highlighted by the above questions. The following paragraphs summarize the organization of the thesis and describe the main topics covered by each chapter.

Chapter 2 proposes a framework to conduct statistical estimations for data-driven methods. This framework constitutes the foundation for most of model-free methods presented in the other chapters. The underlying assumptions for these methods are discussed in details. Several theoretical analyses are also presented to investigate the effect of different metering and system conditions on performance of proposed methods.

Chapter 3 presents a data-driven and model-free scheme for assessment of open-loop VVCs. The structure for this assessment method is established using the estimation framework developed in chapter 2. AMI data is considered as the main data input for these methods. Simulation studies are presented to evaluate accuracy of the proposed techniques. Various studies are conducted to reveal the impact of different system and metering conditions on the assessment results. Particularly, the effect of DER presence is investigated in the results.

Chapter 4 develops a data-driven VVC scheme. The scheme operates using the AMI data without the need to system models. The structure for controlling VR and capacitor equipment by such VVC scheme is laid out in details. Various simulation studies are presented to demonstrate the feasibility and effectiveness of this scheme. The simulation tests include DER generation to study possible negative interaction between DERs and the proposed VVC. Sensitivity studies are also presented to evaluate the effect of system characteristics and availability of AMI data on the proposed method's performance.

Chapter 5 employs the statistical estimation idea to realize a data-driven CVR scheme. Unlike the VVC scheme, the CVR scheme is established without the need to a complete AMI system, rather it can operate by limited number of measurement units on VRs and across the feeder. The algorithmic structure for VR and capacitor controllers are developed accordingly. The efficacy of proposed CVR scheme is demonstrated by simulation studies. Similar to other chapters, the studies are accompanied by supporting sensitivity analysis as well.

Chapter 6 is devoted to VSSE. As a data-driven PQ assessment technique, merits of VSSE are clarified in comparison to other sag estimation methods. A generalized formulation for VSSE is proposed to realize the full potential of modern PQ monitoring devices. Statistical estimation methods are applied as solutions to the proposed VSSE framework. Several simulation studies are presented to verify the accuracy and flexibility of presented VSSE platform.

Chapter 7 summarizes the key conclusions of this thesis. The chapter also discusses different possibilities of continuing studies of this thesis, and the promising research path on this topic for the future.

# Chapter 2

# The Proposed Statistical Framework

The key in a model-free approach is to estimate the indices of interest for different equipment status that cannot be all captured together by measurement in one instant of operation. The obvious solution is to find a function which relates such indices to parameters which are available by measurements. Once this relationship is identified, the measurement data can be organized into proper sample sets, so that a regression analysis as described in the previous chapter[10] can be applied to perform the required estimations. This chapter is mainly devoted to find such appropriate setup for statistical estimations required for model-free VVC and CVR schemes: What sort of functions exist for a distribution feeder that relates different type of available data, and have the indices of interest as their output? What is the role of operation time in this context? Does the data need to be stamped by time prior to estimations? How do we know that the estimation techniques will be reliable for any type of distribution feeder? What are the assumptions required to settle for this estimation framework? What accounts for the estimation errors? How much of the error can be avoided by improving the measurements? The theoretical discussions in this chapter are aiming to address these questions.

Throughout this chapter, several assumptions will be made regarding the distribution feeder to allow for rigorous theoretical derivations. A number of these assumptions might seem too restrictive from the practical perspective. However, in the end of this chapter, we will show that most of the constraints imposed by these assumptions can be relaxed with no significant impact on application of developed statistical framework.

## 2.1 What is Essential and Possible to Estimate?

The statistical framework is developed for a basic VVC as defined in section 1.1 of the previous chapter. Later in chapter 5, we will show how this framework can be simply applied for other control objectives such as CVR. A statistical framework for the basic VVC needs to predict how the main indices of interest (power loss and maximum/minimum voltage) change with different capacitor states[11] and VR tap positions. We generalize the objective of framework to prediction of power loss and system's voltage vector. Obviously, the maximum/minimum voltage can be directly derived from the voltage vector, afterward.

---

[10] See section 1.4

[11] Switching state of a capacitor will be simply referred to as 'capacitor state' in this thesis.

The first intuitive option is to utilize measurement data to establish functions for direct estimation of indices of interest. For example, one can consider:

$$P_{loss}(t) = f_x(\overrightarrow{a(t)}, \overrightarrow{C(t)}) , \tag{2.1}$$

and then, tries to estimate function $f_x$ using the measurement data. However, this approach is very problematic. For one reason, $f_x$ is apparently a time-variant function because loads, DER generation, etc. can change during operation. The other reason is the unruly large variable space resulting from this simplistic approach. For example, a system with two capacitors and four VRs (each with 32 possible tap positions) will lead to a discrete variable space in size order of $\sim 10^6$. A reliable estimation on such input space will need a tremendous amount of data, which is not possible to collect in practice. Besides, if one tries to eliminate the time-variant nature of $f_x$ by introducing a time-dependent variable in it, the variable space will even grow larger. Indeed, this condition makes it almost impossible to collect enough data to directly estimate the relationships between every indices and the control variables here.

A possible solution for this matter can be inspired from the fact that effect of VRs on power loss is much less compared to that of capacitors ([39]-[40]). Besides, voltage in downstream of VRs approximately change in proportion to VR's tap ratio for a radial distribution feeder [38]. Such approximations can significantly reduce the estimation burden on the statistical framework. Therefore, in our framework, we only focus on changes in indices of interest due to capacitor switching. In chapters 4 and 5, we will see how such capacitor-based-only platform can still serve model-free VVC or CVR platforms on the systems with VRs. Before explaining the proposed statistical framework in details, a simple example is considered in the next section to give a taste on the overall procedure of this chapter.

## 2.2 A Simple Example of Model-Free Approach

In this section, the example of a simple data-driven approach is given. The example single-bus system is with one capacitor as shown on Figure 2.1. We assume that one can only measure the voltage of this bus during operation of the system. Now, the objective is to predict the voltage changes due to switching of the capacitor without using system model's information. In order to keep the problem simple, we assume that the impedances $Z_1$ and $Z_2$ are constant in this system, and only the voltage source ($V_x$) is variant. Before establishing the model-free approach, we need to look into the relationships governing parameters of interest in this system. As shown on Figure 2.1, $V$ and $V+\Delta V$ represent the bus voltage before and after switching ON the capacitor. Using circuit theory, one can easily derive the following equations for this system:

$$\begin{cases} V = \dfrac{Z_2}{Z_1 + Z_2} V_x \\ V + \Delta V = \dfrac{Z_{2,C}}{Z_1 + Z_{2,C}} V_x \text{ where } Z_{2,C} \triangleq \dfrac{Z_2 \cdot Z_C}{Z_2 + Z_C} \end{cases} \tag{2.2}$$

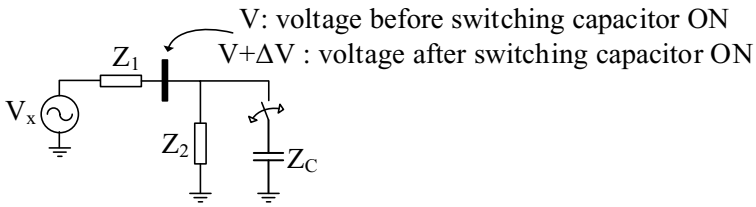


Figure 2.1 The single-bus example system

The two equations in (2.2) can combined by eliminating $V_x$:

$$\Delta V = \overbrace{\left(\frac{Z_1 + Z_2}{Z_1 + Z_{2,C}} \times \frac{Z_{2,C}}{Z_2} - 1\right)}^{\alpha} V \tag{2.3}$$

Therefore, there is a linear relationship between $\Delta V$ and $V$: $\Delta V = \alpha V$. The $\alpha$ coefficient is constant for all OFF to ON switching events since the time-variant element $V_x$ is already eliminated from the equation. By collecting the data from different OFF to ON switching events, one can have several samples for the pair of $V$, $\Delta V$, and $\alpha$ can be found solving a simple LLS problem[12]. Once $\alpha$ is known, $\Delta V$ can be predicted for any future OFF to ON switching of the capacitor given $V$ right before the switching event. Another coefficient similar to $\alpha$ also exists for the ON to OFF switching events. This coefficient can be also determined using the data of ON to OFF switching events. This overall process will meet the objective of model-free approach for this simple system.

Even for this simple system, if the value of either $Z_1$ or $Z_2$ was variant instead of $V_x$, the problem would become more complicated, and we would not face the linear relationship reached in (2.3). Besides, if more than one of the parameters were become time-variant, the mere measurement of the single-bus voltage was not sufficient for the predictions.

The above example sheds light on possible challenges of developing a statistical framework for a realistic distribution feeder. The rest of this chapter is devoted to develop such framework. We will identify the assumptions one has to make to reach time-invariant equations (similar to (2.3) for the example system) which can be used for required estimations for VVC or CVR operation of a distribution feeder. Meanwhile, the errors that can be expected from such predictions, and the practical value of the proposed framework is discussed as well.

[12] See section 1.4 for background information on regression analysis

## 2.3 A Time-Invariant Framework for Estimations

We will demonstrate that for a general radial distribution feeder, a time-invariant framework can be used for estimation of voltage or power loss changes due to capacitor switching. Intuitively, one might initially assume that a time-invariant framework is not suitable here since the effect of a capacitor switching can be quite different at different times of operation. For example, switching a capacitor ON generally helps with provision of reactive power demand at peak hours and thus reduces the losses. While, the same action during light-load hours can lead to unnecessary reactive power flow in the system and creates extra losses and a poor voltage profile. However, although counterintuitive, a time-invariant framework is still effective here by using system voltages before the capacitor switching as the input for estimations. The key characteristic which allows for such time-invariant framework is that during operation of a distribution feeder, the power-line impedances and the general configuration remain constant[13]. The main parameters changing by time are those associated with customers' demands and generations of DERs. Fortunately, the variation of these time-variant parameters can be captured by measuring the system voltages: since system line admittances are constant, the measured voltages thoroughly determine the power injection/absorption of loads/DERs at every node. Hence, the effect of each capacitor switching event can be fully determined using the system voltages right before the switching happens.

The main advantage of time-invariant feature is that the data samples are not required to be stamped by their switching times. For example, there is no need to make a distinction between the data recorded from two switching events when one happened at a previous hour and the other happened on two days ago. The voltages recorded before these two events are sufficient to distinguish them for the purpose of estimations.

The following theorem is presented to theoretically support the feasibility of a time-invariant framework for estimations. The theorem needs a number of assumptions on the subject system. Later, however, we will show such assumptions can be relaxed for practical applications of the framework. Violation of each of the assumptions can introduce time-dependent factors which can be source of error to the estimations. Thus, one merit of this theorem is that it also clarifies the source of possible estimation errors in the proposed framework.

**Theorem 2.1:** For a distribution system operating under the constraints imposed by the following *Assumptions 2.1~2.7*, and for any capacitor switching event (which can be fully specified by changes in capacitor's switching status $\overrightarrow{\Delta C}$) on this system, unique and time-invariant set of equations exists that relates changes in system voltages ($\overrightarrow{\Delta V}$) and losses ($\Delta P_{loss}$) to $\overrightarrow{\Delta C}$ and the voltages ($\overrightarrow{V(t)}$) and tap-positions

[13] Feeder reconfigurations are not considered in the data-driven schemes developed in this thesis, and are considered as a subject for future research.

($\overrightarrow{a(t)}$) of the system before the switching event ($t$ is the instant right before switching happens). In addition, such set of equations is not underdetermined when treating $\overrightarrow{\Delta V}$ and $\Delta P_{loss}$ as unknown variables[14].

***Assumption 2.1:*** the system is with one source at the substation.

***Assumption 2.2:*** the system configuration and power-line impedances are constant during operation (i.e. they are independent of $t$).

***Assumption 2.3:*** at each node, there is one and only one of load, DER or capacitor equipment[15]. For example, no DER or loads are connected to the same node.

***Assumption 2.4:*** voltage-dependency characteristics of loads and DERs do not change during operation[15].

***Assumption 2.5:*** the amount of nominal loads and nominal DER generations do not change during a capacitor switching event[16].

***Assumption 2.6***: tap position of VRs and SLTC (Substation Load Tap Changer) do not change during a capacitor switching event (i.e. $\overrightarrow{a(t)} = \overrightarrow{a(t+\Delta t)}$).

***Assumption 2.7***: the source voltages are constant during operation[15].

**Proof of Theorem 2.1:** A number of vector operations will appear throughout this proof which are defined as follows. Consider two generic vectors of $x$ and $y$ each with the elements labelled as below:

$$\vec{x} = [x_1 \quad x_2 \quad \cdots \quad x_n]^T \,,\, \vec{y} = [y_1 \quad y_2 \quad \cdots \quad y_n]^T ; \tag{2.4}$$

we define the following operators on these two vectors:

$$\begin{aligned} &\vec{x} \odot \vec{y} \triangleq [x_1 y_1 \quad x_2 y_2 \quad \cdots \quad x_n y_n]^T \\ &\frac{\vec{x}}{\vec{y}} \triangleq [x_1 / y_1 \quad x_2 / y_2 \quad \cdots \quad x_n / y_n]^T \\ &\vec{x}^{\,2} \triangleq \vec{x} \odot \vec{x} \\ &\left|\vec{x}\right| = [|x_1| \quad |x_2| \quad \cdots \quad |x_n|]^T \end{aligned} \quad . \tag{2.5}$$

*Assumption 2.1* allows us to define the $V_S$ vector to represent the (phasor) voltages of different phases at substation:

$$\overrightarrow{V_S} = [V_{S,1} \quad V_{S,2} \quad \cdots \quad V_{S,N_s}]^T \tag{2.6}$$

---

[14] A set of equations is called 'underdetermined' if number of equations is less than number of unknown variables.

[15] Some of these assumption might seem unrealistic especially for an actual-world distribution system. Regarding assumption 2.3, some nodes might have both loads and DERs. Assumption 2.4 is also at question for residential loads, e.g. a house can have totally different loads at different hours with different voltage-dependency characteristics. Assumption 2.7 can be also violated by voltage changes in transmission levels. However, all these assumptions is required at this point for theoretical derivation of the statistical framework. And we will see in the end of this chapter how they can be relaxed in practical applications. Sensitivity studies in the next chapters will also consider practical situations where these assumptions are violated.

[16] It should be noted that the change in load power or reactive power caused by voltage variations due to switching event is still allowed by this assumption.

In the above definition, $N_s=1$ and $N_s=3$ for a single-phase and three-phase system, respectively. The system's voltage vector is also defined below which includes the voltage of every system nodes except the source ones.

$$\vec{V} = [V_1 \quad V_2 \quad V_3 \quad \cdots \quad V_{N_{nodes}}]^T \tag{2.7}$$

It should be noted that in this thesis, each phase of a bus is treated as an individual node. This makes it easier to manage unbalanced lines/loads which are commonplace in distribution feeders. The first step of the proof is to derive the general power flow equations for the distribution feeder at instant of *t* which is right before a capacitor switching.

*Assumption 2.2* implies that the only time-variant factor in admittance matrix of the network is tap ratio of SLTCs and VRs[17]. Therefore, we can denote it as a function of tap ratios at time *t.* The admittance matrix can be itself considered as composition of four parts to account for substation and other nodes separately. The current injection vector *I* is defined for every node excluding the substation ones, and it will be related to voltage vectors *V* and $V_S$ as follows:

$$\begin{aligned} &\overrightarrow{I(t)} = \mathbf{Y_S}(\overrightarrow{a(t)})\overrightarrow{V_S(t)} + \mathbf{Y}(\overrightarrow{a(t)})\overrightarrow{V(t)} \\ &\vec{I} \in \mathbb{R}^{N_{nodes}},\ \vec{V} \in \mathbb{R}^{N_{nodes}},\ \overrightarrow{V_S} \in \mathbb{R}^{N_S} \\ &\mathbf{Y_S} \in \mathbb{R}^{N_{nodes} \times N_S},\ \mathbf{Y} \in \mathbb{R}^{N_{nodes} \times N_{nodes}} \end{aligned} \tag{2.8}$$

In above, $\mathbf{Y_s}$ represents the part of admittance matrix relating current injection to voltage of substation buses, and $\mathbf{Y}$ is the other part for voltage of other system nodes. Consequently, the vector for apparent power injection for all the system nodes (except the substation ones) will be:

$$\overrightarrow{S(t)} = \overrightarrow{V(t)} \odot \overrightarrow{I(t)}^* \ \Rightarrow\ \overrightarrow{S(t)} = \overrightarrow{V(t)} \odot [\mathbf{Y_S}(\overrightarrow{a(t)})\overrightarrow{V_S(t)}]^* + \overrightarrow{V(t)} \odot [\mathbf{Y}(\overrightarrow{a(t)})\overrightarrow{V(t)}]^* \tag{2.9}$$

In order to complete the power flow equations for the system, we need to derive *S(t)* based on load, DER, capacitor characteristics, too. Here, we need to define the *C* vector which represents the capacitor(s) state:

$$\vec{C} = [C_1 \quad C_2 \quad C_3 \quad \cdots \quad C_{N_C}]^T \tag{2.10}$$

If the $i^{th}$ capacitor is not multi-step, $C_i$ can only adopt zero and one values for its possible OFF and ON states, respectively. However, if it is a multistep capacitor bank, $C_i$ represents the number of the capacitor modules that are switched ON. If phases of a three-phase capacitor or capacitor bank are controlled separately, three elements are considered in the *C* vector for that capacitor equipment, each representing switching status of one phase. The $Q_C$ vector also contains the nominal kvar size of each capacitor (or size of each capacitor step in case of capacitor-bank) in the *C* vector:

$$\overrightarrow{Q_C} = [Q_{C,1} \quad Q_{C,2} \quad Q_{C,3} \quad \cdots \quad Q_{C,N_C}]^T \tag{2.11}$$

[17] Here, capacitors are not considered in the admittance matrix, but they will be treated based on their current injection in the power flow equations.

*Assumptions 2.3 ad 2.4* allow us to express the active and reactive power injection vectors as follows[18] (which are real and imaginary parts of *S(t)* vector respectively):

$$\begin{cases} \mathrm{Re}\{\overrightarrow{S(t)}\} = \overrightarrow{P_o(t)} \odot \overrightarrow{f_P}(\overrightarrow{V(t)}) \\ \mathrm{Im}\{\overrightarrow{S(t)}\} = \overrightarrow{Q_o(t)} \odot \overrightarrow{f_Q}(\overrightarrow{V(t)}) \end{cases} \tag{2.12}$$

The above $\overrightarrow{P_o(t)}$ and $\overrightarrow{Q_o(t)}$ represent the amount of nominal load (or DER generation, etc.) at time *t*, while, $f_P$ and $f_Q$ functions denote the voltage-dependency nature of the loads, DERs or capacitors. *Assumption 2.4* makes it possible to use time-invariant functions of $f_P$ and $f_Q$ in the above equations. For example, suppose the $i^{th}$ capacitor is connected to $n^{th}$ node. The $n^{th}$ element of these vectors will be:

$$\begin{aligned} &P_{o,n}(t) = 0,\ f_{P,n}(\vec{V}) = 1 \\ &Q_{o,n}(t) = C_i(t) \times Q_{C,i},\ f_{Q,n}(\vec{V}) = (\frac{|V_n|}{V_{Nom,C_i}})^2 \end{aligned} \tag{2.13}$$

As another example, if a load with a ZIP model ([14]) is on the $n^{th}$ node, $n^{th}$ element of $\overrightarrow{P_o(t)}$ and $\overrightarrow{Q_o(t)}$ will correspond to nominal[19] value of load at time *t*, and $n^{th}$ element of $f_P$ and $f_Q$ will be as below:

$$\begin{aligned} f_{P,n}(\vec{V}) &= -a_{z,i}(\frac{V_n}{V_{Nom,Load_i}})^2 - a_{I,i}(\frac{V_n}{V_{Nom,Load_i}}) - a_{P,i} \\ f_{Q,n}(\vec{V}) &= -b_{z,i}(\frac{V_n}{V_{Nom,Load_i}})^2 - b_{I,i}(\frac{V_n}{V_{Nom,Load_i}}) - b_{P,i} \end{aligned} \tag{2.14}$$

where $(a_{z,i}, a_{I,i}, a_{P,i})$ and $(b_{z,i}, b_{I,i}, b_{P,i})$ are ZIP coefficients for active and reactive power of the $i^{th}$ load, respectively.

Obviously, the elements of $\overrightarrow{P_o(t)}$ and $\overrightarrow{Q_o(t)}$ for a node without any DER, load or capacitor will be always zero.

A capacitor switching event that happens at time *t* makes a change in *C* vector, denoted as $\Delta C$ which can be written as:

$$\overrightarrow{\Delta C} = \overrightarrow{C(t+\Delta t)} - \overrightarrow{C(t)}\ , \tag{2.15}$$

where $t+\Delta t$ corresponds to the time right after the switching happens.

Based on *Assumption 2.5* and above definitions, one has $\overrightarrow{P_o(t)} = \overrightarrow{P_o(t+\Delta t)}$ and $\overrightarrow{Q_o(t)} = \overrightarrow{Q_o(t+\Delta t)}$; accordingly, the power injections for $t+\Delta t$ can be written be as follows:

[18] Indeed, it is by *Assumption 2.4*, that we can write $\overrightarrow{f_P}(\overrightarrow{V(t)})$ instead of $\overrightarrow{f_P}(\overrightarrow{V(t)}, t)$.

[19] Nominal value of a load stands for its amount of power usage at a *1pu* voltage.

$$\begin{cases} \mathrm{Re}\{\overrightarrow{S(t+\Delta t)}\} = \overrightarrow{P_o(t)} \odot \overrightarrow{f_P}(\overrightarrow{V(t+\Delta t)}) \\ \mathrm{Im}\{\overrightarrow{S(t+\Delta t)}\} = \overrightarrow{Q_o(t)} \odot \overrightarrow{f_Q}(\overrightarrow{V(t+\Delta t)}) + \vec{\Gamma}\left[\overrightarrow{\Delta C} \odot \overrightarrow{Q_C}\right] \odot \left( \dfrac{|\overrightarrow{V(t+\Delta t)}|}{\vec{\Gamma}\left[|\overrightarrow{V_{Nom,C}}|\right]} \right)^2 \end{cases} \tag{2.16}$$

The $\Gamma$ operator in above equation is used to project the vectors associated with capacitors to nodes of the system. Its definition is expressed below:

$$\vec{y} = \vec{\Gamma}\left[\vec{x}\right] \Leftrightarrow y_n = \begin{cases} x_i & \text{if } i^{th} \text{ capacitor is on } n^{th} \text{ node} \\ \text{else} & 0 \end{cases} \quad \text{for } n = 1 \to N_{Nodes} \tag{2.17}$$

where $x_i$ denotes $i^{th}$ element of the $x$ vector.

*Assumption 2.6* implies $\overrightarrow{a(t)} = \overrightarrow{a(t+\Delta t)}$, and *Assumption 2.7* allows us to treat source voltages as a constant vector (i.e. $\overrightarrow{V_S(t)} = \overrightarrow{V_S}$). Therefore, the equations in (2.9) can be also written for $t+\Delta t$ as below:

$$\overrightarrow{S(t+\Delta t)} = \overrightarrow{V(t+\Delta t)} \odot [\mathbf{Y_S}(\overrightarrow{a(t)})\overrightarrow{V_S}]^* + \overrightarrow{V(t+\Delta t)} \odot [\mathbf{Y}(\overrightarrow{a(t)})\overrightarrow{V(t+\Delta t)}]^* \tag{2.18}$$

Once all combined, equations (2.9),(2.12),(2.16) and (2.18) fully describe the constraints on system voltages before and after the capacitor switching event. The vectors $\overrightarrow{S(t)}$ and $\overrightarrow{S(t+\Delta t)}$ can be eliminated by combining (2.9) with (2.12) and (2.16) with (2.18), respectively, as shown below:

$$\begin{cases} \mathrm{Re}\{\overrightarrow{V(t)} \odot [\mathbf{Y_S}(\overrightarrow{a(t)})\overrightarrow{V_S}]^* + \overrightarrow{V(t)} \odot [\mathbf{Y}(\overrightarrow{a(t)})\overrightarrow{V(t)}]^*\} = \overrightarrow{P_o(t)} \odot \overrightarrow{f_P}(\overrightarrow{V(t)}) \\ \mathrm{Im}\{\overrightarrow{V(t)} \odot [\mathbf{Y_S}(\overrightarrow{a(t)})\overrightarrow{V_S}]^* + \overrightarrow{V(t)} \odot [\mathbf{Y}(\overrightarrow{a(t)})\overrightarrow{V(t)}]^*\} = \overrightarrow{Q_o(t)} \odot \overrightarrow{f_Q}(\overrightarrow{V(t)}) \\ \mathrm{Re}\{\overrightarrow{V(t+\Delta t)} \odot [\mathbf{Y_S}(\overrightarrow{a(t)})\overrightarrow{V_S}]^* + \overrightarrow{V(t+\Delta t)} \odot [\mathbf{Y}(\overrightarrow{a(t)})\overrightarrow{V(t+\Delta t)}]^*\} = \overrightarrow{P_o(t)} \odot \overrightarrow{f_P}(\overrightarrow{V(t+\Delta t)}) \\ \mathrm{Im}\{\overrightarrow{V(t+\Delta t)} \odot [\mathbf{Y_S}(\overrightarrow{a(t)})\overrightarrow{V_S}]^* + \overrightarrow{V(t+\Delta t)} \odot [\mathbf{Y}(\overrightarrow{a(t)})\overrightarrow{V(t+\Delta t)}]^*\} = \overrightarrow{Q_o(t)} \odot \overrightarrow{f_Q}(\overrightarrow{V(t+\Delta t)}) + \vec{\Gamma}\left[\overrightarrow{\Delta C} \odot \overrightarrow{Q_C}\right] \odot \left( \dfrac{|\overrightarrow{V(t+\Delta t)}|}{\vec{\Gamma}\left[|\overrightarrow{V_{Nom,C}}|\right]} \right)^2 \end{cases} \tag{2.19}$$

Next, one can derive $\overrightarrow{P_o(t)}$ and $\overrightarrow{Q_o(t)}$ from the first two equations and replace those into the third and fourth equations to arrive into following set of equations. $\overrightarrow{V(t+\Delta t)}$ is also stated as summation of $\overrightarrow{V(t)}$ and $\overrightarrow{\Delta V}$:

$$\begin{aligned} &\mathrm{Re}\{(\overrightarrow{V(t)} + \overrightarrow{\Delta V}) \odot [\mathbf{Y_S}(\overrightarrow{a(t)})\overrightarrow{V_S}]^* + (\overrightarrow{V(t)} + \overrightarrow{\Delta V}) \odot [\mathbf{Y}(\overrightarrow{a(t)})(\overrightarrow{V(t)} + \overrightarrow{\Delta V})]^*\} = \\ &\mathrm{Re}\{\overrightarrow{V(t)} \odot [\mathbf{Y_S}(\overrightarrow{a(t)})\overrightarrow{V_S}]^* + \overrightarrow{V(t)} \odot [\mathbf{Y}(\overrightarrow{a(t)})\overrightarrow{V(t)}]^*\} \odot \frac{\overrightarrow{f_P}(\overrightarrow{V(t)} + \overrightarrow{\Delta V})}{\overrightarrow{f_P}(\overrightarrow{V(t)})} \end{aligned} \tag{2.20}$$

$$\mathrm{Im}\{(\overrightarrow{V(t)}+\overrightarrow{\Delta V})\odot[\mathbf{Y_S}(\overrightarrow{a(t)})\overrightarrow{V_S}]^*+(\overrightarrow{V(t)}+\overrightarrow{\Delta V})\odot[\mathbf{Y}(\overrightarrow{a(t)})(\overrightarrow{V(t)}+\overrightarrow{\Delta V})]^*\}=$$

$$\mathrm{Im}\{\overrightarrow{V(t)}\odot[\mathbf{Y_S}(\overrightarrow{a(t)})\overrightarrow{V_S}]^*+\overrightarrow{V(t)}\odot[\mathbf{Y}(\overrightarrow{a(t)})\overrightarrow{V(t)}]^*\}\odot\frac{\overrightarrow{f_Q}(\overrightarrow{V(t)}+\overrightarrow{\Delta V})}{\overrightarrow{f_Q}(\overrightarrow{V(t)})}+\vec{\Gamma}\left[\overrightarrow{\Delta C}\odot\overrightarrow{Q_C}\right]\odot\left(\frac{|\overrightarrow{V(t)}+\overrightarrow{\Delta V}|}{\vec{\Gamma}\left[|\overrightarrow{V_{Nom,C}}|\right]}\right)^2 \tag{2.21}$$

Total power loss can be also expressed as summation of active power injection into every node including substation ones. Hence, there is one more equation relating $\Delta P_{loss}$ to the other variables:

$$\Delta P_{loss}=Sum\left(\mathrm{Re}\{\left[\frac{\overrightarrow{V_S}}{\overrightarrow{V(t)}+\overrightarrow{\Delta V}}\right]\odot[\mathbf{Y_{all}}(\overrightarrow{a(t)})\left[\frac{\overrightarrow{V_S}}{\overrightarrow{V(t)}+\overrightarrow{\Delta V}}\right]]^*\}\right)-Sum\left(\mathrm{Re}\{\left[\frac{\overrightarrow{V_S}}{\overrightarrow{V(t)}}\right]\odot[\mathbf{Y_{all}}(\overrightarrow{a(t)})\left[\frac{\overrightarrow{V_S}}{\overrightarrow{V(t)}}\right]]^*\}\right)$$

$$\mathbf{Y_{all}}\in\mathbb{R}^{(N_{nodes}+N_S)\times(N_{nodes}+N_S)} \tag{2.22}$$

Except for vectors of $\overrightarrow{V(t)}$ and $\overrightarrow{a(t)}$, there is no other time-variant term in above equations of (2.20), (2.21) and (2.22). Therefore, the equations relating $\overrightarrow{\Delta V}$ and $\Delta P_{loss}$ to $\overrightarrow{V(t)}$ and $\overrightarrow{a(t)}$ are completely time-invariant. Equations in (2.21) and (2.22) are in a vector format where each vector contains $N_{nodes}$ entities. Hence, $2N_{nodes}+1$ nonlinear equations are available through (2.20), (2.21) and (2.22). Now, if we consider $\overrightarrow{\Delta V}$ and $\Delta P_{loss}$ as the unknown variables for these set of equations, we will also have $2N_{nodes}+1$ unknown variables (the elements of $\Delta V$ are complex variables, therefore number of unknown variables will be twice of the vector size). Therefore, this set of equations is not underdetermined when being solved to find $\Delta V$ and $\Delta P_{loss}$. Thus, the proof for Theorem 2.1 is complete.

■

The most useful implication of the above theorem is that the equations are time-invariant. Inspired from this feature, we can define the below functions for estimation of changes due to a capacitor switching. These functions can be viewed as the solution to nonlinear equations of (2.20), (2.21) and (2.22) which the theorem demonstrated not to be underdetermined. Since the equations are time-invariant, these functions are not dependent on time as well:

$$\overrightarrow{\Delta V}=\overrightarrow{h_V}(\vec{V},\vec{a},\overrightarrow{\Delta C})\quad,\quad\Delta P_{loss}=h_P(\vec{V},\vec{a},\overrightarrow{\Delta C}) \tag{2.23}$$

In analogy to the example system in section 2.2, the above time-invariant equations have the same role of (2.3) for estimations. The above result allows one to collect vectors of $\vec{V}$, $\vec{a}$, $\overrightarrow{\Delta C}$, $\Delta P_{loss}$ and $\overrightarrow{\Delta V}$ for each of the system's switching and perform statistical estimation to predict $\Delta P_{loss}$ and $\overrightarrow{\Delta V}$ for the future switching events. If such time-invariant relationships did not exist, one had to include time as another parameter in the estimations which would further complicate the estimation problems.

However, there is still one difficulty if the functions in (2.23) are to be used for statistical estimations in our framework. This difficulty is due to large space of input variables as discussed in the beginning of this chapter. Based on the present formulations, one has to collect data at every different possible combination of tap ratios ($a$) for different capacitor switching events ( $\overrightarrow{\Delta C}$ ) to ensure accurate estimations. As aforementioned, this limitation is itself enough to make our data-driven approach infeasible. To tackle this issue, we will utilize the fact of high correlation between the voltages ( $\vec{V}$ ) and tap-ratios ( $\vec{a}$ ) in a radial distribution feeder. In the next section, a new unified vector is defined which can substitute for both of the highly correlated $V$ and $a$ vectors in the equations.

## 2.4 Modified Voltage Vector

The voltage values are modified by subtracting the part of voltages which are directly determined by tap ratios of SLTC and VRs. This modification gives a modified voltage vector representing all the system nodes (except substation ones). Before presenting the mathematical definition of modified voltage vector, we need to label phase of each system's node. We define the function *Phase(n)* for this purpose. *Phase(n)* gives the identifier number of the substation's node which corresponds for the phase of the $n^{th}$ node in the system. Considering example of a three-phase system, naturally A, B and C phases of substation for this system will be assigned with the identifier numbers of *1*, *2* and *3*, respectively. Now, supposing that $n$ and $m$ are respectively the identifier number for one phase-A node and one phase-C node of the system, it follows that *Phase(n)=1* and *Phase(m)=3*.

The modified voltage vector ( $\overrightarrow{V'}$ ) is a vector with the same length of the original voltage vector ( $\vec{V}$ ), where each of its element are defined as below:

$$\overrightarrow{V'} = [V'_1 \quad V'_2 \quad V'_3 \quad \cdots \quad V'_{N_{nodes}}]^T \ , V'_n \triangleq V_n - V_{S,phase(n)} \times \prod_{i \in R_n} a_i \quad \text{for } n = 1 \rightarrow N_{nodes} \tag{2.24}$$

where $R_n$ is a set including identifier numbers of all tap-changing equipment upstream of $n^{th}$ system node.

The importance of the above definition becomes clear by the following theorem. Before stating the theorem, some more assumptions are required as stated bellow.

***Assumption 2.8***: No (active/reactive) power generating/consuming equipment such as loads, DER or capacitor is directly connected to primary of secondary of VRs. Moreover, primary of SLTC is not immediately connected to the substation source.

**Theorem 2.2:** For a radial distribution feeder constrained with *Assumption 2.8*, and with a known substation voltage(s), knowledge of modified voltage vector ( $\overrightarrow{V'}$ ) is sufficient to determine the voltage vector ( $\vec{V}$ ) and tap ratios of SLTC and every VRs (i.e. the $\vec{a}$ vector).

The proof for the above theorem is presented in Appendix A. From mathematical standpoint, what the theory implies is that unique functions $M_V$ and $M_a$ exist such that:

$$\vec{V} = \overrightarrow{M_V}(\vec{V'}) \ , \ \vec{a} = \overrightarrow{M_a}(\vec{V'}) \tag{2.25}$$

The above functions help to rewrite the function for $\overrightarrow{\Delta V}$ in (2.23) as follows:

$$\overrightarrow{\Delta V} = \overrightarrow{h_V}(\vec{V}, \vec{a}, \overrightarrow{\Delta C}) \Rightarrow \overrightarrow{\Delta V} = \overrightarrow{h_V}(\overrightarrow{M_V}(\vec{V'}), \overrightarrow{M_a}(\vec{V'}), \overrightarrow{\Delta C}) \tag{2.26}$$

On the other hand, based on definition of modified voltage vector ($\overrightarrow{V'}$), we already know that inverse of the functions in (2.24) exists as follows[20]:

$$\overrightarrow{V'} = \overrightarrow{M_V^{-1}}(\vec{V}, \vec{a}) \tag{2.27}$$

Therefore, $\overrightarrow{\Delta V'}$ can be also stated in terms of $\vec{V}$ , $\overrightarrow{\Delta V}$ , and $\vec{a}$ :

$$\overrightarrow{\Delta V'} = \overrightarrow{M_V^{-1}}(\vec{V} + \overrightarrow{\Delta V}, \vec{a}) - \overrightarrow{M_V^{-1}}(\vec{V}, \vec{a}) \tag{2.28}$$

By combining (2.25)-(2.26) and (2.28), we arrive at a time-invariant function that relate changes of modified voltage vector due to a switching event to its original value before the switching:

$$\overrightarrow{\Delta V'} = \overrightarrow{H_V}(\overrightarrow{V'}, \overrightarrow{\Delta C}) \tag{2.29}$$

A similar logic leads to the same conclusion for changes in power loss:

$$\Delta P_{loss} = H_P(\overrightarrow{V'}, \overrightarrow{\Delta C}) \tag{2.30}$$

Therefore, the voltage vector modification leads to a much more convenient statistical estimation framework. One only needs to derive modified voltage vectors for each capacitor switching event, and that will be sufficient to be organized as the input for the statistical estimation process. It should be noted that the described technique limits the application of proposed framework to radial feeders. Developing a framework for meshed systems will be considered in future research on this topic.

## 2.5 Organizing the Measurement Data

Since the nature of $\Delta C$ and $V'$ is different, it is more convenient to define separate functions for each type of capacitor switching. For example, if there is only one (not multi-step) capacitor in the system, $\overrightarrow{\Delta C}$ will be a single variable adopting only two possible values of either *-1* or *1* for turning it OFF or ON. In this example, estimations could be done on two separate functions as below:

$$\begin{aligned} \Delta P_{loss} &= H_P^{ON}(\overrightarrow{V'}) = H_P(\overrightarrow{V'}, \overrightarrow{\Delta C})\,|_{\overrightarrow{\Delta C}=[1]} \\ \Delta P_{loss} &= H_P^{OFF}(\overrightarrow{V'}) = H_P(\overrightarrow{V'}, \overrightarrow{\Delta C})\,|_{\overrightarrow{\Delta C}=[-1]} \end{aligned} \tag{2.31}$$

[20] Which is indeed definition of $V'$ in (2.24).

Obviously, if there are more capacitors or capacitor banks, one has to define more of such functions. By this technique, $V'$ will be the only input variable left for the estimations.

***Assumption 2.9***: The measurement system records the voltage phasor (i.e. both magnitude and phasor angles) of every system nodes[21].

Supposing the measurement system has recorded the following data of $\overrightarrow{V'}$ and $P_{loss}$ for the operation instants of $t_1, t_2, \ldots, t_T$ where $T$ is the number of recorded instants[22]:

$$\{\overrightarrow{V'(t_1)},\overrightarrow{V'(t_2)},\overrightarrow{V'(t_3)}\cdots,\overrightarrow{V'(t_T)}\}\ ,\ \{P_{loss}(t_1),P_{loss}(t_2),P_{loss}(t_3),\cdots,P_{loss}(t_T)\} \tag{2.32}$$

one can organize this measurement data into separate sample sets for $H_P^{ON}$ and $H_P^{OFF}$ functions. For example, the input and output samples for $H_P^{ON}$ will be as follows.

$$\begin{aligned} X\left[H_P^{ON}\right] &= \{\overrightarrow{V'(t_n)} \mid n \in \{1,2,\cdots,T-1\} \wedge \overrightarrow{C(t_n)} = [0] \wedge \overrightarrow{C(t_{n+1})} = [1]\} \\ Y\left[H_P^{ON}\right] &= \{P_{loss}(t_{n+1}) - P_{loss}(t_n) \mid n \in \{1,2,\cdots,T-1\} \wedge \overrightarrow{C(t_n)} = [0] \wedge \overrightarrow{C(t_{n+1})} = [1]\} \end{aligned} \tag{2.33}$$

Similarly, one can perform this organization of data for estimating changes in modified voltage vector and establish sample data for $H_V^{ON}$ and $H_V^{OFF}$ functions. Once the modified voltage is estimated for a switching event, the original voltage vector can be also reconstructed by inversing the formula in (2.24).

## 2.6 Regression Technique

Thus far, we have arrived at a desirable time-invariant function and its associated data-samples appropriate for applying a regression method to realize a statistical data-driven framework. The difference between parametric and non-parametric regressions were discussed earlier in chapter 1. The non-parametric option seems more suitable for the developed framework here. As the first reason, the number of parameters will be too large if one tries to employ a parametric regression. As the development of the estimation functions in the previous sections show, several parameters such as power line impedances, voltage dependency variables for loads and DERs will be among the unknown parameters. As the second reason, even if one could handle this large number of unknown parameters, it is too difficult to model everything by well-known mathematical functions. Because the whole estimation model is essentially rooted in nonlinear equations of (2.20), (2.21) and (2.22) which are almost analytically unsolvable[23]. However, there is still possibility of using 'Feature Selection' techniques in the field of statistical/machine learning to make

[21] This assumption is particularly too restrictive for practical purposes. Later, we will show how it can be mostly abandoned for practical applications of the proposed statistical framework.

[22] Measurements surely do not measure V' directly, but rather record V vector, however V' can be simply derived using (2.24). Section 3.2 in the next chapter will discuss how a measurement system such as AMI can provide the power loss ($P_{loss}$) data.

[23] Here, a problem is called analytically solvable if its solution can be stated in form of well-known mathematical functions.

parametric regression techniques feasible in this context [15]. Such approach is not pursued any further in this thesis, and is left as the future research work on this subject. Therefore, non-parametric regression is only considered here.

One of the simplest, yet effective and popular non-parametric techniques, known as K-Nearest Neighbor (KNN), is employed in this thesis. In principle, KNN predicts unknown output for a new input of a function based on the average of output samples belonging to the most similar input samples [15]. The method can be mathematically illustrated on an example (unknown) function *f* in a multi-dimension space:

$$\vec{y} = f(\vec{x}). \tag{2.34}$$

Supposing to have the following data sample sets for *f*:

$$\mathrm{X}[f] = \{\vec{x_1}, \vec{x_2}, ..., \vec{x_S}\},\ \mathrm{Y}[f] = \{\vec{y_1}, \vec{y_2}, ..., \vec{y_S}\}, \tag{2.35}$$

the KNN estimation will be as follows:

$$\hat{f}(\vec{x}) \cong \frac{1}{k} \sum_{x_i \in N_k(\vec{x})} \vec{y_i} \tag{2.36}$$

where $N_k(x)$ is a set consisting of $k$ closest $x_i$ vectors to $x$ , and closeness is defined in terms of Euclidian distance. For selection of $k$ parameter in KNN, the studies of this thesis adopt a popular rule of thumb and sets it as square root of number of samples (i.e. $k=S^{1/2}$) [16].

By means of theoretical statistics literature such as [18], we can be assured that KNN is a *Consistent* non-parametric estimator. It means that estimations of KNN are guaranteed to converge to their actual values with collection of enough sample data. Therefore, at least from the theoretical perspective, the data-driven methods that will be later developed based on this framework can be expected to give satisfactory results. The key factor is then collecting enough sample data for them.

As we will see in chapter 4 and 5, when this statistical framework is used for model-free operations such as VVC or CVR, the controller needs a prediction on the estimation error as a criteria to determine whether enough data is collected or not. The average error of the estimated values can be predicted using a Leave-One-Out Cross Validation method [15]. Supposing the estimation output is in scalar format (i.e. $y_s$ are not vectors), this method gives the following formula to calculate estimation error based on the available sample data in (2.34):

$$Estimation\ \ Error \cong \sqrt{\frac{1}{S}\sum_{s=1}^{S}[\hat{f}(\vec{x_s}) - y_s]^2} \tag{2.37}$$

## 2.7 Dimension Reduction

As observed from the previous sections, the input set of data samples are in form of modified voltage vectors[24]. Length of these vectors can become too large when there are several nodes in the system. In addition to computational difficulties, such big vectors can be also problematic for the KNN method due to 'Curse of Dimensionality' phenomenon [3],[15]. Therefore, application of a dimension reduction technique is essential for our proposed data-driven framework. In this thesis, Principal Component Analysis (PCA) [17] is used to reduce size of the input vectors before applying KNN.

The overall procedure can be mathematically illustrated on the unknown function *f* and its samples formulated in the previous section. In order to apply PCA, a matrix of input samples ($\boldsymbol{X_{Input}}$) needs to be built as shown below.

$$\mathbf{X}_{Input} = \begin{bmatrix} \overrightarrow{x_1}^T \\ \overrightarrow{x_2}^T \\ \vdots \\ \overrightarrow{x_S}^T \end{bmatrix} \tag{2.38}$$

Since PCA generally performs better on real values, in case that input vectors contain complex values[25], $X_{Input}$ is alternatively defined as:

$$\mathrm{X}_{Input} = \begin{bmatrix} \mathrm{Re}\{\overrightarrow{x_1}\}^T & \mathrm{Im}\{\overrightarrow{x_1}\}^T \\ \mathrm{Re}\{\overrightarrow{x_2}\}^T & \mathrm{Im}\{\overrightarrow{x_2}\}^T \\ \vdots & \vdots \\ \mathrm{Re}\{\overrightarrow{x_S}\}^T & \mathrm{Im}\{\overrightarrow{x_S}\}^T \end{bmatrix}. \tag{2.39}$$

The PCA technique gives a transformation matrix that transforms the input data into new dimensions, where the first components bear the maximum variation of the original data:

$$U_{Mat} = X_{Input} \times W_{PCA} \tag{2.40}$$

By keeping the first *p* (*p* is smaller than size of input vectors) columns of *U*, the transformed vectors can be defined as below:

$$\overrightarrow{u_i} = \begin{bmatrix} u_{i,1} & u_{i,2} & \cdots & u_{i,p} \end{bmatrix}^{\mathrm{T}} \quad i = 1 \rightarrow S \tag{2.41}$$

where each $u_{i,j}$ is one entity of $U_{Mat}$ matrix. Now, the PCA has transformed data to a smaller dimension, and, the KNN method can be based on this transformed data. In order to estimate outcome of function '*f* ' for a new input vector of *x*, the transformed vector will be:

[24] See (2.33) as an example.
[25] For instance, if the measurement data includes complex phasor voltage values.

$$\vec{u} = [\text{first } p \text{ elements of } (W_{PCA}^{T} \times \vec{x})] \tag{2.42}$$

And the estimated output of function using KNN combined with this PCA process will be:

$$\hat{f}(\vec{x}) \cong \frac{1}{k} \sum_{\vec{u}_i \in N_k(\vec{u})} \vec{y}_i \tag{2.43}$$

where $N_k(u)$ is a set consisting of $k$ closest $\vec{u_i}$ vectors to $\vec{u}$ (similar to definition of $N_k(x)$ in previous section).

## 2.8 Impact of Assumptions and Data Availability

As promised, this section investigates how all the assumptions adopted in this chapter affect the performance of proposed statistical framework for a practical application. Among all the assumptions, only 2.1 and 2.6 seem nonnegotiable, since the concept of modified voltage vector introduced in this thesis is only meaningful and useful for a radial distribution feeder where tap ratios of SLTCs and VRs do not change during capacitor switching events.

Fortunately, one can relax the constraints imposed by all the other assumptions (i.e. except 2.1 and 2.6), by introducing a probabilistic error in addition to the deterministic time-invariant function that is estimated. The probabilistic error can also account for the measurement errors. For example, considering the $H_P^{ON}$ function in (2.30), the equation in (2.30) is only valid if all the assumptions are fully met. Now, by relaxing those assumptions a probabilistic error will be added to the equation which is itself a function of $\overrightarrow{V'}$, $t$ and some other probabilistic variables:

$$\Delta P_{loss} = H_P^{ON}(\overrightarrow{V'}) + H_{err}(\overrightarrow{V'}, t, \varepsilon_1, ..., \varepsilon_n) \tag{2.44}$$

where $\varepsilon_1$, $\varepsilon_2$,…, $\varepsilon_n$ quantify the impact of uncertainties such as measurement noise, load changes during switching, variation of load characteristics by time and etc. Dependence of $H_{err}$ on $t$ stems from the fact that most of the relaxed assumptions were considering some time-variant characteristics of an actual system to be time-invariant. For example, *Assumption 2.4* and *Assumption 2.7* were considering constant voltage-dependency characteristic of loads and voltage source for the system during operation.

According to the literature in statistics [18], results of *Consistent* regression method such as KNN converge to the true expected value of the estimated output parameter conditioned on the input parameter in the sample data. Therefore, there will be a difference between a parameter and its estimated value as follows:

$$\underset{T\to\infty}{Lim}\left[\hat{\Delta P}_{loss}\,|_{\text{Estimated by KNN}}\right] = \Delta P_{loss}\,|_{\text{Actual}} - \overbrace{\mathrm{E}\left[H_{err}(\overrightarrow{V'}, t, \varepsilon_1, ..., \varepsilon_n)\,|\,\overrightarrow{V'}\right]}^{\text{Inevitable Error}} \tag{2.45}$$

As highlighted above, the eventual result of relaxing the assumptions will be an inevitable error in estimations of the proposed framework. One possibility that might reduce this inevitable error is inclusion

of switching times in the estimations. Albeit the potential benefit, having time as one of the input variables accompany its own complications. For example, further assumptions will be required on the behavior of the system from *Time Series* perspective to allow for the estimations. Nonetheless, upgrading the proposed framework with inclusion of time variable has been considered as future research to the topic of this thesis. For some special conditions such as a system that goes under significant feeder reconfigurations, inclusion of time as an estimation variable seems unavoidable for this framework.

Due to practical reasons, *Assumption 2.9* needs to be abandoned for the most part. The first reason is that no measurement system can give voltages for every node of a distribution feeder; for example, AMI systems can only provide voltage recording at customer nodes. The second reason is general lack of synchro-phasor capability in measurement systems such as AMI; the existing AMI systems are at least incapable to provide phasor angles for the measured voltages. As will be shown in the simulation studies of next chapters, these limitations might not cause a problem for the proposed statistical framework at all. This is mostly due to high correlation in voltages of nearby nodes, and also the high correlation between magnitude and angle of voltage for each node in a radial feeder. Hence, voltage magnitudes of limited number of nodes are found sufficient to reflect all the key state variations in the system. Therefore, since the dimension reduction process (PCA) eventually keeps only main components of variation, exclusion of voltages of some nodes or absence of phasor angle data becomes unimportant for the estimations.

The other possible concern with AMI data is its time resolution. The time resolution of the gathered data will be affected by latency and bandwidth of AMI communications in conjunction with the metering technology [12]. A large time resolution in the data can drop accuracy of estimations in the proposed statistical framework, because of a wider time gap between input and output sample values provided for estimations in $H$ functions of (2.31)[26]. For most of simulation studies in this thesis, a time resolution of 1 minute is considered. This value might seem visionary in respect to the characteristics of AMI systems installed on existing distribution feeders; however, it can better demonstrate the full potential of proposed methods. In fact, such feasibility studies on data-driven operation methods can eventually play a part in encouraging utilities to install improved communication technologies for future AMI systems in the grids. Nonetheless, effect of higher (and more practical) time resolutions such as 15 minutes will be also considered in the simulations.

## 2.9 Summary

This chapter presented a statistical framework suitable for VVC/CVR control and assessment on radial distribution feeder. Although the framework only focuses on predicting indices due to capacitor switching,

[26] In another perspective, a large time resolution can be viewed as a contrast to *Assumption 2.5*.

they are still applicable to a system with VR equipment. The estimation framework is time-invariant, therefore, the measurement data can be used for estimations without the need of being labelled by operation time. Two theorems were also presented to support the validity of this framework. The assumptions in premise of these theorems were rigorously stated as well. The discussion in the last section clarified that these assumptions do not obstruct practical application of the framework.

Suitable functions were also identified for estimations. The process of organizing the measurement data prior to estimations was presented, too. KNN and PCA were respectively introduced as regression analysis and dimension reduction methods used in the studies of this thesis. The next chapters will show how this statistical framework aids one to realize different model-free techniques for assessment and control of distribution grids.

# Chapter 3

# Model-free Assessment of Volt-Var Control (VVC)

This chapter presents a technique to assess benefits of VVC schemes using the data collected from an AMI system and the statistical framework developed in chapter 2. The VVC schemes under consideration of this chapter are capacitor-based[27] and open-loop. The open-loop characteristic implies that the VVC algorithm is not using any online feedback from system measurements such as voltage meters or AMI. The common examples of open-loop VVCs are usage of preset times for switching capacitors or a VVC running based on offline model-based computer simulations[28]. The proposed method is able to estimate, statistically, the amount of feeder losses saved due to switched capacitors during a given test period such as a week. Feasibility of the method will be demonstrated by simulation studies on an Elementary System and the IEEE 123 node test feeder.

## 3.1 Literature Review

Despite their obvious advantages, implementation of VVC schemes can be expensive, making it essential to assess their true benefits in the operation of a distribution feeder. Indeed, this need has driven a separate research stream to develop methods for VVC benefit assessment [13],[19]. Papers such as [20] and [21] have used model-based analyses and simulations to evaluate performance of VVCs. On the other hand, research works in [22]-[24] have also employed limited measurement data in conjunction with model-based simulations to improve the assessment results.

As discussed earlier in chapter 1, a proper benefit assessment of any automation scheme must be independent of system models, and, this rule apparently holds no exception regarding VVC schemes. Indeed, network owners are increasingly interested to actually measure the true benefits of an installed VVC scheme. The result of such assessment is significantly more reliable than computer simulations which themselves might be a part of the tested VVC scheme.

---

[27] The proposed statistical framework in chapter 2 did not include estimation of the power loss changes due to VR tap operations. Although it does not prevent developing a model-free VVC operating VRs (as will be shown in the next chapter), our studies have shown that a VVC controlling both capacitors and VRs cannot be always reliably assessed by a model-free approach based on this framework. Therefore, capacitor-based VVCs are only considered in this chapter.

[28] Model-free assessment of closed-loop VVC algorithms is considered as a future research on this topic.

One intuitive approach for field assessment of VVCs is the so-called "on/off experiment". As the name implies, this method consists of comparing system performance in two separate periods with turning the VVC scheme ON and OFF. Despite being simple and straightforward, this method is hardly capable to recognize load and ambient condition differences between the two periods. Some improvements have been proposed by using corrective factors in assessing the results, however, the improved methods either require prolonged test periods (up to two months) or are yet based on oversimplifying assumptions about system loads and ambient conditions. Nonetheless, on/off experiment has been the only available method used by utilities so far to evaluate VVC schemes independent of the models [25]-[28].The on/off experiment method will be further described in the next section.

## 3.2 Proposed Data-driven Assessment Scheme

### 3.2.1 The basic idea

We consider example of a single-capacitor system shown on Figure 3.1 to illustrate the basic idea behind the proposed method. Figure 3.2(a) shows switching commands from an open-loop VVC controlling this capacitor for a two day periods. Since the VVC is open-loop, its switching commands can be determined even before conducting the test. The objective of VVC assessment is to run a test on the system to derive the curves shown on Figure 3.2(b) where system losses are plotted with and without the example VVC. Unfortunately, both of these two curves cannot be directly measured during a test, since the capacitor can be either OFF or ON at each instant.

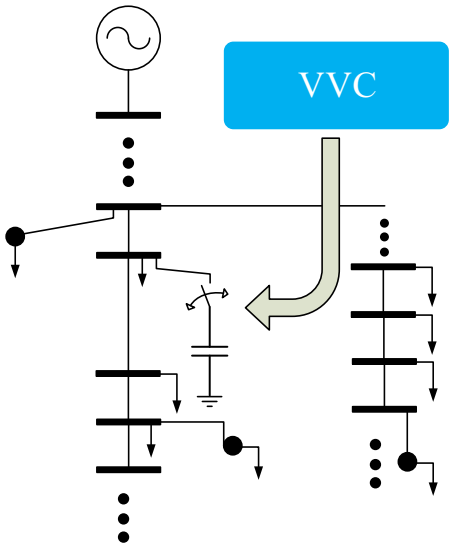


Figure 3.1 Example of a single-capacitor system with an open-loop VVC

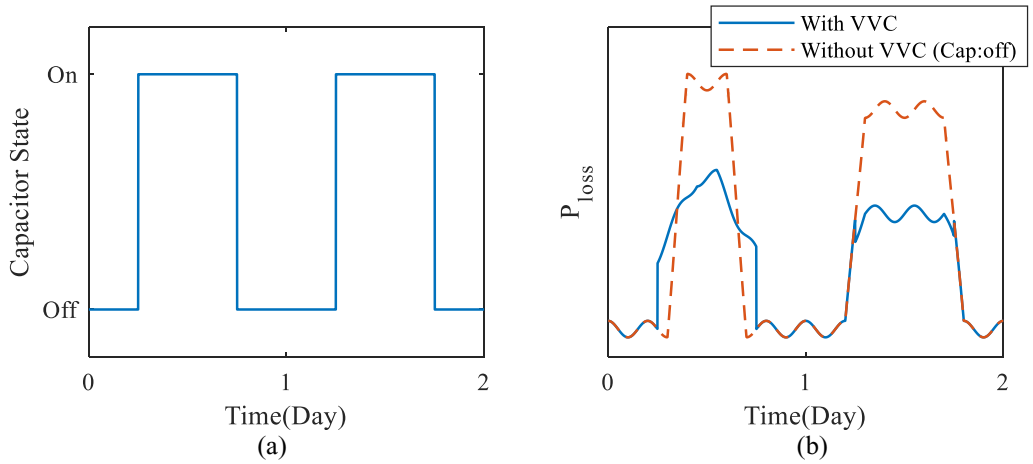


Figure 3.2 Capacitor switching command of example VVC and its performance on the example system

A common method to resolve this issue is conducting the so-called 'ON/OFF experiments'. By this method, the capacitors are switched according to the tested VVC for one day, and are abandoned OFF for the next day. A two-day ON/OFF experiment for the example VVC is shown on Figure 3.3 where on the first day the capacitor is switched according to the VVC and it is left OFF on the second day. By result of this test, the measured power losses of first and second days respectively represent the performance with and without VVC. The remaining problem is the differences of system conditions (e.g. loads, DER generation, etc.) between these two days. Hence, the data from one day cannot be used as a reference for the other day. The common practice to overcome this issue is to continue the test for several days. As Figure 3.4 shows, the system is operated with VVC on odd days and operated without VVC on even days (or vice versa). Instead of comparing two single days, average of power loss on even days and odd days are obtained and compared to assess VVC benefits. The averaging process aids to filter out the differences between the test days. Based on the studies reported in literature [25]-[28], the tests might need to be as long as two months to achieve reliable results.

One idea to avoid a very long test period is to increase the frequency of ON/OFF experiments. For example, instead of running VVC for one day and turning it OFF for the next day, the VVC algorithm can be turned ON and OFF repeatedly at each hour. Figure 3.5 shows this idea on the example VVC where the capacitor is switched by the VVC commands every other hour. It should be noted that this idea is only feasible for testing an open-loop VVC which does not rely on any measurement feedback.

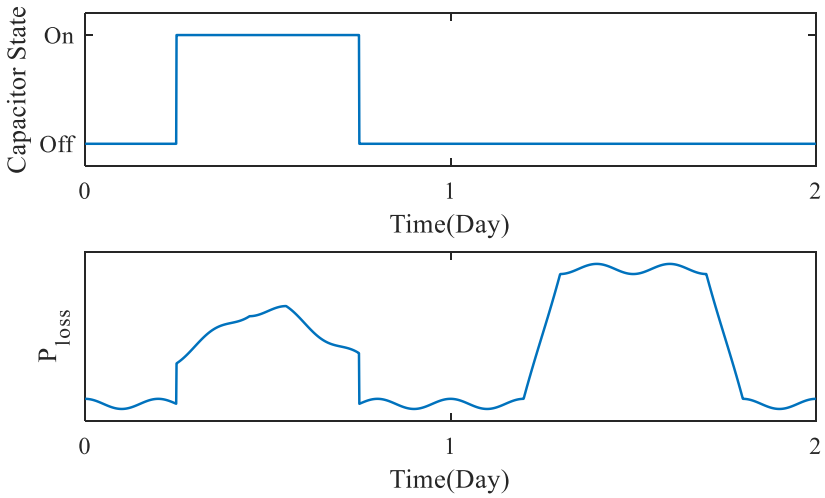


Figure 3.3 Two-day illustration of ON/OFF experiment for example VVC

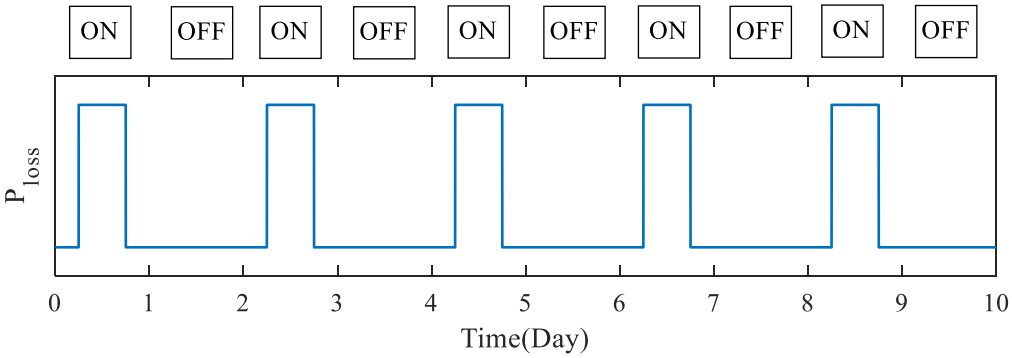


Figure 3.4 Capacitor switching pattern for a ten-day 'ON/OFF experiment' method of assessing example VVC

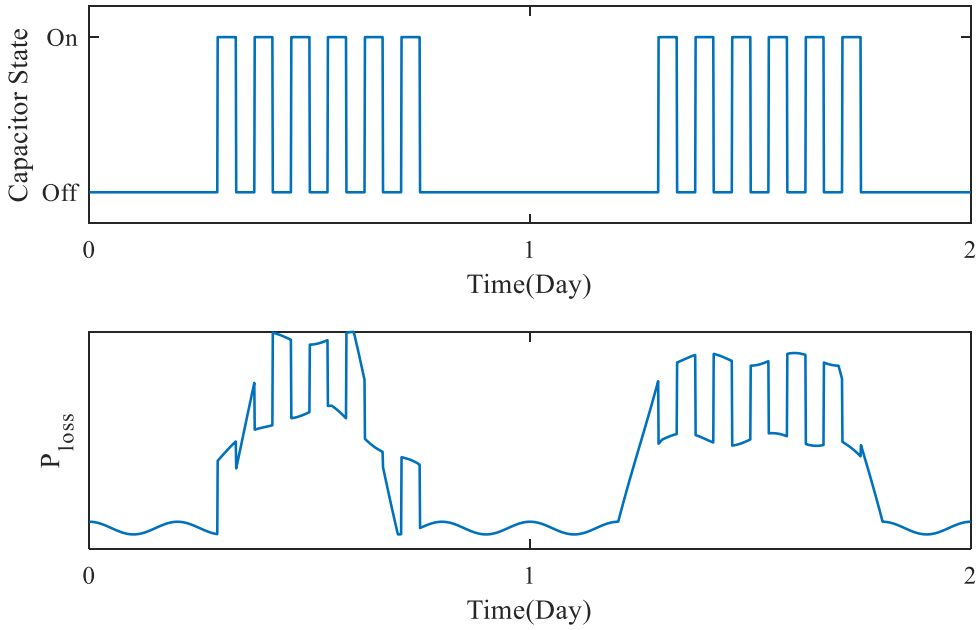


Figure 3.5 Testing the VVC by frequent ON/OFF experiment

The value of data achieved by this test can be even increased if the frequent switching of capacitor also extends to the hours that VVC switching command is OFF. As Figure 3.6 shows, the capacitor can be repeatedly switched at every hour. By this method, the measured power loss provides samples of both ON and OFF curves shown on Figure 3.7. If switching events are frequent enough, both of these curves can be estimated using interpolation on the data of this test. Once these curves are derived, the performance of any open-loop VVC algorithm can be assessed against the case of no-VVC including both conditions of leaving the capacitor OFF or ON.

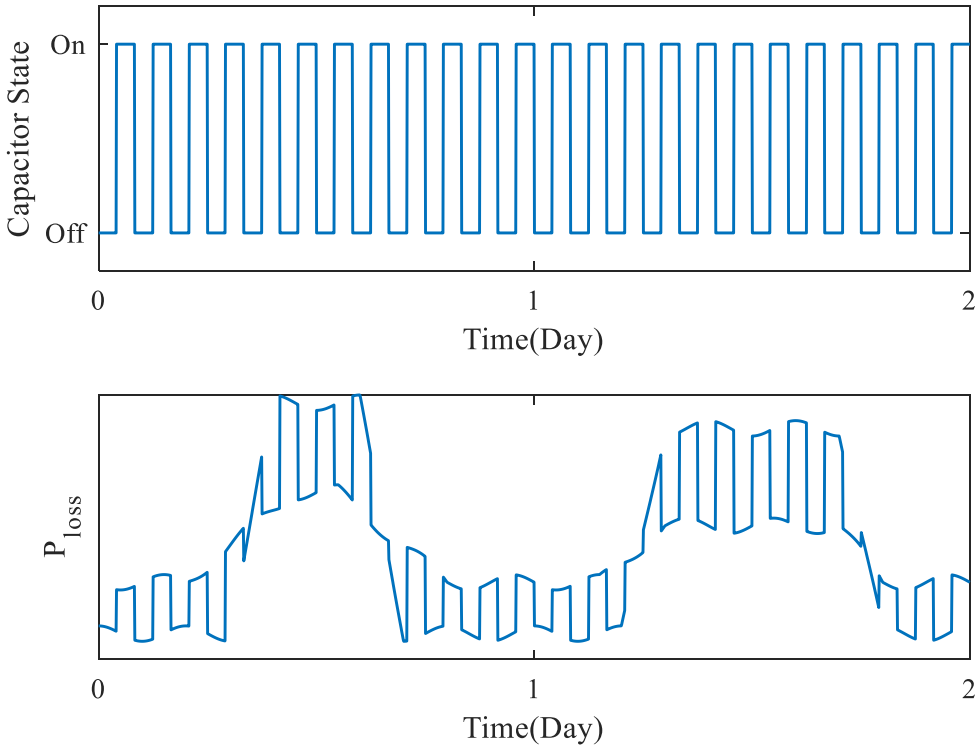


Figure 3.6 VVC assessment by frequent switching of the capacitor

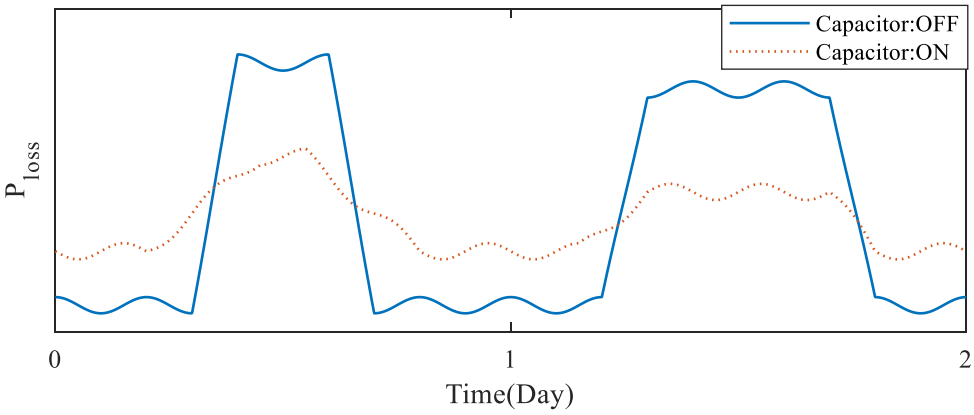


Figure 3.7 Power loss of the example system for two possible states of the capacitor

The problem with this simplistic approach is the huge number of switching events required to achieve accurate results. Fortunately, instead of relying only on interpolation, one can also use the data associated with each switching event. Each switching event presents a valuable sample revealing how power loss would change if the capacitor was in another state. Each sample point consists of the voltages before switching and the power loss change due to the switching. Using this additional data also can reduce the number of switching events required for the test. Instead of fixed time intervals, capacitor can be also switched in random times to reveal more general information regarding the tested system. The described idea is the core of the VVC assessment method presented in this thesis. The proposed method is illustrated in Figure 3.8 for the example VVC on how to estimate the complete profile of capacitor being ON. Similarly, the same method can build the power loss profile of the capacitor being OFF during whole profile. As aforementioned, having these two curves and knowing the VVC commands, the power loss curve resulted from the VVC can be also constructed, and its benefits get assessed accordingly.

Instead of estimating both OFF and ON curves independently and then constructing the curve for the considered VVC, the proposed method in this chapter uses the described procedure to directly estimate power loss resulting from the VVC. The estimations are performed according to the statistical framework developed in the second chapter. The method is also generalized to the scenarios of having more than a single capacitor, and estimation of other two indices of interest (i.e. minimum and maximum voltage). The detailed procedure is given in the next sections.

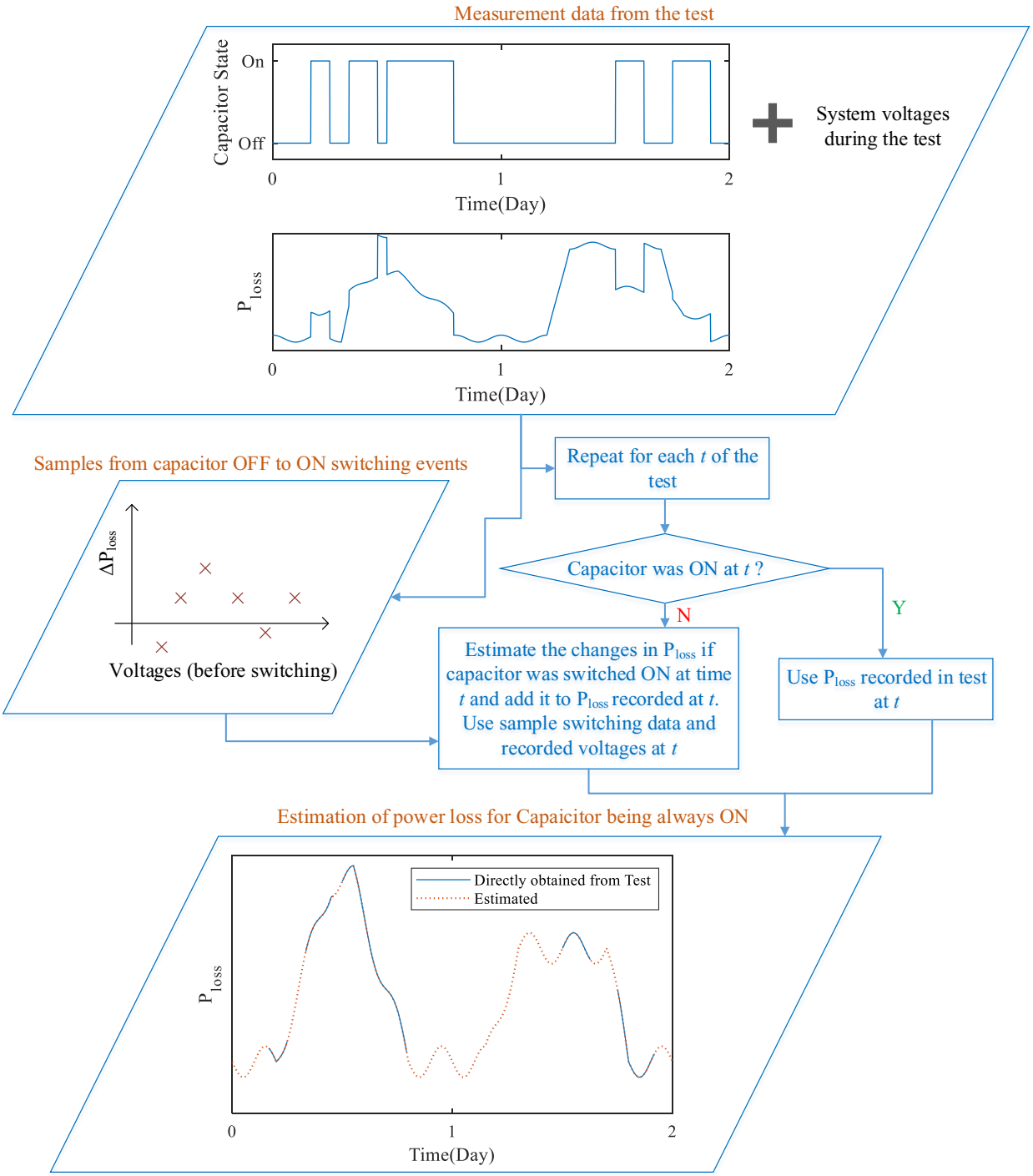


Figure 3.8 Illustration of the core idea: procedure for estimating power loss profile for ON state of capacitor using test data for the example system

### 3.2.2 Assessment Scheme

Main functions of an effective VVC are feeder loss reduction and support to voltage regulation. The first role can be evaluated in terms of the decrease in system total power loss. One can also assess the voltage regulation role by measuring maximum and minimum voltages of the system and confirming whether VVC contributes in holding them within the standard limit. Therefore, three indices of interest can be identified as essential assessment criterion: (a) total system power loss (b) system maximum voltage, and (c) system minimum voltage. The proposed method employ the data from AMI system to evaluate VVC impact on these three indices of interest. As shown on Figure 3.9, each smart meter provides the amount of power consumed (or produced) by each customer[29]. The scheme also collects the overall feeder power measured by a substation meter. Hence, it is able to calculate system's total power loss ($P_{loss}$):

$$P_{Loss} = P_{Sub} - \sum_{m=1}^{M} P_m^{SM} \tag{3.1}$$

The voltages recorded by smart meters can be also used to establish an approximation of system's total voltage vector:

$$\vec{V} \cong [V_1^{SM} \quad V_2^{SM} \quad \cdots \quad V_M^{SM}]^T \tag{3.2}$$

Absolute maximum and minimum entities inside the voltage vector represent an acceptable approximation of overall feeder's maximum and minimum voltages (since the customers' voltages are of the main regulation concern in a VVC). Overall, the scheme has access to measurement of key indices of interest for a basic VVC operation.

As thoroughly described before, the main challenge in such model-free approach is the lack of measurement data for every capacitor states at each instant of the test period. In fact, the measurement gives the data for only one capacitor state for each specific time. However, we need the information for every capacitor states to fully assess the effects of different VVC algorithms. This problem is overcome by using statistical estimation methods introduced in Chapter 2. Figure 3.9 shows the modular scheme for the proposed VVC assessment technique. The scheme is capable to estimate the expected performance of the feeder for different open-loop VVC algorithms. The capacitors are switched randomly to observe how voltages and total losses change at different capacitor states. Through this test, input data for statistical estimation process is collected. On the other hand, since the tested VVCs are open-loop, their switching commands are available to the scheme independent of the test. The statistical estimation procedure employs all of these data sets to predict the performance of the system on the same test period as if it was operated under these VVC algorithms.

[29] If the meter only sends the energy reading, consumed/produced power can be determined from incremental increase/decrease in energy reading.

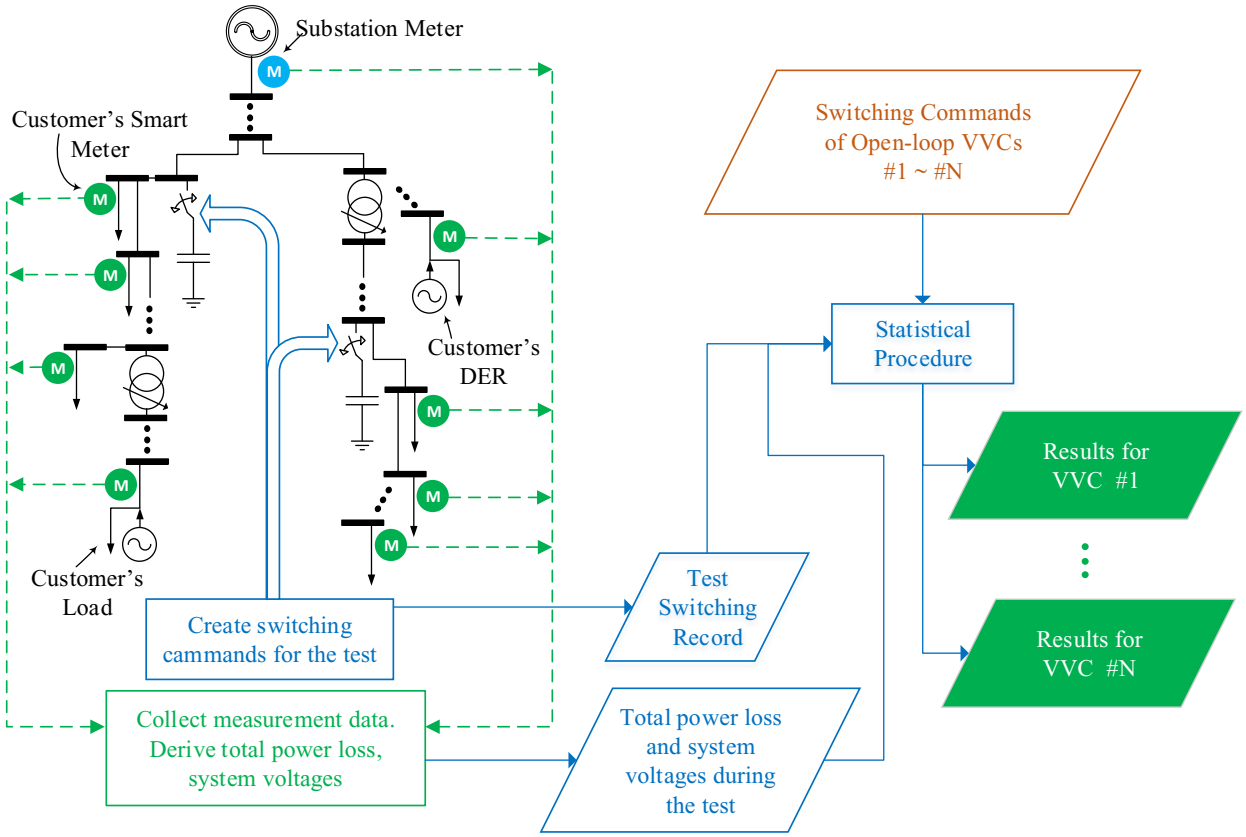


Figure 3.9 Scheme of proposed VVC assessment technique

If the system models were to be used, the procedure to determine system indices with different VVC algorithms would be all straight-forward. However, statistical estimation based on the measured data is the only option in the proposed model-free approach.

## 3.3 Statistical Estimation Module

The following sections develop the required definitions and computation procedure to realize the statistical framework as the core module in the proposed VVC assessment technique (see Figure 3.9).

### 3.3.1 Estimation Objective

The data from AMI is discrete with a time resolution depending on meter reading and data transmission frequency. Assuming that $T$ instants are recorded during the test at times $t=t_1, t_2,\dots, t_T$, the total raw data available for estimations can be labelled as follows:

$$\left\{ \overrightarrow{C_{VVC}(t_i)}, \overrightarrow{C(t_i)}, P_{loss}(t_i), \overrightarrow{V(t_i)} \right\}, i = 1,2,...,T \tag{3.3}$$

where $C_{VVC}(t)$ represents the capacitor switching commands from the VVC algorithm under consideration at time $t$. And $C(t)$ stands for capacitors state at time $t$ of the test. Since the proposed framework in chapter 2 operates based on modified voltage vector rather than the original voltage vectors, we can rewrite the raw data and expected outcome of estimations as follows:

$$\left\{ \overrightarrow{C_{VVC}(t_i)}, \overrightarrow{C(t_i)}, P_{loss}(t_i), \overrightarrow{V'(t_i)} \right\} , \; i = 1,2,...,T \tag{3.4}$$

Based on definition of $V'$ in chapter 2, one can easily derive (3.4) from (3.3). The expected outcome of estimation will be power loss and voltage vector of the system for the whole test period as if the system was operated according to VVC commands:

$$\left\{ P_{loss}^{VVC}(t_i), \overrightarrow{V^{VVC}(t_i)} \right\} , \; i = 1,2,...,T \tag{3.5}$$

Again, it becomes more consistent with the proposed statistical framework if we rewrite the expected outcome in terms of the modified voltage vector:

$$\left\{ P_{loss}^{VVC}(t_i), \overrightarrow{V'^{VVC}(t_i)} \right\} , \; i = 1,2,...,T \tag{3.6}$$

Once the estimations are performed, one can easily reconstruct $V$ from $V'$ based on the instructions in chapter 2.

### 3.3.2 Creating Data Sample Sets

The statistical platform developed in chapter 2 is used here. For the $n^{th}$ capacitor of the system we use groups of $H_P$ and $H_V$ functions[30] to predict changes due to different switching state of this capacitor:

$$\begin{aligned} &\Delta P_{loss} = H_P^{C_n,ON}(\overrightarrow{V'}) \; , \; \Delta P_{loss} = H_P^{C_n,OFF}(\overrightarrow{V'}) \\ &\overrightarrow{\Delta V'} = H_V^{C_n,ON}(\overrightarrow{V'}) \; , \; \overrightarrow{\Delta V'} = H_V^{C_n,OFF}(\overrightarrow{V'}) \end{aligned} \tag{3.7}$$

As per the procedure discussed in chapter 2, one can establish the data samples for these functions from the raw data (3.4) as follows:

[30] See section 2.5 for details on philosophy behind this type of functions.

$$
\begin{aligned}
&X\left[H_V^{C_n:ON}\right] = X\left[H_P^{C_n:ON}\right] = \left\{\overrightarrow{V'(t_i)} \mid i \in \{1,2,\cdots,T-1\} \wedge \Phi\left[\overrightarrow{C(t_{i+1})} - \overrightarrow{C(t_i)}\right] = n\right\} \\
&Y\left[H_P^{C_n:ON}\right] = \left\{P_{loss}(t_{i+1}) - P_{loss}(t_i) \mid i \in \{1,2,\cdots,T-1\} \wedge \Phi\left[\overrightarrow{C(t_{i+1})} - \overrightarrow{C(t_i)}\right] = n\right\} \\
&Y\left[H_V^{C_n:ON}\right] = \left\{\overrightarrow{V'(t_{i+1})} - \overrightarrow{V'(t_i)} \mid i \in \{1,2,\cdots,T-1\} \wedge \Phi\left[\overrightarrow{C(t_{i+1})} - \overrightarrow{C(t_i)}\right] = n\right\} \\
&X\left[H_V^{C_n:OFF}\right] = X\left[H_P^{C_n:OFF}\right] = \left\{\overrightarrow{V'(t_i)} \mid i \in \{1,2,\cdots,T-1\} \wedge \Phi\left[\overrightarrow{C(t_{i+1})} - \overrightarrow{C(t_i)}\right] = -n\right\} \\
&Y\left[H_P^{C_n:OFF}\right] = \left\{P_{loss}(t_{i+1}) - P_{loss}(t_i) \mid i \in \{1,2,\cdots,T-1\} \wedge \Phi\left[\overrightarrow{C(t_{i+1})} - \overrightarrow{C(t_i)}\right] = -n\right\} \\
&Y\left[H_V^{C_n:OFF}\right] = \left\{\overrightarrow{V'(t_{i+1})} - \overrightarrow{V'(t_i)} \mid i \in \{1,2,\cdots,T-1\} \wedge \Phi\left[\overrightarrow{C(t_{i+1})} - \overrightarrow{C(t_i)}\right] = -n\right\}
\end{aligned}
\tag{3.8}
$$

where the $\Phi[\ ]$ operator on a vector $x$ is defined as below:

$$
\Phi\left[\vec{x}\right] = \begin{cases} n & \text{if there is } n \text{ such that } x_n = 1 \text{ and for any } m \neq n:\ x_m = 0 \\ -n & \text{if there is } n \text{ such that } x_n = -1 \text{ and for any } m \neq n:\ x_m = 0 \\ 0 & \text{else} \end{cases} \tag{3.9}
$$

as examples of applying $\Phi[\ ]$: $\Phi\left[\begin{bmatrix}1 & 0\end{bmatrix}^T\right] = 1, \Phi\left[\begin{bmatrix}0 & -1\end{bmatrix}^T\right] = -2, \Phi\left[\begin{bmatrix}1 & -1\end{bmatrix}^T\right] = 0, \Phi\left[\begin{bmatrix}2 & 0\end{bmatrix}^T\right] = 0$.

In order to maximize the number of sample points for each function, the test switching commands should only switch one capacitor at a time (if two capacitors are switched simultaneously, it won't be counted as a sample based on structure of data sample sets in (3.8)).

### 3.3.3 Estimation Procedure

The estimation for each instant needs to be done separately. As discussed in chapter 2, KNN and PCA are used as the regression analysis and the dimension reduction method, respectively. At each instant, one should see how the capacitor states differ in the VVC commands from the measured test, and apply estimation on a chain of functions in (3.7) to arrive at the indices resulting from VVC. The whole procedure is illustrated by the following pseudocode:

$$
\begin{aligned}
&\text{for } i = 1 \to T \\
&\quad \text{set } \overrightarrow{\Delta C} = \overrightarrow{C_{VVC}(t_i)} - \overrightarrow{C(t_i)} \\
&\quad \text{set } \overrightarrow{V_x'} = \overrightarrow{V'(t_i)} \\
&\quad \text{set } P_{loss}^{VVC}(t_i) = P_{loss}(t_i) \\
&\quad \text{for } n = 1 \to N_C \\
&\qquad \text{if } \overrightarrow{\Delta C}(n) = 1 \\
&\qquad\quad \text{estimate } H_V^{C_n,ON}(\overrightarrow{V'}) \text{ and } H_P^{C_n,ON}(\overrightarrow{V'}) \text{ for } \overrightarrow{V'} = \overrightarrow{V_x'} \text{ using data samples in (3.8) and KNN+PCA} \\
&\qquad\quad \text{set } \overrightarrow{V_x'} = \overrightarrow{V_x'} + \hat{H}_V^{C_n,ON}(\overrightarrow{V'}) \\
&\qquad\quad \text{set } P_{loss}^{VVC}(t_i) = P_{loss}^{VVC}(t_i) + \hat{H}_P^{C_n,ON}(\overrightarrow{V'}) \\
&\qquad \text{endif} \\
&\qquad \text{if } \overrightarrow{\Delta C}(n) = -1 \\
&\qquad\quad \text{estimate } H_V^{C_n,OFF}(\overrightarrow{V'}) \text{ and } H_P^{C_n,OFF}(\overrightarrow{V'}) \text{ for } \overrightarrow{V'} = \overrightarrow{V_x'} \text{ using data samples in (3.8) and KNN+PCA} \\
&\qquad\quad \text{set } \overrightarrow{V_x'} = \overrightarrow{V_x'} + \hat{H}_V^{C_n,OFF}(\overrightarrow{V'}) \\
&\qquad\quad \text{set } P_{loss}^{VVC}(t_i) = P_{loss}^{VVC}(t_i) + \hat{H}_P^{C_n,OFF}(\overrightarrow{V'}) \\
&\qquad \text{endif} \\
&\quad \text{endfor} \\
&\quad \text{set } \overrightarrow{V'^{VVC}(t_i)} = \overrightarrow{V_x'} \\
&\text{endfor}
\end{aligned}
\tag{3.10}
$$

The above code processes the raw data of (3.4) to obtain the expected estimated result stated in (3.6). Finally, the original voltage vectors can be easily reconstructed from the estimated modified voltages, and the system' maximum/minimum voltage is determined as well.

## 3.4 Simulation Study Setup

Simulation studies were performed to evaluate the proposed methodology. Load flows were conducted by OpenDSS interface in Matlab. The statistical estimation process was also implemented by Matlab codes. Two systems were tested: an abstract Elementary system and the IEEE 123 Node Test Feeder [29]. The first system is a basic one suitable for illustration of the statistical estimation process, on the other hand, the latter one is closer to actual systems since it has more nodes and is unbalanced including both single and three-phase lines. Hence, it is used to test the feasibility of the proposed technique.

Simulation procedure was as follows: first, a number of abstract VVC commands were considered for each system. Then, the system was simulated for a specific test period where the capacitors were randomly switched, and the measurement data was collected as per the proposed scheme shown on Figure 3.9. The statistical estimation was also conducted to give the results of VVC assessment. Next, the system was separately simulated according to switching commands of each VVC for the test period. The results of these

simulations were considered as 'actual' performance of the system under that specific VVC. The actual results aid to assess accuracy of the data-based assessment methods.

For each system, three possible scenarios were considered regarding the capability of the AMI system:

**Scenario 3.1:** As a visionary scenario, AMI system was assumed to give the phasor angle of voltages. Thus, voltage vector were created by complex phasor values of voltages. The data resolution was assumed 1 minute.

**Scenario 3.2:** AMI system was assumed to give the voltage magnitudes only (closer to practical situation). Thus, voltage vector were created by magnitudes of voltages. The data resolution was assumed 1 minute similar to first scenario.

**Scenario 3.3:** Similar to previous scenario, but the data resolution was considered 15 minute.

For each system and each scenario, three indices are shown as the result of evaluating a VVC:

- Total Power loss of feeder ($P_{loss}$)
- Maximum voltage of system nodes ($V_{max}$)
- Minimum voltage of system nodes ($V_{min}$)

## 3.5 Simulation Studies on Elementary System

The assumed Elementary system is a *25kV* single-line feeder consisting of 10 similar sections and serving 10 loads as depicted in Figure 3.10. Every feeder sections are equal, each with length of *5km* and impedance of $Z=1.5+j1.5\ \Omega/km$. Loads are also evenly distributed along the feeder. The peak value of each load is *1500 kW* with constant Power Factor of *0.75*. A bell-shaped abstract load profile as shown in Figure 3.10 was also assumed for this system. The switchable capacitor is placed at the $7^{th}$ bus of the system with size of $Q_{C,1}=3000\ kvar$. Smart meters are assumed to be on each bus of the system to read and send its voltage and the power of the load.

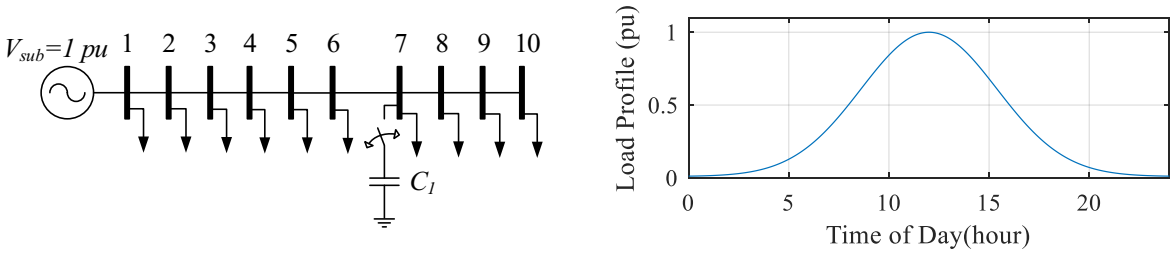


Figure 3.10 The schematic and load profile assumed for the Elementary system

### 3.5.1 Base Test Description

The base test was performed for a one day period with 14 switching operations of the capacitor at randomly chosen times. Figure 3.11 shows the raw data obtained from this test for *Scenario 3.2*.

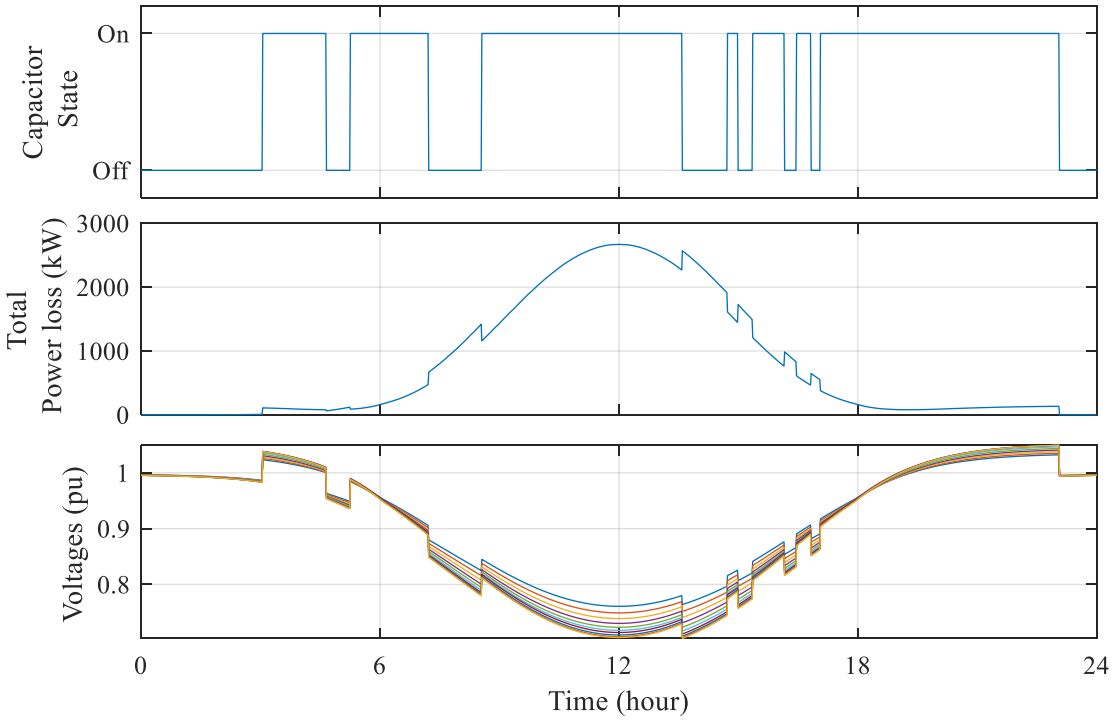


Figure 3.11 Raw measurement data from base test on Elementary system (Metering *Scenario 3.2*)

Using the proposed framework, three open-loop VVCs were evaluated using the data from this test system. Their switching commands are plotted on Figure 3.12.

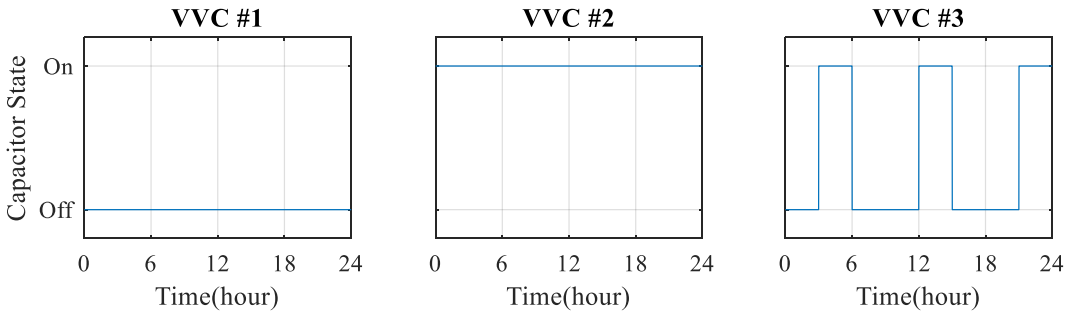


Figure 3.12 Capacitor switching commands of the tested VVC algorithms for Elementary System

The number of principal components kept for estimations was four (i.e. $p=4$ in PCA process described in chapter 2).

### 3.5.2 Base Results

Figure 3.13 and Figure 3.14 show the VVC assessment results for the base test. As the results show the proposed method has successfully estimated the performance of the three VVC algorithms for all the three indices of interest. For this system, all the three metering scenarios seem to be effective.

Table 3-A shows the errors of the estimation averaged for the whole test period and the three VVCs[31]. The results show that the negative impact of higher time resolution is not significant for this system. However, the estimations tend to be more accurate when voltage phasor angles are measured too, while the result without phasor angles is still quite acceptable.

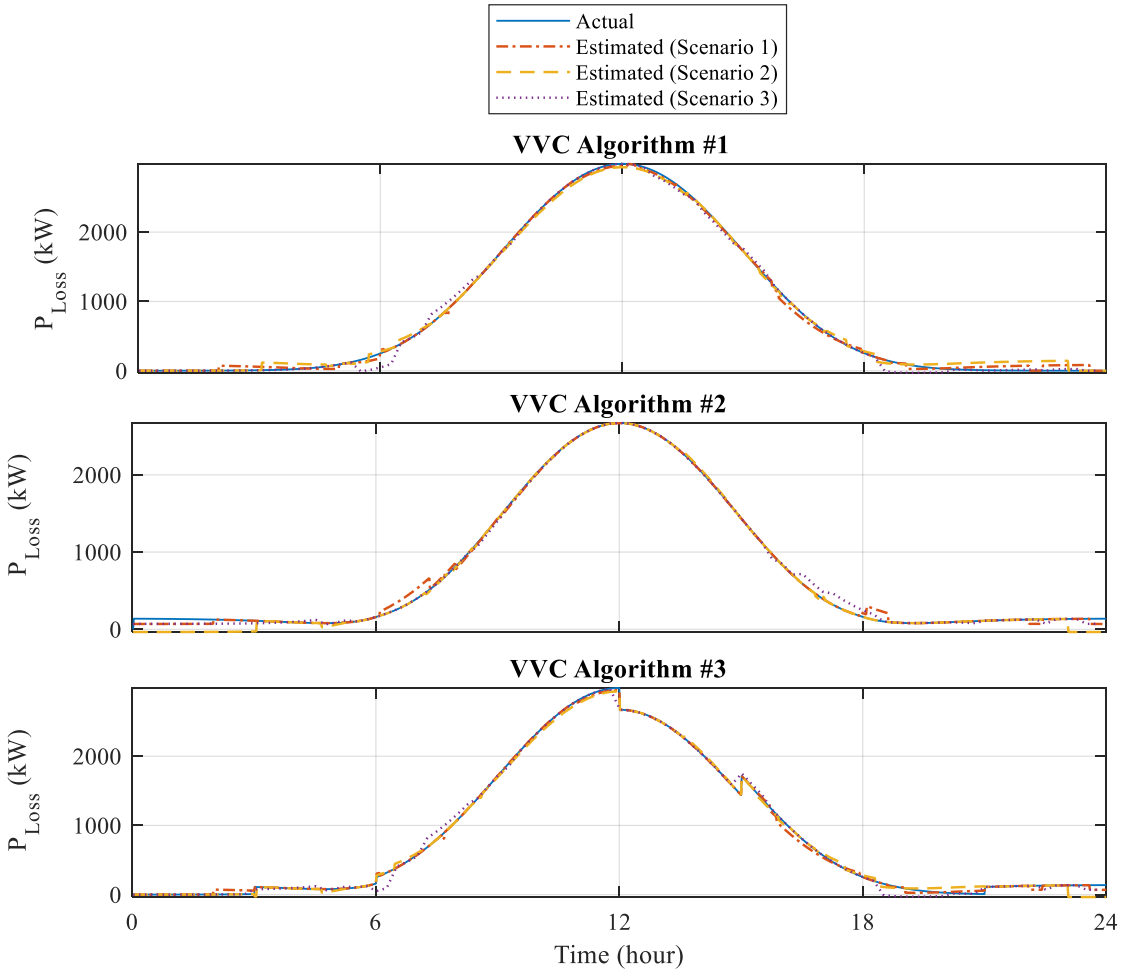


Figure 3.13 Data-driven assessment results for the Elementary System: Total Power Loss

[31] Since the indices such as power loss reach a very small value for some periods, the percentage of error is calculated as dividing average of error over average of index (i.e. average{error}/average{index}×100), rather than direct average of error (i.e. average{error/index}×100)

Table 3-A Average Estimation Errors for VVC assessment on Elementary System

| Average Estimation Error (%) | Metering Scenario | | |
|---|---|---|---|
| | 3.1: With phasor and 1 minute resolution | 3.2: Without phasor and 1 minute resolution | 3.3: Without phasor and 15 minute resolution |
| for Power Loss | 2.30 | 3.70 | 3.09 |
| for Minimum Voltage | 0.15 | 0.17 | 0.10 |
| for Maximum Voltage | 0.01 | 0.04 | 0.05 |

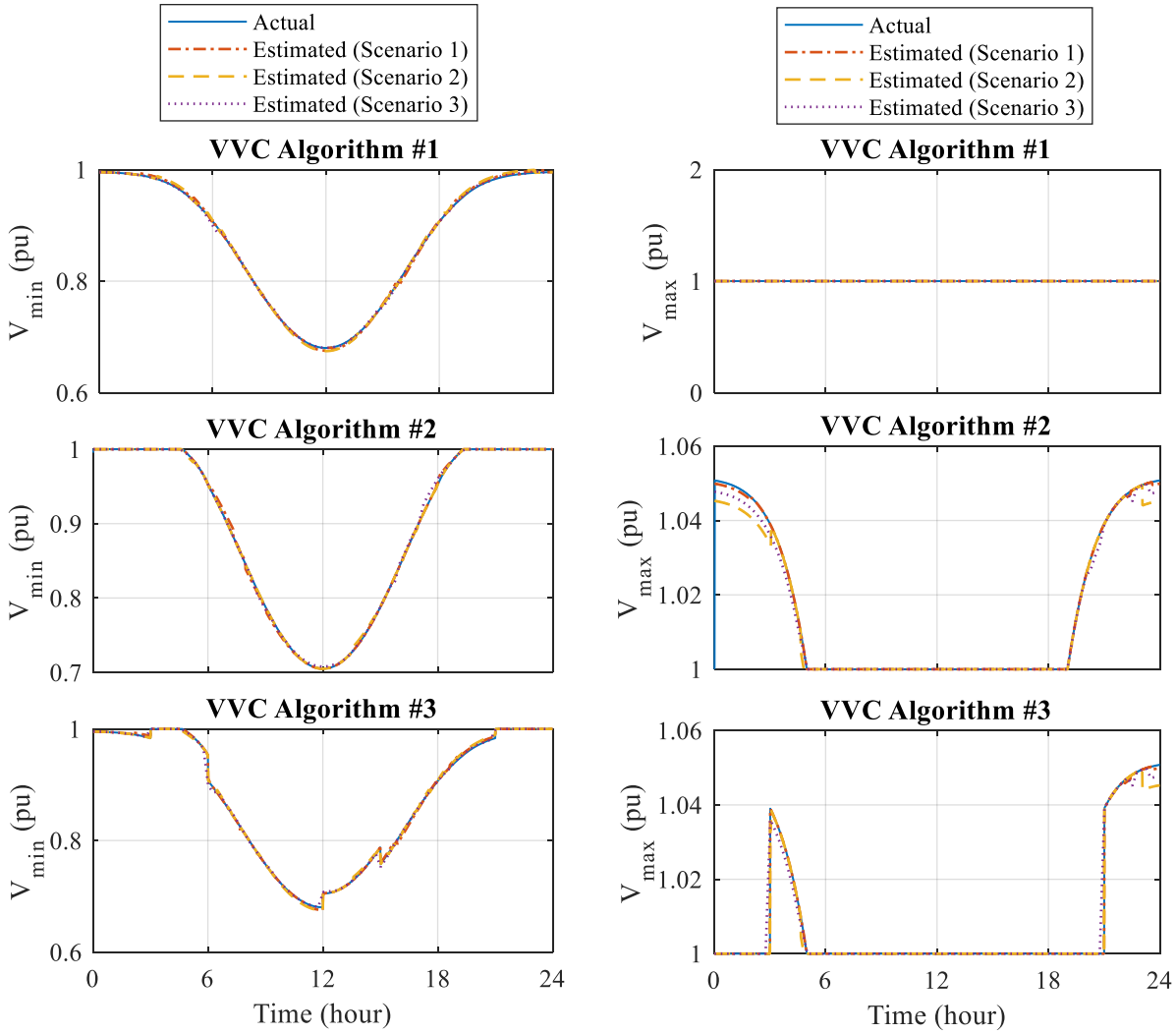


(a)Minimum Voltage of the System (b) Maximum Voltage of the System

Figure 3.14 Data-driven assessment results for the Elementary System

### 3.5.3 Sample Data Illustration

For illustration purpose, one example of the data collected for estimations is presented in this section. Figure 3.15 shows the sample data for a test on Elementary system with 65 capacitor switching events. The

example data is shown as organized for estimations of $H_P^{C:ON}$ and $H_P^{C:OFF}$ based on the first two principle components ($u_1$ and $u_2$ in the figure).

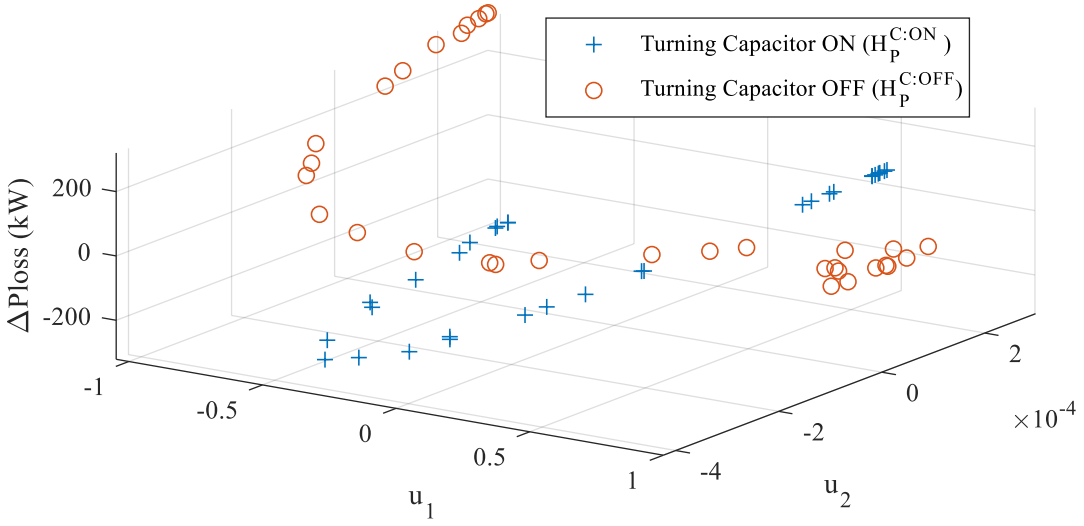


Figure 3.15 Data sample points from a test on Elementary System (X and Y axis represents the first two principal components)

### 3.5.4 Sensitivity Studies

The test was repeated with different number of capacitor switching events. Figure 3.16 shows how the average estimation error changes by switching the capacitor more frequently. There are fluctuations in the results, because in each case the switching times are chosen randomly. Therefore, more number of switching times does not necessarily guarantee more accurate results. However, as intuitively expected, the error generally reduces with switching the capacitor more often during the test because of providing larger data sample sets for the estimations. There seems to be a saturation effect too; the estimation error is not significantly lowered if the capacitor is switched more than 40 times during the one-day test on the Elementary system.

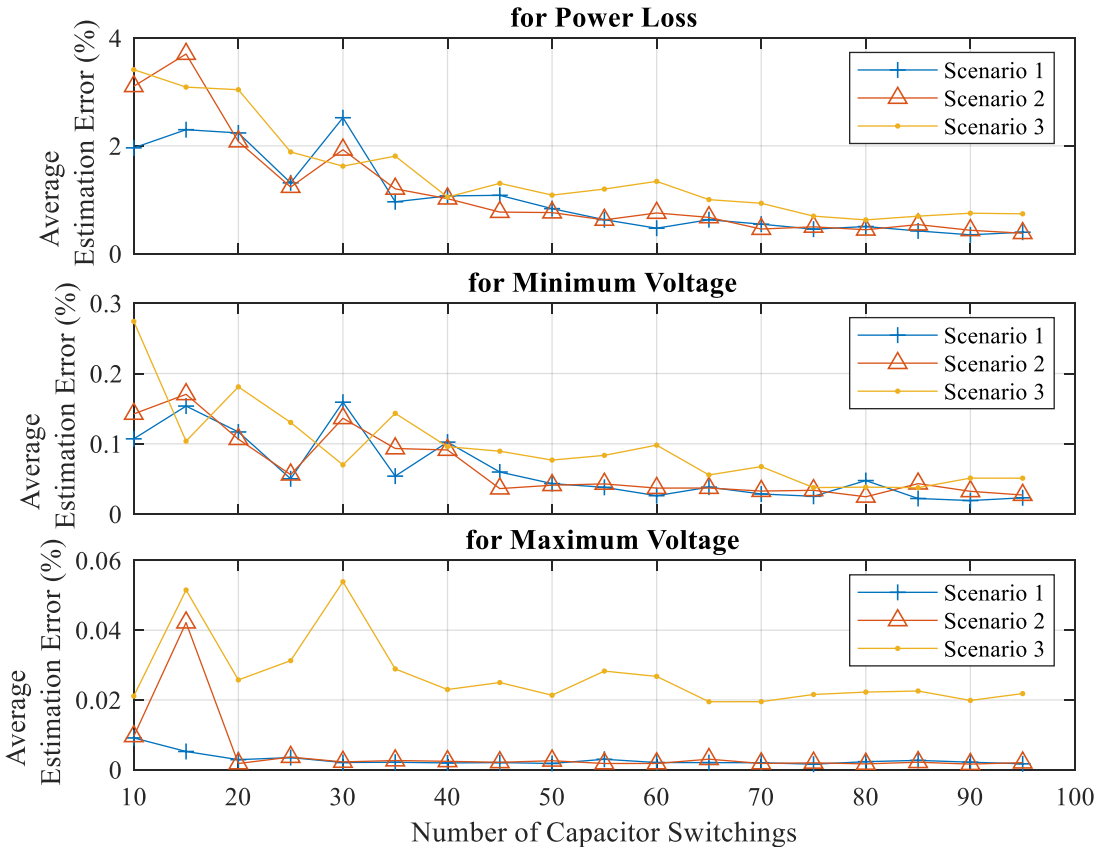


Figure 3.16 Average Estimation Error for different number of capacitor switching events

## 3.6 Simulation Studies on IEEE 123 Nodes Test Feeder

Figure 3.17 shows the schematic of IEEE 123 Nodes Test system (full details such as load info and network model are given in [29]). There are several unbalanced loads and powerlines with different number of phases in the IEEE 123 Node system, hence, it can present a serious test to feasibility of the proposed method. For this study, 70% of the loads were assumed to be residential. The bottom-up modeling technique, described in [30], was employed to derive sample daily profiles for the residential loads. Figure 3.18 shows average of the profiles assigned to residential loads. For the rest 30% of the loads, constant daily profiles were assumed. The load profiles are for a 10 day period with the 6th and 7th days assumed as weekend. Fifteen DER units were also added to this system as listed in Table 3-B. DERs were assumed to be of solar photovoltaic nature with the generation profile as shown on Figure 3.18. All DERs units were considered to operate with a constant power factor of one (*PF=1*). Simulations were performed for both cases of including and excluding these DER units on the system.

Two switchable capacitors were placed inside the test system as shown on Figure 3.17 ($Q_{C,1}$= *1200 kvar*, $Q_{C,2}$= *600 kvar*). The assessed VVC algorithms control these two capacitors. Each bus with one load or a

DER or both was assigned with one smart meter that reads and sends its voltage magnitude and power usage.

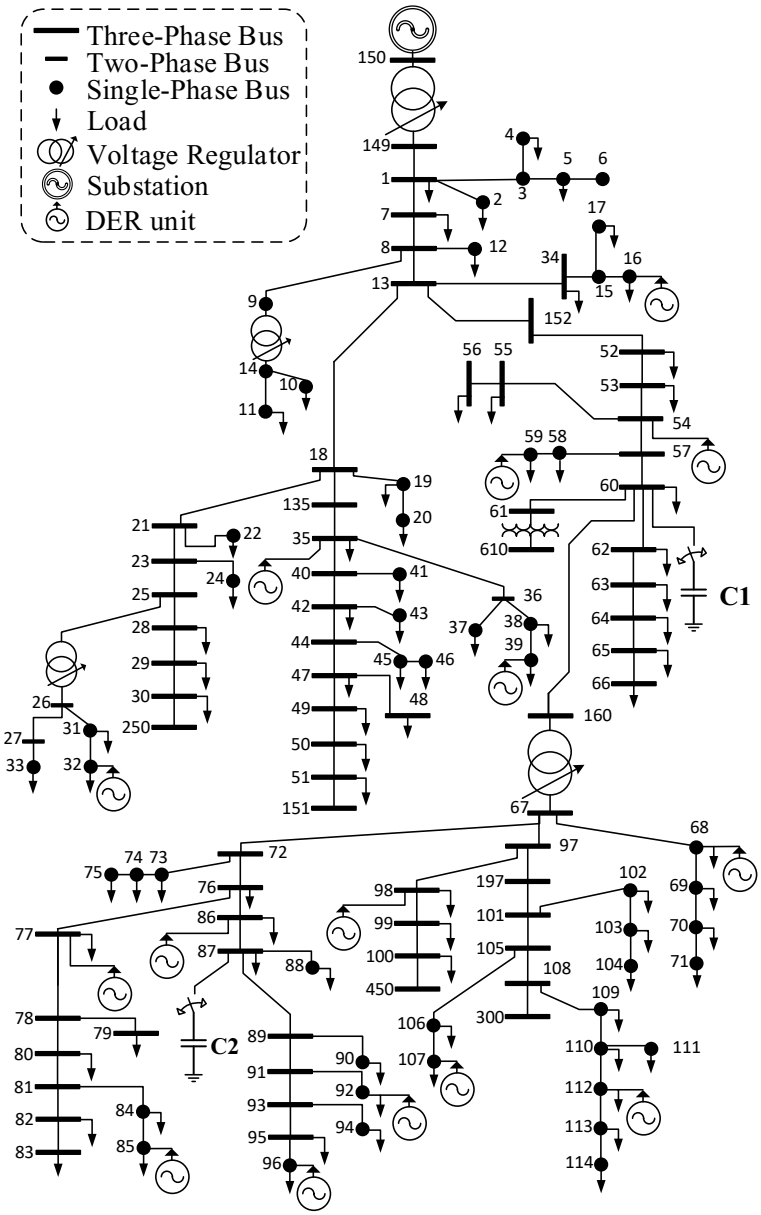


Figure 3.17 Schematic of IEEE 123 Nodes Test System

Table 3-B List of added DER units to IEEE 123 Node Test System

| Phases | Size | Nodes |
|---|---|---|
| 3-phase | 300 kW | 35, 54, 77, 86, 98 |
| 1-phase | 120 kW | 39, 59, 85, 96, 112 |
| 1-phase | 80 kW | 16, 32, 68, 92, 107 |

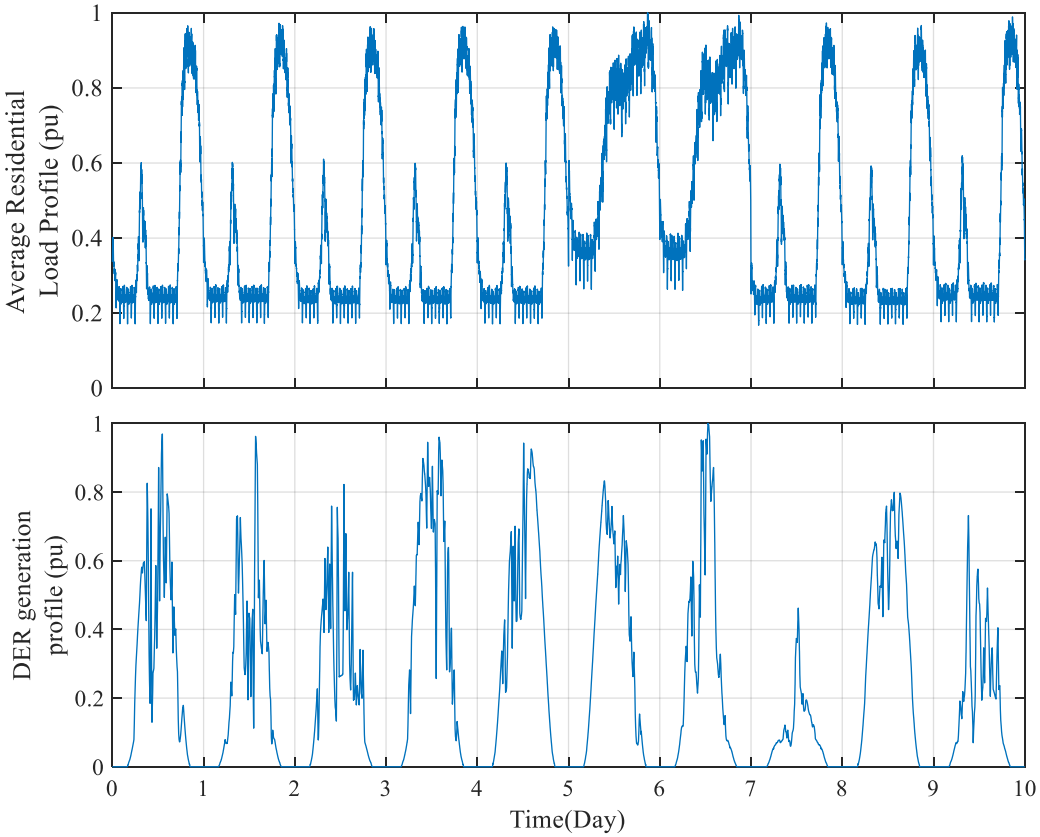


Figure 3.18 Average Profile of residential loads and Generation profile of DER units adopted for simulation studies on IEEE 123 Nodes System

### 3.6.1 Base Test Description

The base test was performed for a one-week (7 days) period with each capacitor randomly switched 10 times per day. As explained early in section 3.3.2, simultaneous switching of capacitors were avoided to provide better sample data sets for the estimations. Two base tests were performed; in one the DERs were assumed OFF the system, while they were included in the circuit for the other test. Since the proposed assessment method is only applicable to capacitor-based VVCs, tap position of all VRs were kept at the neutral mode (i.e. a constant tap ratio of one for every VRs) during the test. Figure 3.19 and Figure 3.20 show the raw data obtained from this test under metering *Scenario 3.2* for the cases of without DER and with DERs, respectively.

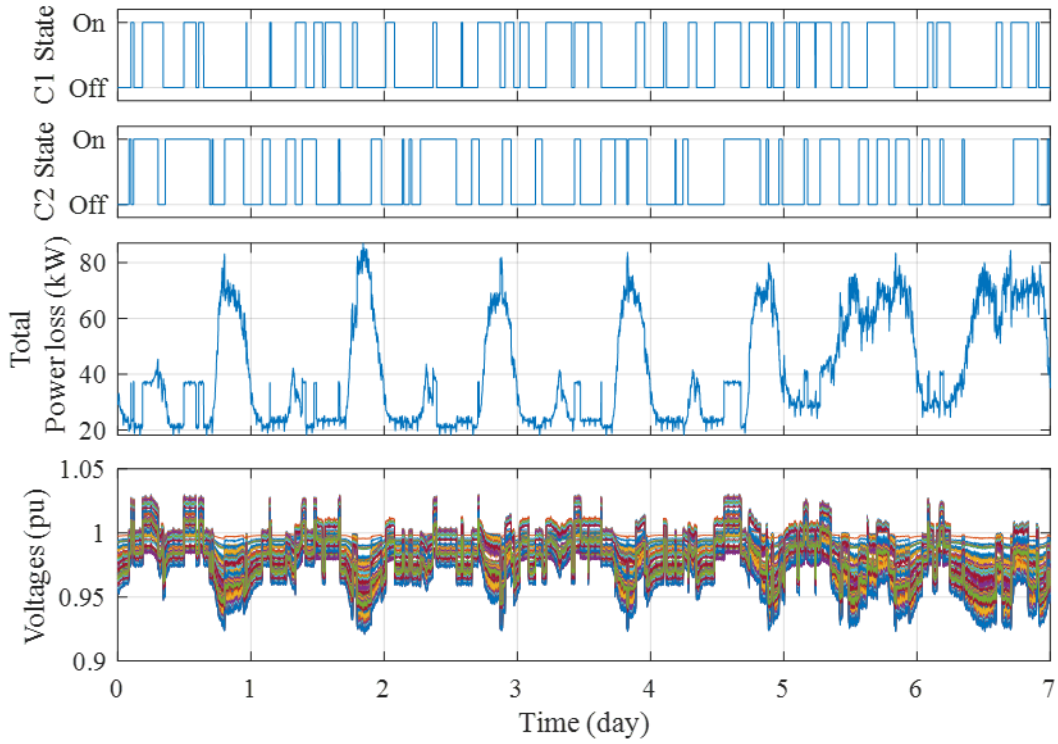


Figure 3.19 Raw measurement data from base test on IEEE 123 Node System: without DERs (Metering *Scenario 3.2*)

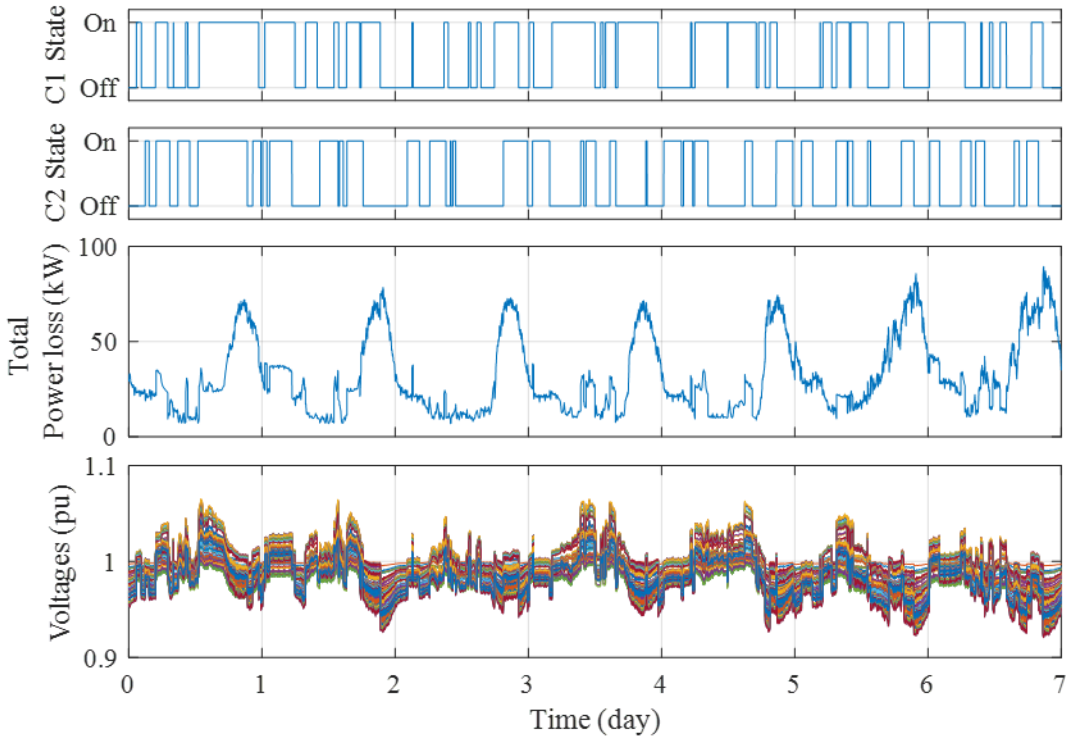


Figure 3.20 Raw measurement data from base test on IEEE 123 Node System: with DERs (Metering *Scenario 3.2*)

Using the data from the tests and proposed method, performance of the system under four different open-loop VVCs were assessed. Figure 3.21 shows the capacitor commands from these assumed VVC algorithms. The number of principal components kept for estimations was four (i.e. $p=4$ in PCA process described in chapter 2).

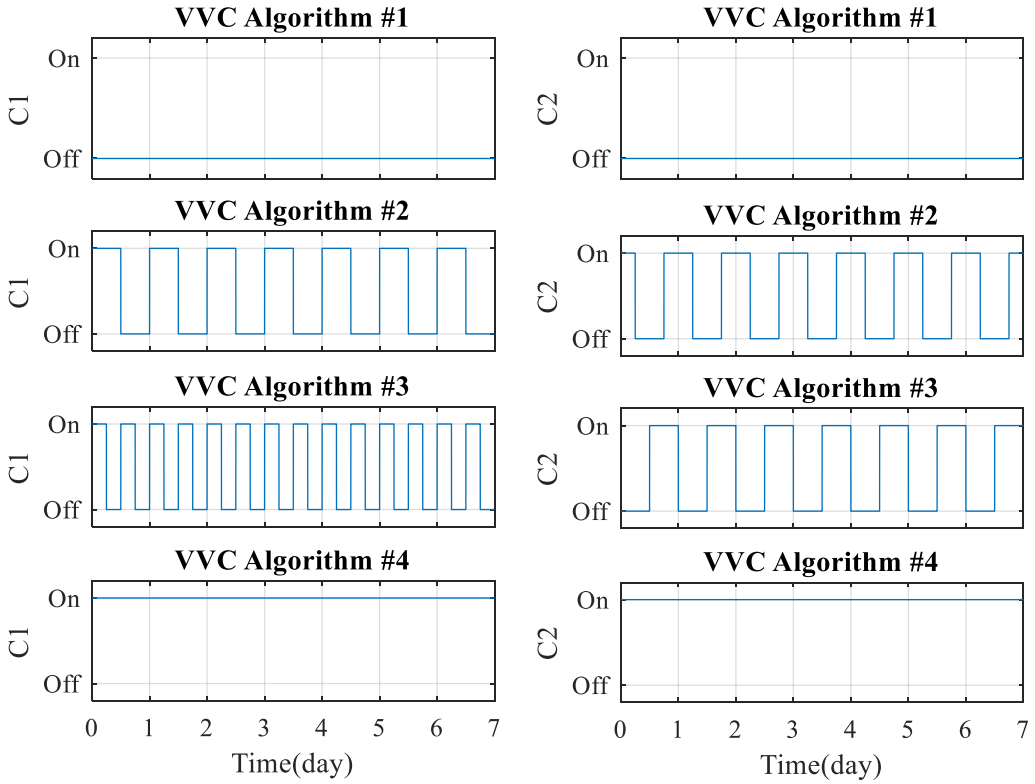


Figure 3.21 Capacitor switching commands of the tested VVC algorithms for IEEE 123 Nodes Test Feeder

### 3.6.2 Base Results

The VVC assessment results are shown and compared with the actual values on Figure 3.22. The results demonstrate efficacy and accuracy of the proposed method. Table 3-C also presents the average estimation errors for different indices and metering scenarios. Overall, the results are found more accurate when DERs are not present. This observation was intuitively expected, since DERs can complicate power flows and performance in the system. However, the results are still quite acceptable when DERs are present. In general, the estimation error is higher for power loss estimation compared to the two voltage indices. It is also understandable since power loss has a more complicated relationship with system voltages which makes it more difficult to accurately estimate. In other words, $H_p$ functions defined in Chapter 2 are more complicated than $H_V$ functions. The highest accuracy is obtained when the voltage phasors are available

(i.e. *Scenario 3.1*), however, the method has remained efficient even when voltage phasor angles are not available (i.e. *Scenario 3.2* and *Scenario 3.3*). Interestingly, the results for *Scenario 3.2* and *Scenario 3.3* are quite close to each other which means the 15 minute time resolution has not impacted the estimation outcome significantly.

Table 3-C Average Estimation Errors for VVC assessment on IEEE 123 Nodes System

| Average Estimation Error (%) | | Metering Scenario | | |
|---|---|---|---|---|
| | | *3.1:* With phasor and 1 minute resolution | *3.2:* Without phasor and 1 minute resolution | *3.3:* Without phasor and 15 minute resolution |
| Without DERs | for Power Loss | 2.16 | 2.21 | 4.15 |
| | for Minimum Voltage | 0.03 | 0.02 | 0.09 |
| | for Maximum Voltage | 0.01 | 0.01 | 0.04 |
| With DERs | for Power Loss | 5.19 | 7.89 | 9.20 |
| | for Minimum Voltage | 0.03 | 0.02 | 0.12 |
| | for Maximum Voltage | 0.02 | 0.02 | 0.07 |

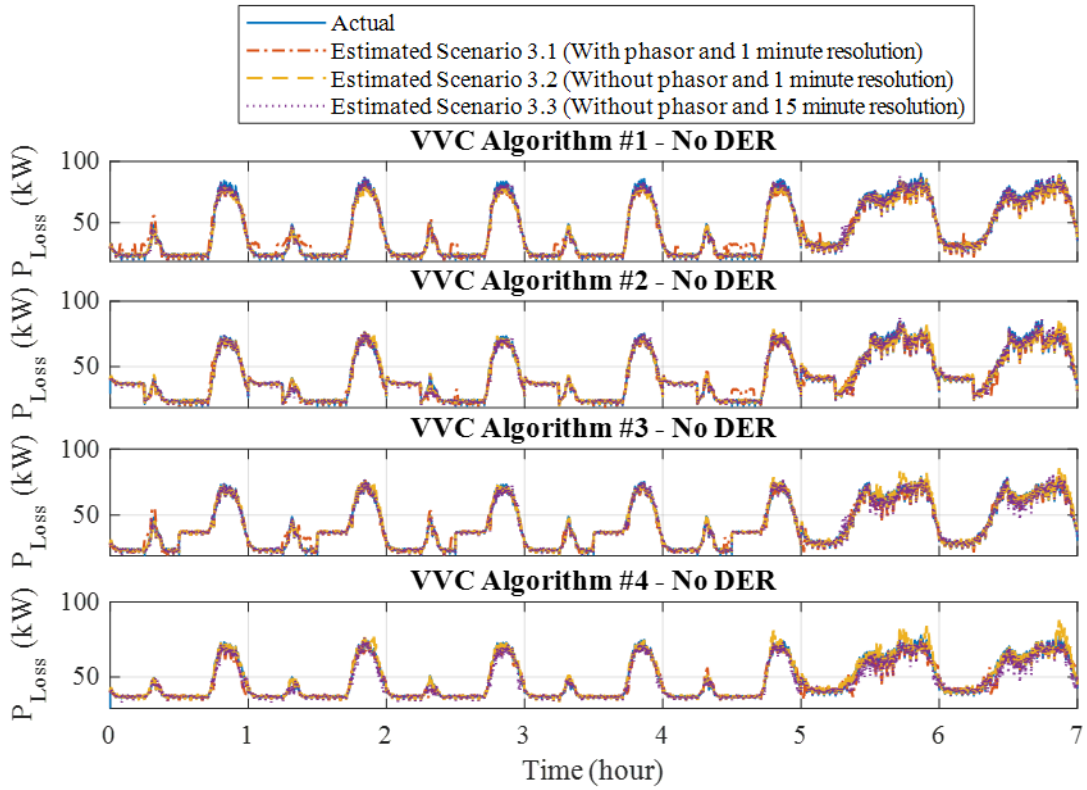


(a) Total power loss – without DERs

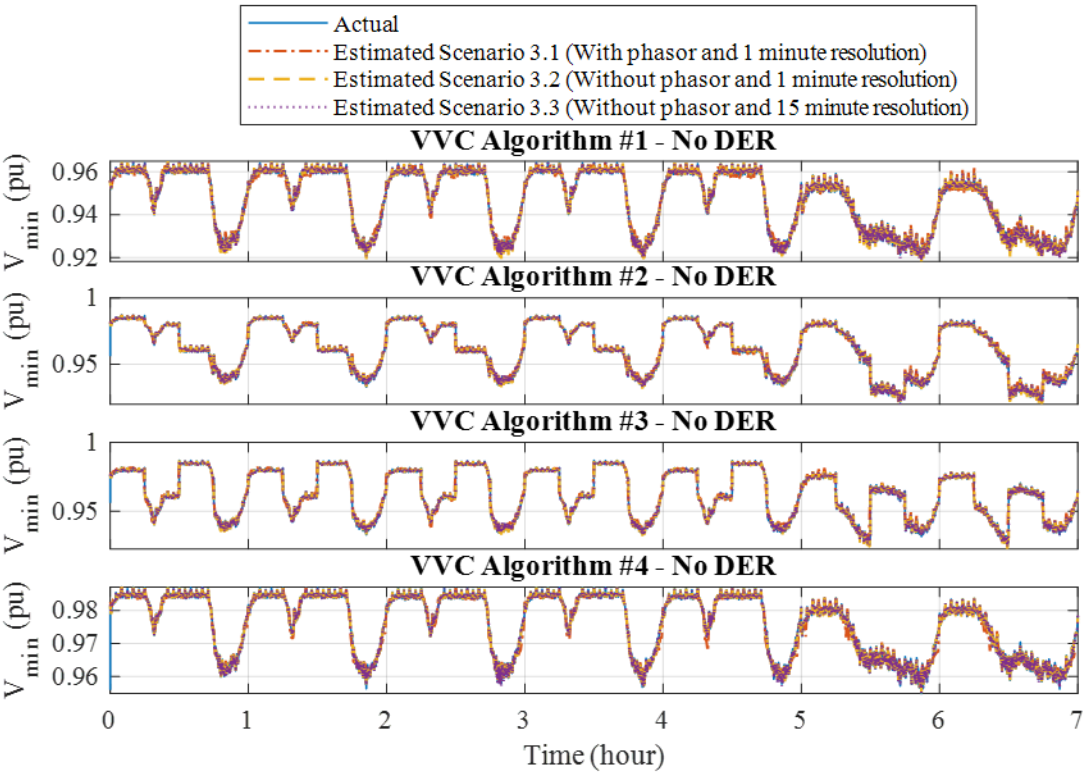


(b) System's minimum voltage – without DERs

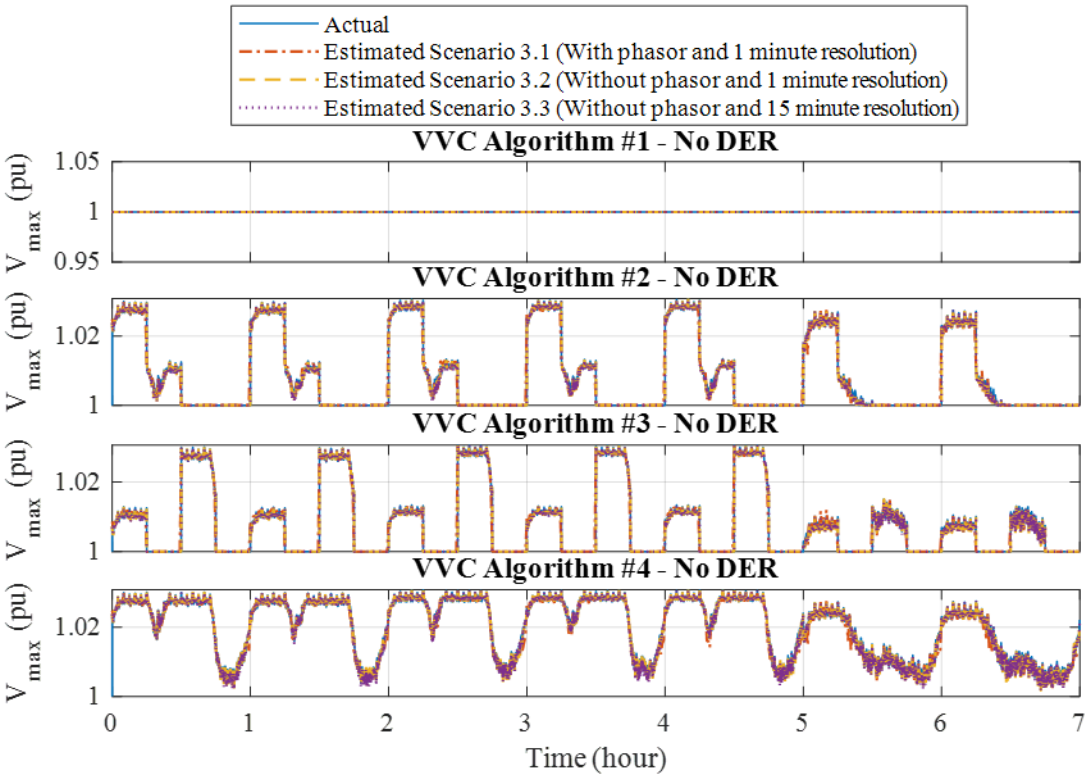


(c) System's maximum voltage – without DERs

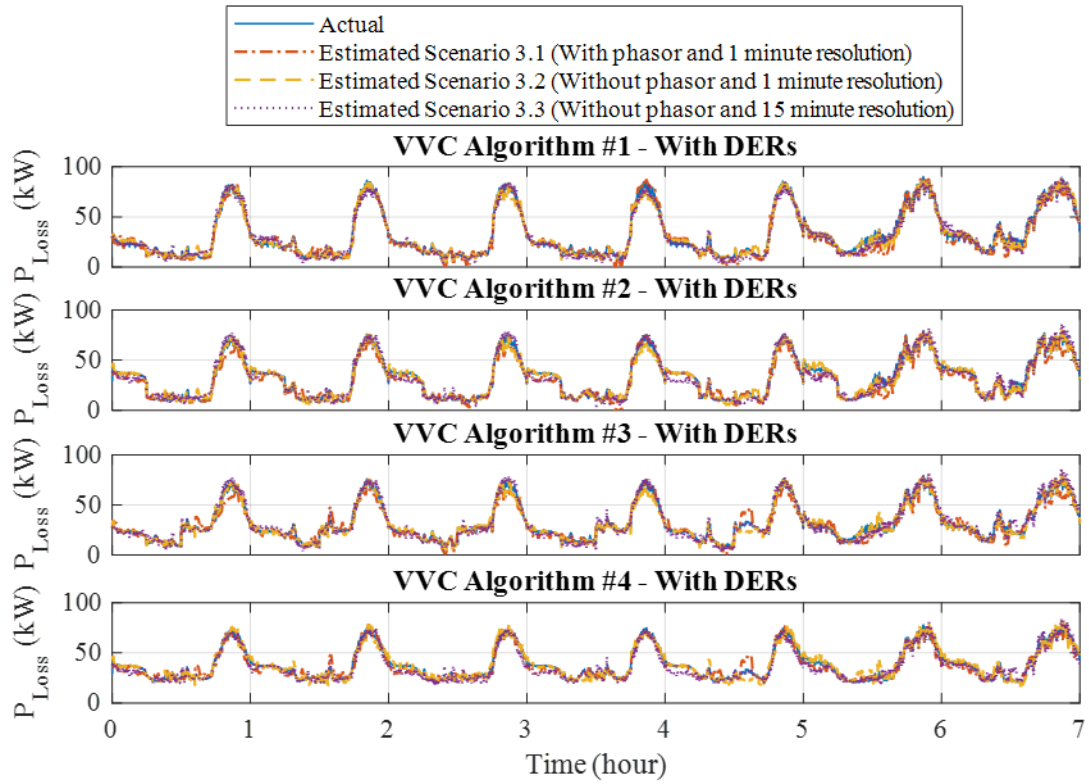


(d) Total power loss – without DERs

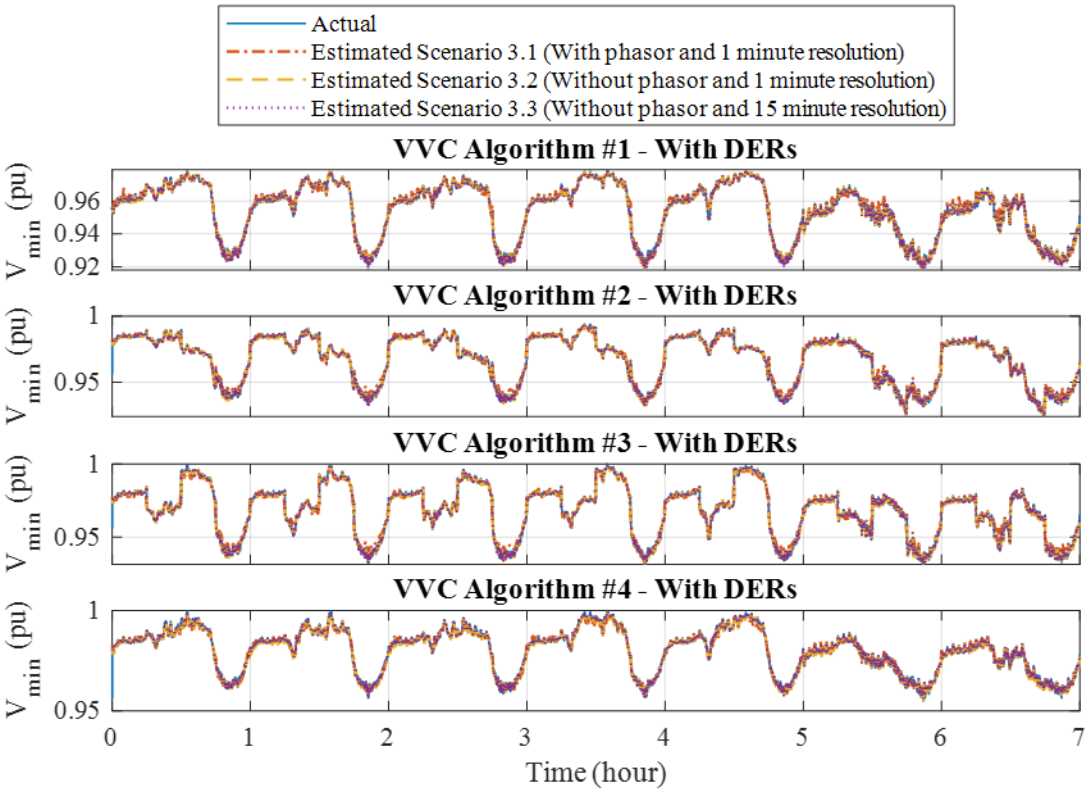


(e) System's minimum voltage – with DERs

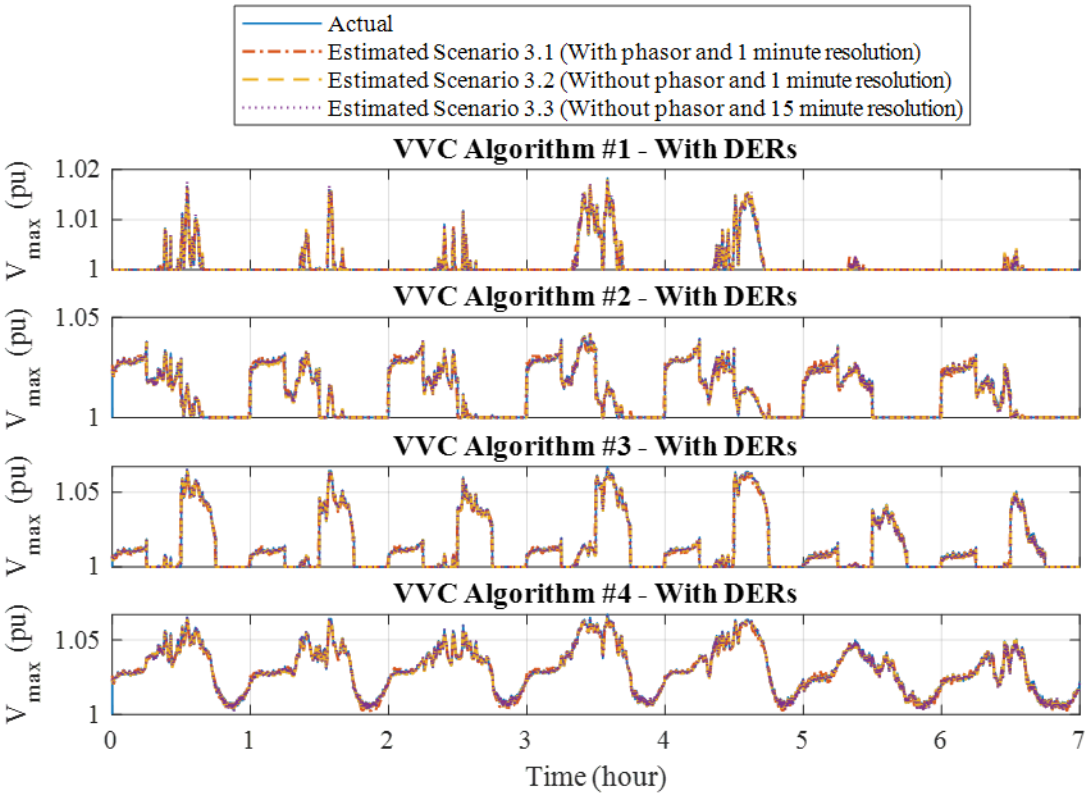


(f) System's maximum voltage – with DERs

Figure 3.22 Data-driven VVC assessment results for the base tests on IEEE 123 Nodes System

### 3.6.3 Sensitivity Studies

#### a. Number of Capacitor Switching Events

The base tests were repeated with different number of capacitor switching events per day. Figure 3.23 shows the resulted estimation error for this sensitivity study. For all three indices and metering scenarios, increasing the number of capacitor switching beyond 20 times per day hasn't shown a significant effect on the accuracy of results. For less than 20 switching events per day, the estimation error generally tend to decrease by increasing number of switching times. Among the three indices, accuracy of power loss estimation is found the most sensitive one to the number of switching events. For estimation of minimum/maximum system voltage, even 5 times switching per day has given very satisfactory accuracy for all the studied cases (estimation error is less than 0.1%).

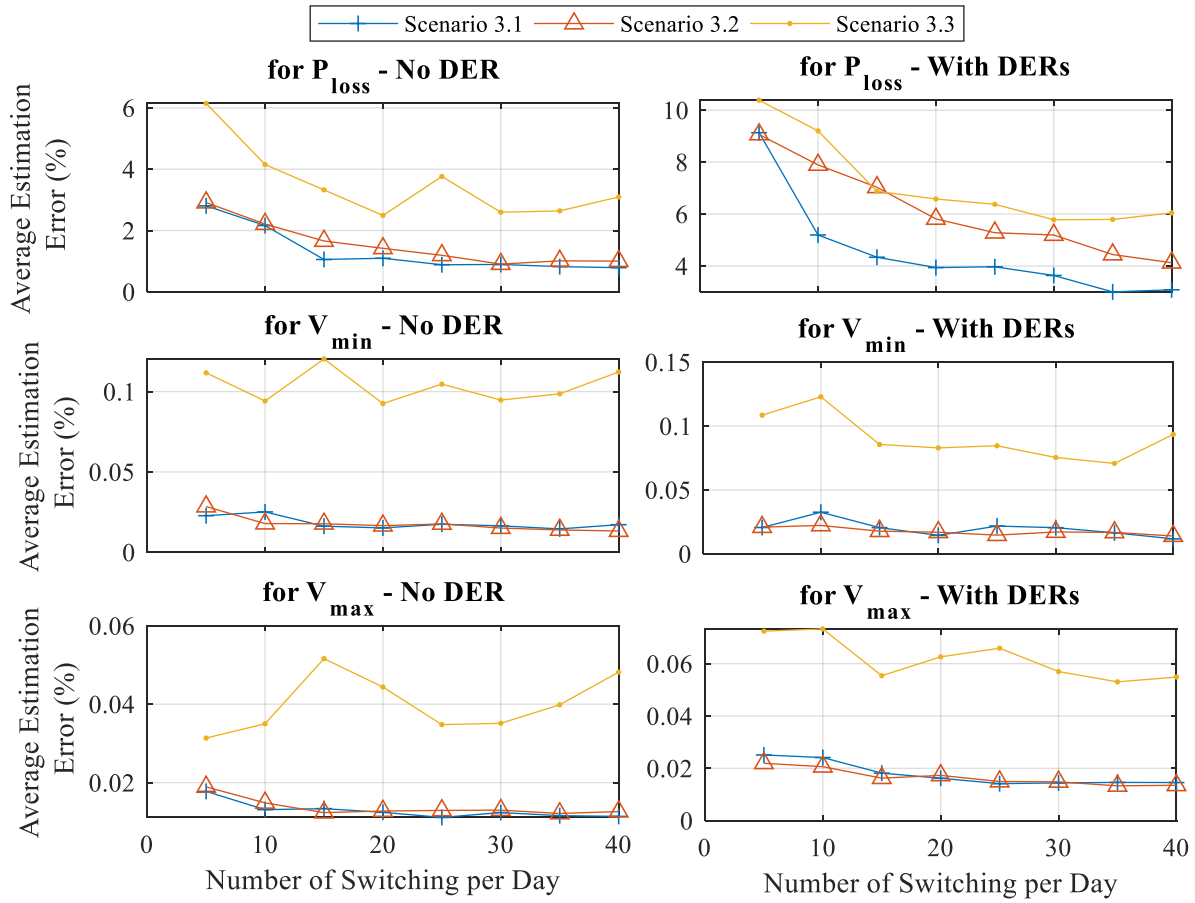


Figure 3.23 Estimation Error for different number of capacitor switching events[32]

[32] The number of switching events is stated as per day per each capacitor

### b. Measurement Error

In this sensitivity study, intentional error with a Gaussian distribution is added to measurement of each meter. Different percentage of noises from 0.01% up to 10% was considered. The case without DERs and metering *Scenario 3.2* was chosen as the basis for this study. Figure 3.24 summarizes the accuracy of results for the three indices of interest. As expected, the average estimation error increases with higher levels of measurement noise. Overall, the method is found completely robust against measurement noises up to 1%.

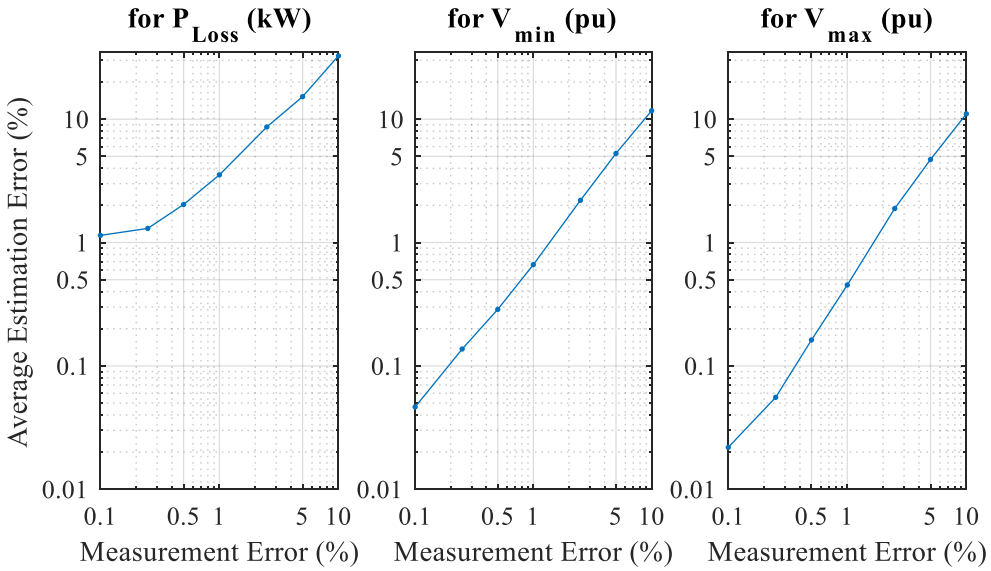


Figure 3.24 Average Estimation Error resulting from different level of measurement noise

### c. Number of Principal Components

For the base results, four of the principal components were used in estimations (i.e. $p=4$ in PCA process described in chapter 2). A sensitivity study was also conducted to investigate the impact of this parameter in the estimation accuracy. Two sets of raw measurement data associated with *Scenario 3.1* and *Scenario 3.2* from the base case without DER (see section 3.6.1) were chosen as the basis for this study. The statistical estimation process on this raw data was repeated with different number of principal components (i.e. changing $p$ in PCA). Figure 3.25 summarizes the results by plotting the average estimation error resulting from different cases. The results show that keeping only 3 or 4 of the principal components are sufficient for the estimations on this system. Indeed, the estimation accuracy is not observed to improve by $p$ if $p$ is already higher than 3.

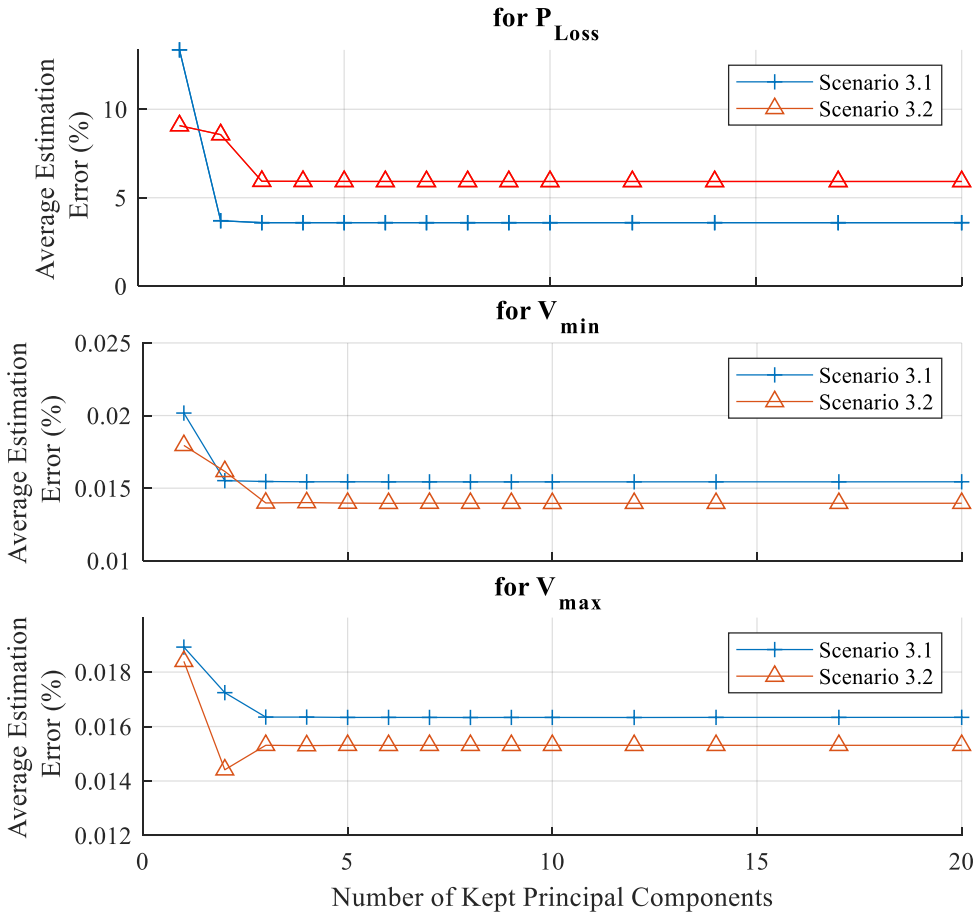


Figure 3.25 Average estimation error resulting from different number of principal components used for estimations

### d. Substation Impedance and Variant Load Nature

The proposed statistical framework was built on the assumption that feeder voltage at substation is constant and that voltage-dependency characteristic of loads don't change by time (see *Assumption 2.4* and *Assumption 2.7* in chapter 2). As already mentioned in chapter 2, these type of assumptions might be violated in actual systems, however, it does not necessarily undermine the efficiency of estimations. In this sensitivity study, we investigate this possible effect on the IEEE 123 Nodes system. In one sensitivity case, an impedance is included in substation source of the feeder which makes the source voltage variant by time. In other case, the voltage-dependency of loads is changed during simulation time:

**Base Case:** normal system as defined for base tests in section 3.6.1 with considering DERs under metering *Scenario 3.2*

**Case X:** similar to Base case, but load models (which describe voltage dependency of load powers on voltages) are considered to randomly vary with the time. More details are given in Appendix B.

**Case Y:** similar to Base case, but a source impedance of $0.1+0.1j$ Ω is added to model of the system used for simulations.

Table 3-D Average Estimation Errors for Different Cases

| No. of capacitor switching per day | For $P_{loss}$ Estimation | | | For $V_{min}$ Estimation | | | For $V_{max}$ Estimation | | |
|---|---|---|---|---|---|---|---|---|---|
| | Base Case | Case X | Case Y | Base Case | Case X | Case Y | Base Case | Case X | Case Y |
| 5 | 9.07 | 10.39 | 11.49 | 0.02 | 0.03 | 0.45 | 0.02 | 0.02 | 0.51 |
| 10 | 7.89 | 7.01 | 10.17 | 0.02 | 0.03 | 0.46 | 0.02 | 0.02 | 0.49 |
| 15 | 7.03 | 6.85 | 9.27 | 0.02 | 0.03 | 0.47 | 0.02 | 0.02 | 0.51 |
| 20 | 5.81 | 5.91 | 8.83 | 0.02 | 0.03 | 0.47 | 0.02 | 0.02 | 0.49 |
| 25 | 5.28 | 5.43 | 7.89 | 0.01 | 0.02 | 0.44 | 0.01 | 0.02 | 0.47 |
| 30 | 5.19 | 4.48 | 7.31 | 0.02 | 0.02 | 0.47 | 0.01 | 0.02 | 0.49 |
| 35 | 4.44 | 4.55 | 7.36 | 0.02 | 0.02 | 0.46 | 0.01 | 0.02 | 0.48 |
| 40 | 4.13 | 4.32 | 6.88 | 0.01 | 0.02 | 0.47 | 0.01 | 0.02 | 0.49 |

The estimation errors for Case X are quite close to those of the Base Case. Therefore, the varying load characteristics do not seem to be problematic for proposed methods. However, the errors for Case Y are mostly higher than the Base Case. The results show that the most negative impact of this case is on estimation of voltage indices. It is understandable since inclusion of substation impedance influence the feeder voltage significantly. Nonetheless, the voltage indices are still estimated with an acceptable error of less than 1%. The errors of Case Y in $P_{loss}$ estimation are also not that much higher than Base case to disprove the efficacy of the method under variant substation voltage.

## 3.7 Summary

A new technique has been presented to assess benefits of open-loop VVC schemes in distribution systems using AMI data analytics. The results are not affected by the uncertainties associated with system models. The accuracy of assessment results were demonstrated by simulation studies on one elementary system as well as IEEE 123 Test Feeder. The simulation results also revealed the following facts regarding the model-free VVC assessment scheme:

- The most accurate results are obtained if smart meters were equipped with synchro-phasor capability to record voltage phasor angles as well. However, the obtained results are still acceptable if phasor angles are not available.

- The lower the time resolution of the data, the more accurate the results are found to be. However, the proposed methods still delivered acceptable assessments for a time resolution up to 15 minutes which is consistent with the AMI technologies installed in existing distribution feeders.
- Estimation of voltage indices are generally more accurate than the ones related to system losses.
- Presence of DERs can reduce the accuracy of estimation results, however, the method could still give satisfactory results even in presence of DERs.
- Increasing number of capacitor switching events or increasing the number of principal components improve the accuracy of assessment result to a limited extent. For example, in simulations of IEEE 123 Nodes system, switching the capacitor more often than 20 times per day, or keeping more than 3 principal components didn't show a significant rise in accuracy of the VVC assessment results.
- The method results remained robust with up to 1% measurement errors.

# Chapter 4

# Model-free Volt-Var Control (VVC)

This chapter presents a new data-driven model-free VVC scheme for operation of radial power distribution systems [31]. Unlike the existing methods available to utilities, the proposed VVC is neither reliant on model-based computer simulations nor limited to intuition/experience-driven rules for operation of switchable capacitors and VR inside a feeder. Despite the model-free feature, the proposed scheme can still give optimal performances by using statistical estimations on the AMI system. Effectiveness and feasibility of this scheme will be evaluated by simulation studies on an Elementary system and IEEE 123 Nodes Test feeder.

## 4.1 Literature Review

Optimization-based techniques constitute a common class of VVC schemes. In these methods, computer simulations based on the network models are usually employed to determine optimum status for different system equipment such as VRs or capacitors. Various optimization algorithms have been introduced in literature ranging from agent-based strategies to evolutionary methods or mixed-integer programming [32]-[34]. Research works such as [35]-[36] have also proposed to employ metering data in conjunction with model information to improve optimization accuracy. In this so-called Hybrid approach, metering data is used as a supplement to improve accuracy of load profiles in the simulations.

As already discussed in chapter 1, albeit their high performance, heavy reliance of optimization methods on circuit models can be a serious obstacle to their actual implementation. In distribution systems, especially, establishing complete and accurate set of models is too difficult. Therefore, model-free VVC approach is by no surprise a common choice in today industry practice. In this category, simplified rules are usually assigned for controlling VVC equipment such as VR or capacitor. For example, the capacitors are preset to switch based on the day time or environment temperature. Alternative type of rules are based on local measurement such as using a local voltage threshold to control a capacitor or VR [38]-[39]. In papers such as [40], the rules are improved to benefit from extra points of measurement on the feeder such as end-of-the-line or few customers. In a more advanced form, the rules might be also dynamically updated based on operation records and experiences [40]-[41]. Rule-based methods can be generally reliable and easy to implement. However, lacking a rigorous technical basis, they cannot guarantee an optimal performance, especially, when loss reduction is a concern. In addition, widespread growth of DER across modern grids

has further jeopardized the effectiveness of traditional VVC rules. Several studies have demonstrated the vulnerability of conventional rule-based VVC schemes in presence of DER [42]-[44].

The above literature review suggests the need for an advanced VVC methods which are theoretically rigorous and yet capable to operate independent of system models. This chapter's goal is to present such scheme.

## 4.2 Proposed Data-driven VVC Scheme

The overall structure of proposed model-free VVC scheme is shown on Figure 4.1. As shown on the figure, the metering part of this scheme is quite similar to that of the VVC assessment method introduced in chapter 3. As elaborated in chapter 3, such metering scheme provides real-time[33] values of total power loss and approximate voltage vector of the system. This data constitutes the essential input for operation of model-free VVC.

In the proposed scheme, the control of capacitors and VRs are implemented in separate modules (see Figure 4.1). The capacitor controller employs the estimations based on measurement data to decide for optimal switching commands. Since the impact of VR control on power loss is generally much less in comparison to the impact of capacitors ([39]-[40]), the VR controller is only tasked to improve the feeder's voltage profile and ensure the compliance with regulatory voltage limits. The working principle of Capacitor and VR controllers is described in the following sections.

[33] As aforementioned in section 2.8 of second chapter, even if the data is not available in a perfect real-time manner, the proposed statistical methods can be expected to perform well.

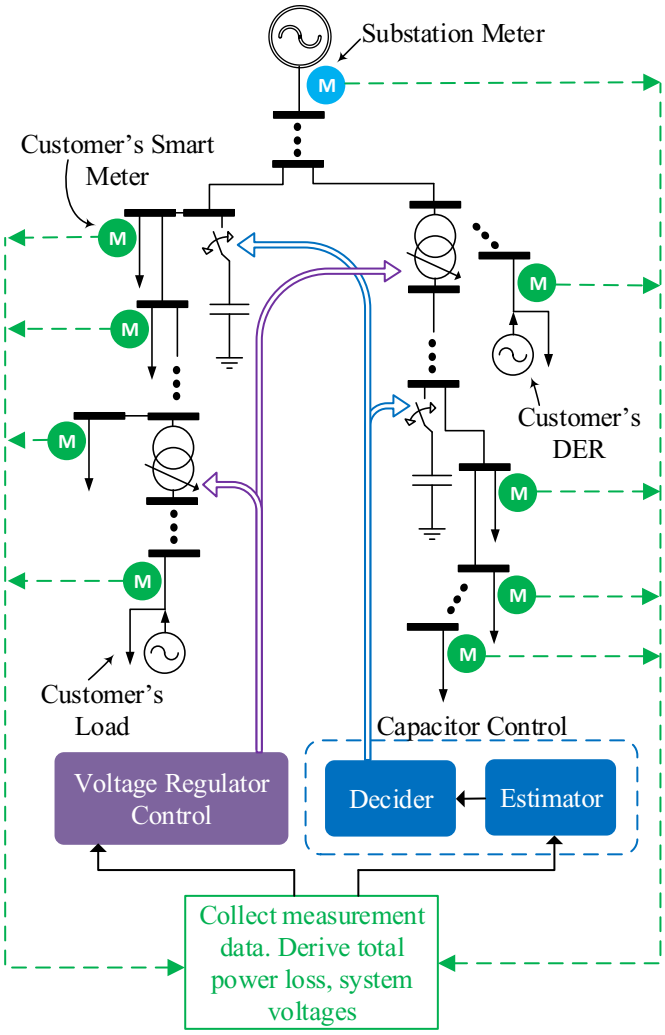


Figure 4.1 Overall structure of proposed model-free VVC scheme

## 4.3 Capacitor Control

As shown on Figure 4.1, the capacitor control module consists of an Estimator and a Decider unit. The Estimator unit statistically processes the recorded data to predict how different capacitor switching events affect different VVC indices of interest. These estimations are then sent to the Decider unit to determine the optimal switching commands.

### 4.3.1 Estimation Procedure

Supposing that at operation time of $t_T$, the measurement data has been collected for times $t=t_1, t_2,\dots, t_T$, the compiled measurement input for the estimations can be labelled as a set in a similar fashion to the previous chapter:

$$\left\{ \overrightarrow{C(t_i)}, P_{loss}(t_i), \overrightarrow{V'(t_i)} \right\},\ i = 1,2,...,T \tag{4.1}$$

The role of estimations is to predict the three indices of interest for time $t_{T+1}$ for different capacitor states. The proposed statistical framework in chapter 2 is applied here. Before introducing the functions for estimation, we need to define an index which assigns a number to each possible state of system switchable capacitors[34]. This index is referred as *CSI* (Capacitor(s) State Identifier) in this thesis:

$$CSI = 1 + \sum_{i=1}^{N_C} C_i 2^{i-1} \tag{4.2}$$

We categorize the functions $H_P$ and $H_V$ developed in chapter 2 based on the above defined *CSI*:

$$\begin{aligned} &\Delta P_{loss} = H_P^{i,j}(\overrightarrow{V'}) \ \text{ where } i = CSI \text{ after switching},\ j = CSI \text{ before switching} \\ &\overrightarrow{\Delta V'} = H_V^{i,j}(\overrightarrow{V'}) \ \text{ where } i = CSI \text{ after switching},\ j = CSI \text{ before switching} \end{aligned} \tag{4.3}$$

The above approach of categorization of *H* functions is different from that of chapter 3 (see (3.7)). In fact, the categorization method introduced here leads to a larger group of functions that need to be estimated. Here, one has two groups of functions each with $2^{N_C}(2^{N_C}-1)$ members, while in chapter 2, $2N_C$ was the number of members in each group. This larger groups of functions lead to smaller sample sets for estimation of each function which intuitively suggests lower quality in the estimations, however, our simulation studies have shown that this approach will produce more effective VVC schemes[35]. Therefore, we replace the capacitor state vector *C* in the raw data set of (4.1) with *CSI* as below:

$$\left\{ CSI(t_i), P_{loss}(t_i), \overrightarrow{V'(t_i)} \right\},\ i = 1,2,...,T \tag{4.4}$$

This data can be organized into sample sets for the *H* functions that need to be estimated:

$$\begin{aligned} X\left[H_V^{i,j}\right] &= X\left[H_P^{i,j}\right] = \left\{ \overrightarrow{V'(t_n)} \,|\, n \in \{1,2,\cdots,T-1\} \wedge CSI(t_{n+1}) = i \wedge CSI(t_n) = j \right\} \\ Y\left[H_P^{i,j}\right] &= \left\{ P_{loss}(t_{n+1}) - P_{loss}(t_n) \,|\, n \in \{1,2,\cdots,T-1\} \wedge CSI(t_{n+1}) = i \wedge CSI(t_n) = j \right\} \\ Y\left[H_V^{i,j}\right] &= \left\{ \overrightarrow{V'(t_{n+1})} - \overrightarrow{V'(t_n)} \,|\, n \in \{1,2,\cdots,T-1\} \wedge CSI(t_{n+1}) = i \wedge CSI(t_n) = j \right\} \end{aligned} \tag{4.5}$$

With the above data samples, the regression technique method described in chapter 2 can be used to estimate indices of interest at different capacitor switching states for $t=t_{T+1}$. Setting modified voltage vector at $t=t_T$ as the input, one can estimate losses and modified voltage vector for time $t_{T+1}$ at any possible capacitor switching state:

[34] The definition of *CSI* is not applicable to multistep capacitor banks.

[35] For example, one drawback of applying chapter 3's approach for model-free VVC stems from the fact that it focuses on switching effect of each capacitor separately. Although such approach does not affect a VVC assessment method, it commonly makes a model-free VVC prone to miss some optimal commands which involve switching of the two capacitors simultaneously.

$$\begin{cases} \hat{P}_{loss}(t_{T+1})\Big|^{CS(t_{T+1})=i} = P_{loss}(t_T) + \hat{H}_P^{i,j}(\overrightarrow{V'}(t_T)) \\ \overrightarrow{\hat{V}'}(t_{T+1})\Big|^{CS(t_{T+1})=i} = \overrightarrow{V'}(t_T) + \hat{H}_V^{i,j}(\overrightarrow{V'}(t_T)) \\ \qquad i = 1 \rightarrow 2^{N_C}, j = CS(t_T) \end{cases} \tag{4.6}$$

As explained in chapter 2, the original voltage vector can be easily reconstructed from the estimation of modified voltage vector, and, feeder's maximum/minimum voltages are determined accordingly.

In this thesis, we assume that the distribution system does not change during VVC operation (except changes of loads and DER generations). If system characteristics are subject to changes such as feeder reconfiguration, a weighting factor can be introduced in the proposed statistical framework in order to prioritize the effect of most recent collected data for the estimations.

### 4.3.2 Control Flowchart

Figure 4.2 shows the overall flowchart for the capacitor controller. Using the procedure described in the previous section, the Estimator unit conducts the essential estimations for the VVC indices of interest. It also assesses the estimation error using the method given in section 2.6. The period in which the estimation error has not reached a stable state means that more sample data needs to be collected, so that an Explore command is sent to Decider unit which is responsible to select the proper switching command. When Explore command is given (i.e. during a period referred to as Exploration period), Decider unit switches all the capacitors randomly between different capacitor states to ensure enough data samples are collected for every pair of before/after switching states. Once the estimation error becomes stable, there is no more Explore command and the decider unit chooses an optimum constrained *CSI* (i.e. the one with lowest feeder loss and maximum/minimum voltages within standard regulation range) based on the predictions from Estimator. The Decider unit also considers the operation limits such as maximum number of switching per day and the minimum time between subsequent switching events.

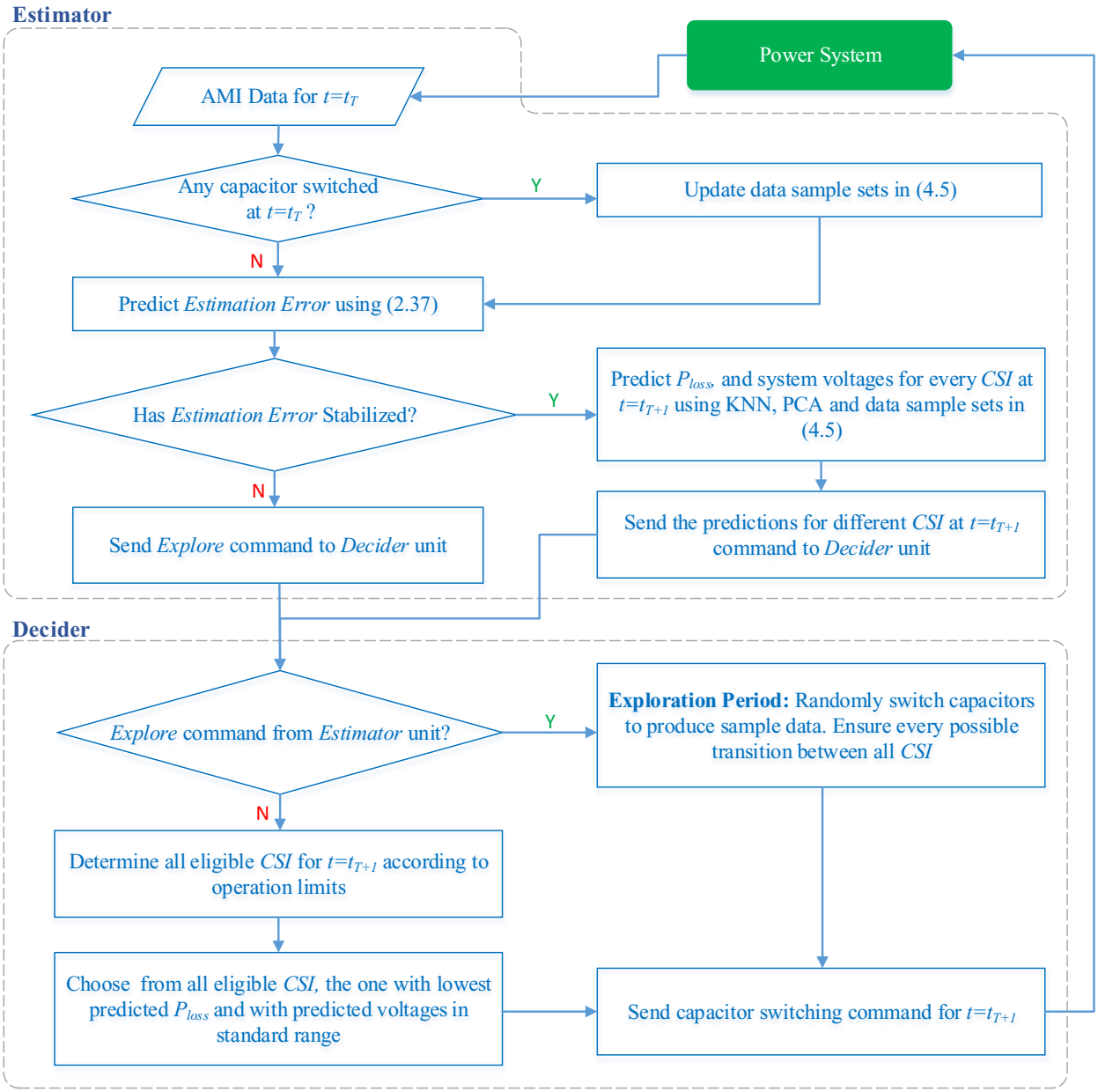


Figure 4.2 Capacitor control flowchart in proposed model-free VVC

## 4.4 Voltage Regulator Control

As explained early, the key objective of VR controller is feeder's voltage regulation. In a radial distribution feeder, voltages of downstream nodes to a VR change almost proportionally to the VR's tap ratio [38]. Therefore, model-free VR control is much more straightforward to implement and does not require any statistical process on the data. The system is divided into a number of voltage zones separated by VRs. The example shown on Figure 4.3 illustrates how the zones are defined. Each VR is controlled

according to the voltages in its downstream zones. The zone directly fed by a VR is referred as a primary one (e.g. *Zone a* is primary zone for VR1 and *Zone c* is primary zone for VR3 in Figure 4.3). The other downstream zones in neighbor to the primary zone are referred to as secondary ones (e.g. *Zone b* and *Zone c* are secondary zones for VR1 in Figure 4.3). Voltages recorded by smart meters inside each zone give an appropriate estimate of maximum and minimum feeder voltage associated with that respective zone. If voltages of one zone deviates the regulatory standard, the upstream VR tap position is increased or decreased accordingly after a time delay. The time delay for primary zone is apparently selected smaller than that of the secondary zones in order to avoid interference. By this scheme, each VR is mainly responsible for voltage regulation of its own primary zone, and as an additional support for the secondary zones.

Beside the main objective of keeping zone voltages within limit, the VR controller also aims for an auxiliary objective of centering the voltages in its primary zone. This objective aids the VVC to achieve an overall smoother feeder's voltage profile. If the controller finds that voltages within primary and secondary zones of one VR are within standard limit, while, the mean of primary zone's voltages has deviated from the reference value (i.e. 1pu), the VR tap is adjusted accordingly. A control bandwidth is also considered here to avoid excessive tap operations for the sole purpose of voltage centering.

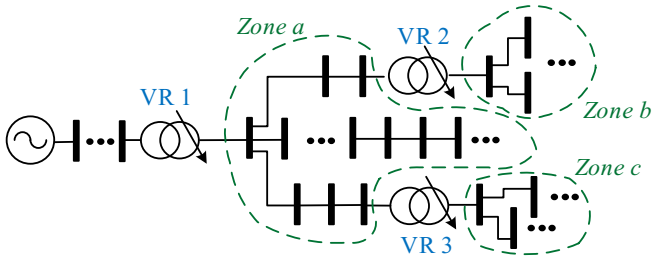


Figure 4.3 Example of a distribution feeder to illustrate VR zones

## 4.5 Simulation Study Setup

Simulation studies were performed to evaluate effectiveness and feasibility of the proposed model-free VVC scheme. Similar to chapter 3 studies, load flows were conducted by OpenDSS interface in Matlab. The statistical estimation process as well as the control algorithms were implemented by Matlab codes. Both of the Elementary and IEEE 123 Nodes Test systems introduced in chapter 3 were also used for the simulation studies of this Chapter.

Three indices were used to evaluate effectiveness of different simulated VVC cases:

- Daily average of feeder total power loss

- Mean of Voltage Deviation (MVD) to assess quality of overall feeder's voltage profile, as defined below:

$$MVD = \frac{1}{N}\sum_{i=1}^{N_{nodes}} \left| |V_i| - V_{ref} \right| \ , \ V_{ref} = 1pu \tag{4.7}$$

- Percentage of the time that voltage of every node is within standard regulation limits (i.e. $\forall i : |V_i| \geq \mathrm{V_{Min,Lim}} \wedge |V_i| \leq \mathrm{V_{Max,Lim}}$). In the studies of this thesis, minimum and maximum voltage limits are assumed to be 0.95 pu and 1.05 pu respectively ($V_{Min,Lim}=0.95pu$ , $V_{Max,Lim}=1.05pu$ ).

## 4.6 Simulation Studies on Elementary System

The Elementary System of Chapter 3 is modified for the studies in this chapter. As Figure 4.4 shows, two VRs are added to the system. Size of each load is also reduced to *250kW* with the same Power Factor of *0.75*. The size of capacitor is also decreased to *500kvar*[36]. Power-line specifications and daily load profile of the system remain quite similar to their definition in chapter 3 (see section 3.5).

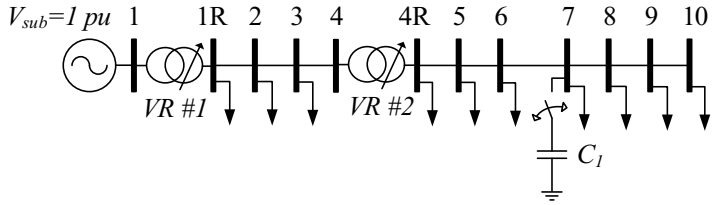


Figure 4.4 Schematic of Elementary system with voltage regulators

### 4.6.1 Base Test Description

The proposed model-free VVC scheme was simulated for a five day period with 15 capacitor switching per day for the Exploration period. The criteria chosen for stability of estimations was: for all capacitor switching combinations, the variation of predicted error of power loss estimation in last 12 hours becomes less than 20% of its initial estimated error value. Four principle components from PCA were also kept for estimations (i.e. $p=4$ in PCA process described in chapter 2). The time resolution of AMI data was assumed 1 minute, and the meters were assumed to provide voltage magnitudes only.

For the VR controller, time delay of 1 minute was assigned for primary zone of VR#1, and 2 minute was assigned for secondary zone of VR #1 and primary zone of VR #2. A *0.01pu* control bandwidth was also considered for voltage centering.

[36] The main reason for reducing size of the loads and capacitor in this chapter is to make it possible to regulate its voltages within the regulatory standard.

As a reference to evaluate performance of model-free VVC, a model-based optimization VVC was also simulated on this system. More details are given in Appendix C on the optimization method.

### 4.6.2 Base Results

Figure 4.5 shows the simulation results for the first three days. After the exploration period ends in the beginning of second day, the proposed model-free VVC commands become very similar to that of model-based optimization. The scheme is also able to decrease the power loss close to the level achieved by model-based optimization. Since there is no exploration period involved in VR controller, the voltages imposed by model-free VVC are within the limit from the first day. Interestingly, the model-free VVC has reduced the MVD even more than the model-based counterpart. This is probably due to optimization objective in model-based case which makes it willing to compromise MVD for power loss reduction (see Appendix C). Overall, the results demonstrate efficacy of proposed model-free VVC on the Elementary system.

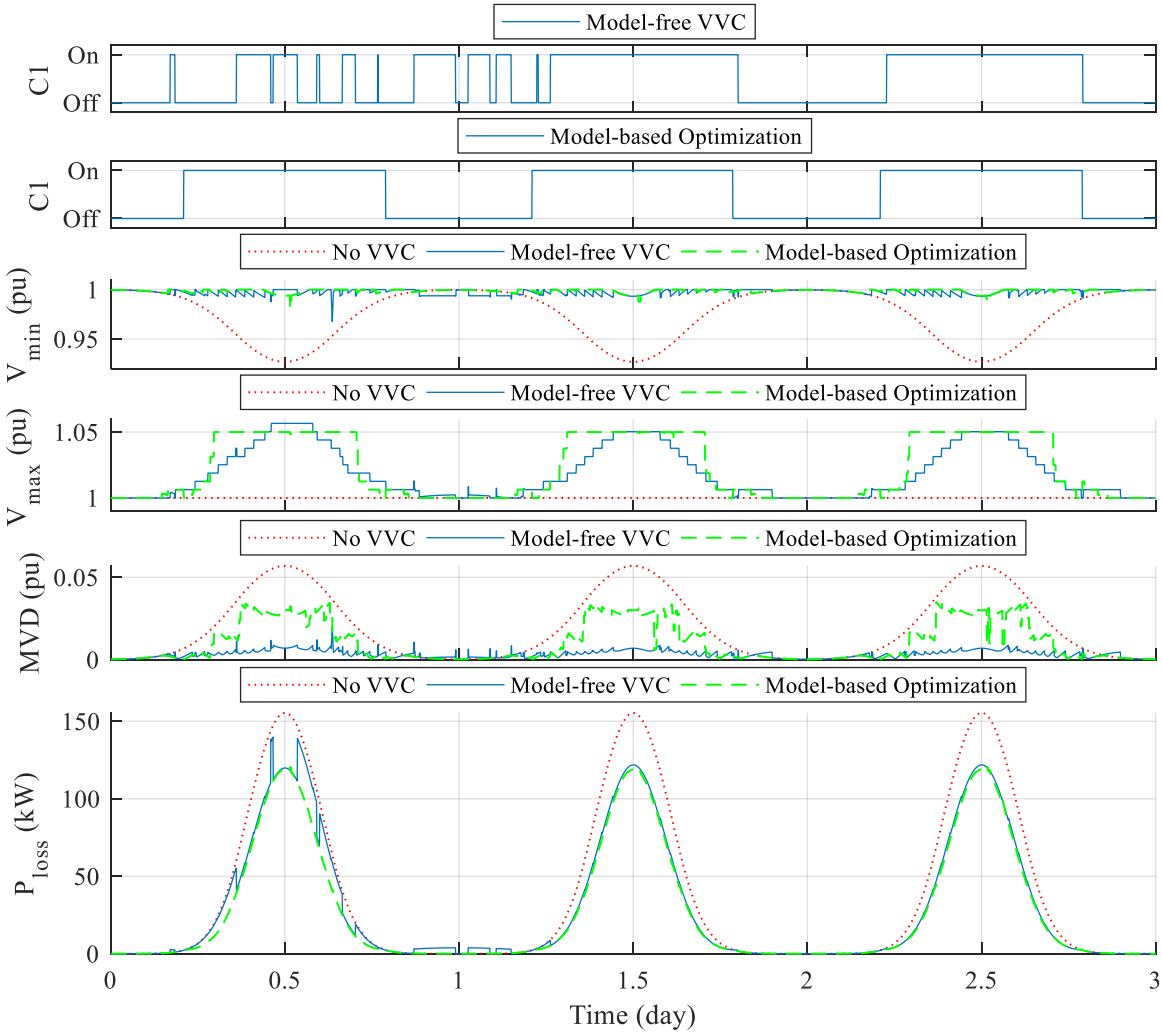


Figure 4.5 Results of Model-free VVC simulation on Elementary System (only first three days are shown for better visualization)

### 4.6.3 Sensitivity Studies

#### a. Metering Condition and Measurement Errors

Different cases were simulated to assess effect of metering characteristics such as measurement errors or absence of phasor angles on the efficacy of proposed model-free VVC. The results are shown on Figure 4.6. The results demonstrate that absence of voltage phasor angles in measurement data does not affect the performance of model-free VVC. The 15 minute time resolution has a negative impact, but the model-free VVC is still performing well even under this condition.

The model-free VVC is found thoroughly robust against the measurement errors up to 1%. The measurement errors equal or higher than 2.5% are observed to deteriorate the VVC performance (in both power loss reduction and improving the voltage profile or decrease of MVD).

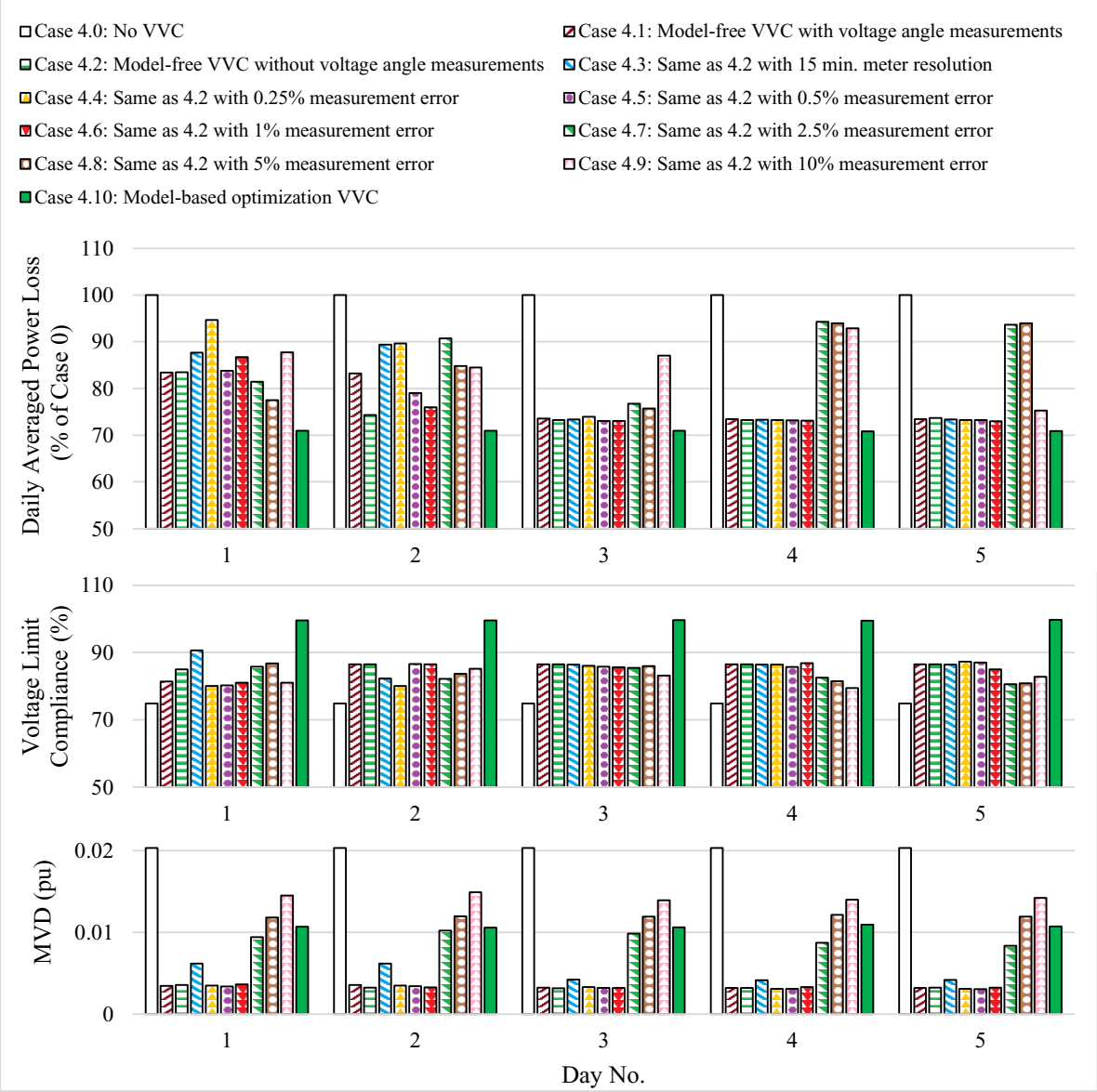


Figure 4.6 Results of VVCs with different metering conditions

### b. Number of Capacitor Switching Events during Exploration

Sensitivity studies were also conducted to assess the effect of number of capacitor switching during the exploration period. The effect is analyzed from two perspectives; one associated with length of the exploration period, while the other is to measure the performance of VVC after the exploration period in terms of reducing power loss and MVD (compared to normal condition when there is no VVC). Figure 4.7

shows the results. More frequent switching during exploration period in general has shortened the exploration period, however, a saturation effect is observed too. Switching the capacitor more than 25 times per day did not significantly reduce the length of exploration period. The results also reveal that too few switching per day such as less than 6 times per day can make the VVC completely ineffective. For any number of switching during exploration, the proposed scheme is found effective, and, the VVC performance after exploration period is not significantly improved by switching the capacitor more often during exploration.

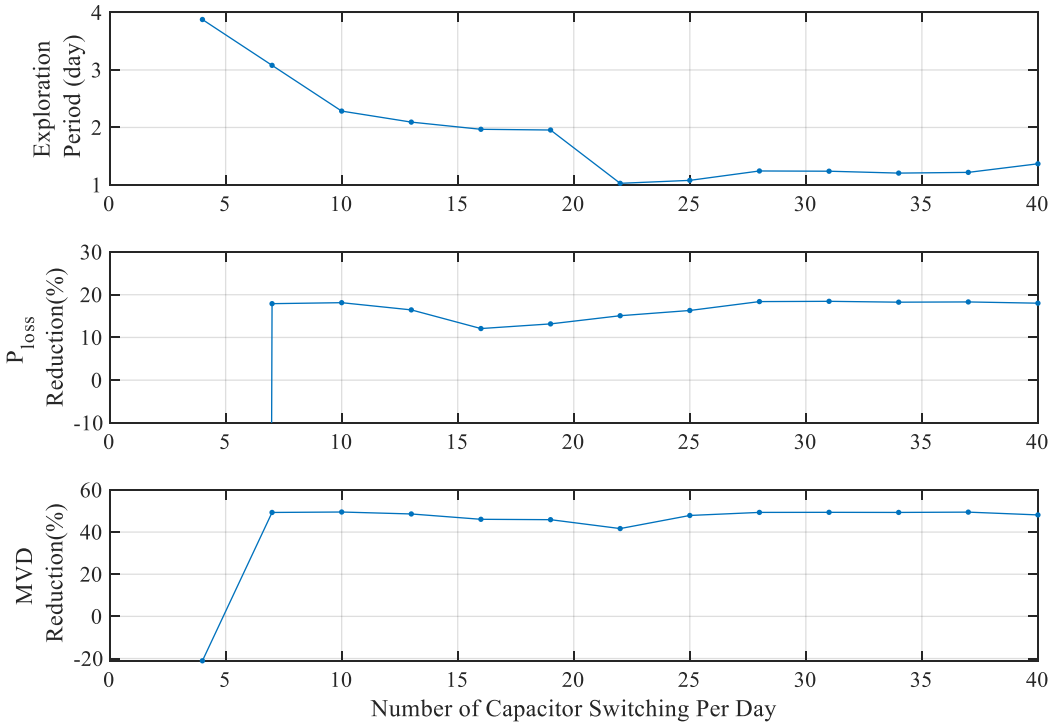


Figure 4.7 Effect of number of Capacitor switching in the exploration period on performance of model-free VVC for the Elementary system

## 4.7 Simulation Studies on IEEE 123 Nodes Test Feeder

The IEEE 123 Nodes Test Feeder was simulated with the similar specifications given in section 3.6 of previous chapter (including load/DER profiles, capacitor size and locations). However, unlike chapter 3, the simulations were performed for the whole 10 day periods, and the case without DERs is not considered here (i.e. DERs are on the circuit for all simulation studies of this chapter). Similar to the simulation case of chapter 3, each bus with one load or a DER or both was assigned with one smart meter that reads and sends its voltage magnitude and power usage to the VVC control center.

### 4.7.1 Base Test Description

For the base test, the proposed model-free VVC scheme was simulated with the following settings in the capacitor controller:

- 50 capacitor switching per day for the Exploration period
- Operation limits (except Exploration period): maximum 10 capacitor switching per day and minimum 10 minutes between consequent switching times
- Criteria for stability of estimations: for all capacitor switching combinations, the variation of predicted error of power loss estimation in last *12* hours becomes less than *20%* of its initial estimated error value
- Four principle components from PCA were kept for estimations (i.e. $p=4$ in PCA process described in chapter 2)

And the following settings for VR controller:

- Time delays for substation VR: 1 and 2 minutes for primary and secondary zones respectively
- Time delays for the other VRs: 4 and 9 minutes for primary and secondary zones respectively
- *0.01pu* safety margin in voltage control (i.e. controller acts based on $V_{Min,Lim}+0.01pu$ and $V_{Max,Lim}-0.01pu$ instead of original $V_{Min,Lim}$ and $V_{Max,Lim}$).
- *0.01pu* control bandwidth in voltage centering

For the base test, time resolution of AMI data was considered to be 1 minute and meters were assumed without synchro-phasor capability (i.e. measurements only included voltage magnitudes). As a reference to evaluate performance of model-free VVC, a model-based optimization VVC was also simulated on this system. More details are given in Appendix C on the optimization method.

### 4.7.2 Base Results

Figure 4.8, shows the performance of the model-free VVC on IEEE 123 Nodes system. The results show that after three days of exploration, the proposed method can give switching commands close to that of model-based optimization. Once the exploration ends, it has successfully reduced total power loss by a similar level to the model-based counterpart. In terms of voltage control, the model-free VVC has reduced MVD and kept the voltages within limit from the first day of operation, since no exploration and sample data collection is required for the VR control part of the proposed scheme.

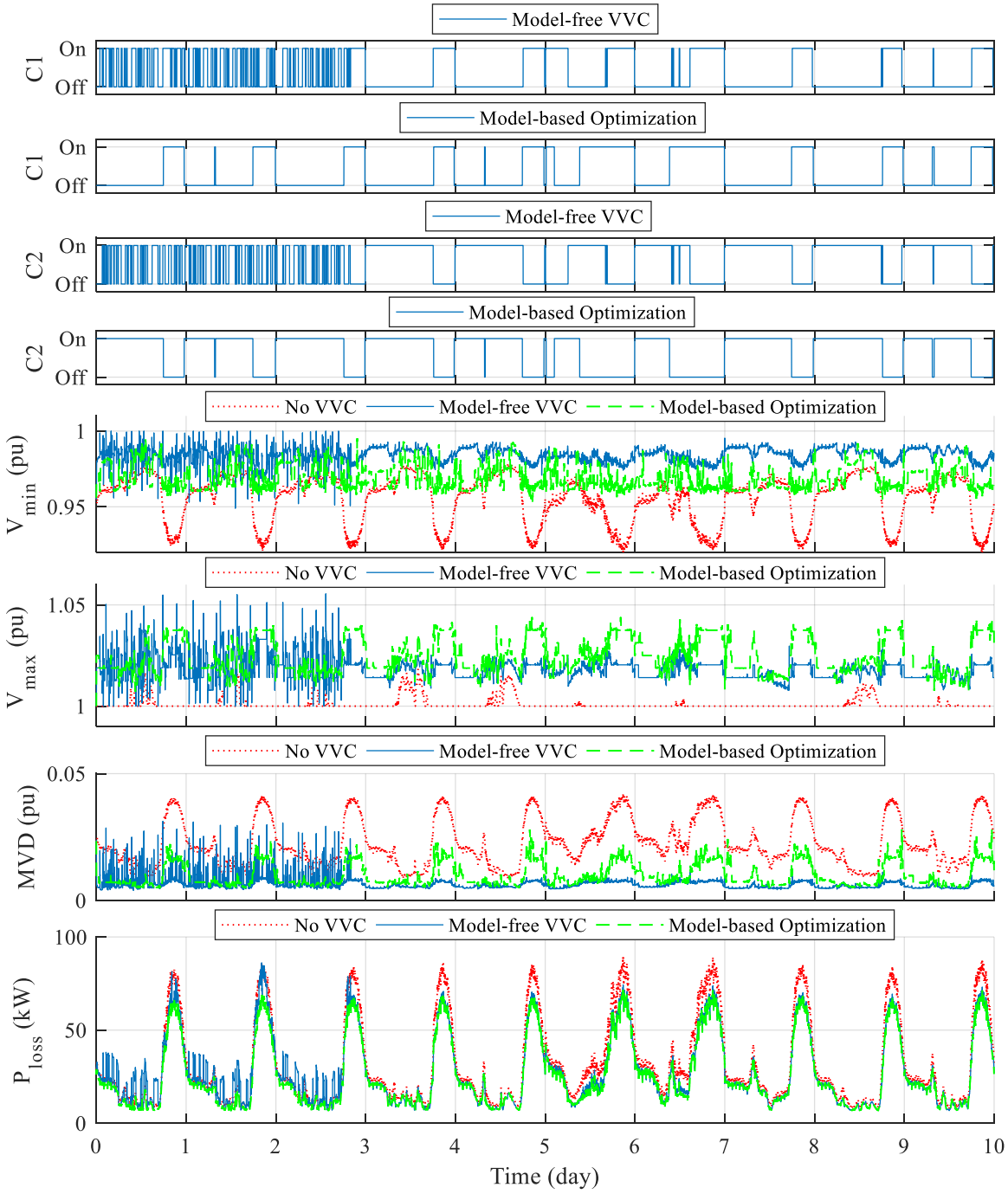


Figure 4.8 Results of Model-free VVC simulation on IEEE 123 Nodes Test System

### 4.7.3 Comparison to Rule-based VVCs

The results of model-free VVC is also compared to its traditional rule-based counterparts. Three rule-based VVC were simulated on the IEEE 123 Nodes test feeder. In these cases, the VRs were locally controlled with default LDC settings as in [29]. Capacitors were switched based on time, voltage or reactive

power rules as explained in [38]. In first one of these rule-based VVCs, the capacitors were switched based on their local voltage measurement. The thresholds for turn ON and turn OFF actions were chosen as 1pu and 1.03pu respectively. In second rule-based VVC, the capacitors were switched based on the local reactive power measurement at their upstream branch. The thresholds selected for switch ON and switch OFF were 40% and -60%[37] of capacitor size respectively. The last rule-based VVC represents a time-based control scenario. The capacitors were switched ON at 6pm and switched OFF at 11pm. In all these rule-based VVC simulation cases, optimal values were assigned to control parameters based on extensive case studies on the simulated system. This act is somehow equivalent to field tuning based on operation experience (or measurement record) in a real-world application.

Figure 4.9 compares the performance of proposed model-free VVC with these rule-based VVC cases. The model-free VVC shows a more effective performance in terms of power loss and MVD reduction, especially after it passes the exploration period of the first three days.

[37] Positive/negative sign means reactive power flowing downstream/upstream

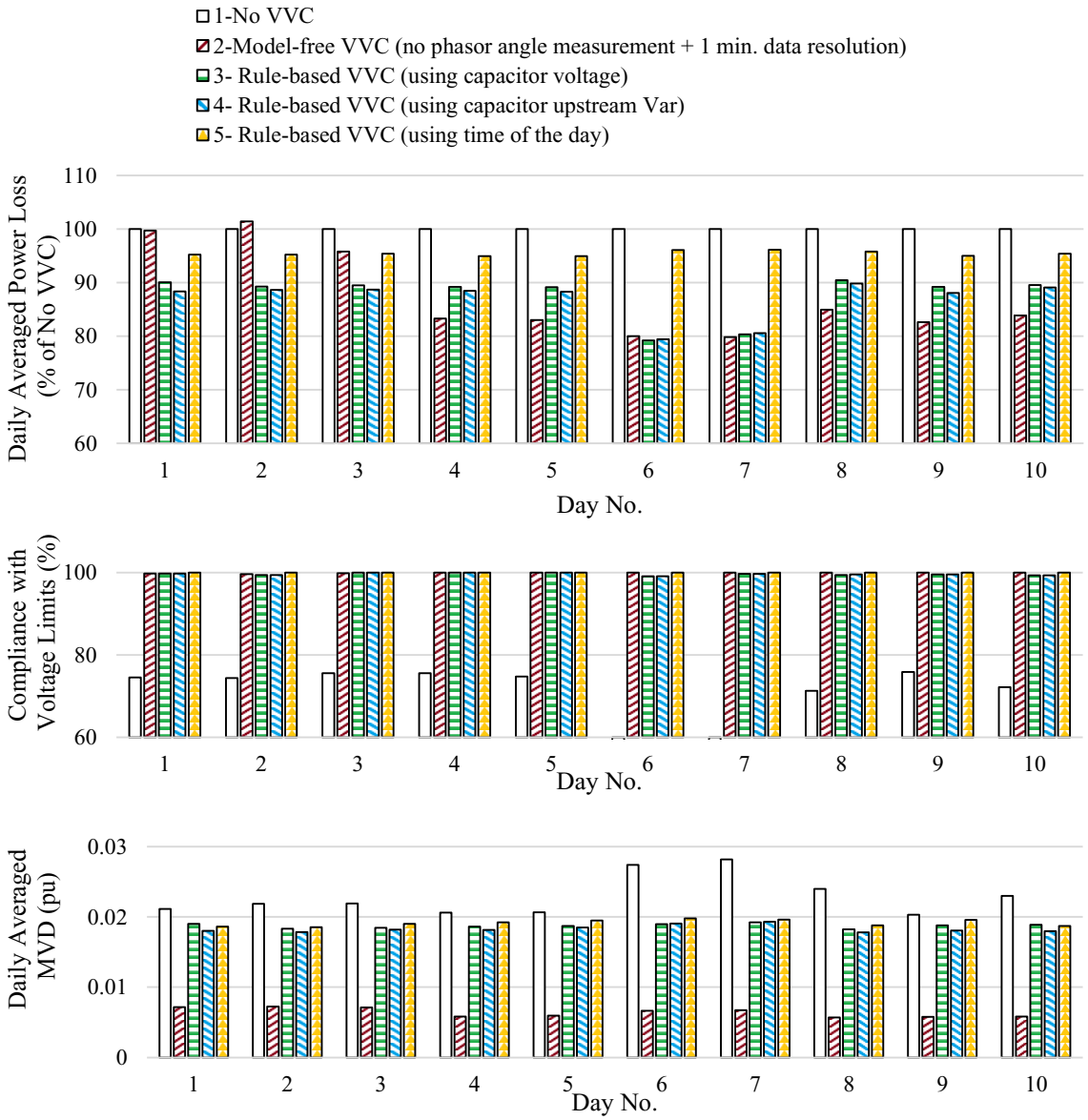


Figure 4.9 Comparing results of Model-free VVC with rule-based VVCs

### 4.7.4 Sensitivity Studies

#### a. Metering Condition and Measurement Errors

The model-free VVC was also tested with different metering conditions such as larger time resolution and presence of phasor angle measurement or measurement noises.

Figure 4.10 shows the results. The results from third and fourth cases are quite close to that of the second case. This observation shows that neither lack of voltage phase angles nor presence of measurement error significantly affect the performance of proposed VVC method. Such negligible effect of voltage phasor angles was expected from the earlier discussions in chapter 2. Tolerance of the proposed method against measurement errors is also understandable considering the averaging nature of KNN technique in addition to automatic noise filtering feature of a dimension reduction process (PCA analysis).

Results of the fifth case show that the proposed scheme is still effective even with a 15 minute time resolution of AMI data. Naturally, performance of this case is not as optimal as Cases 2~4 because of the larger time resolution.

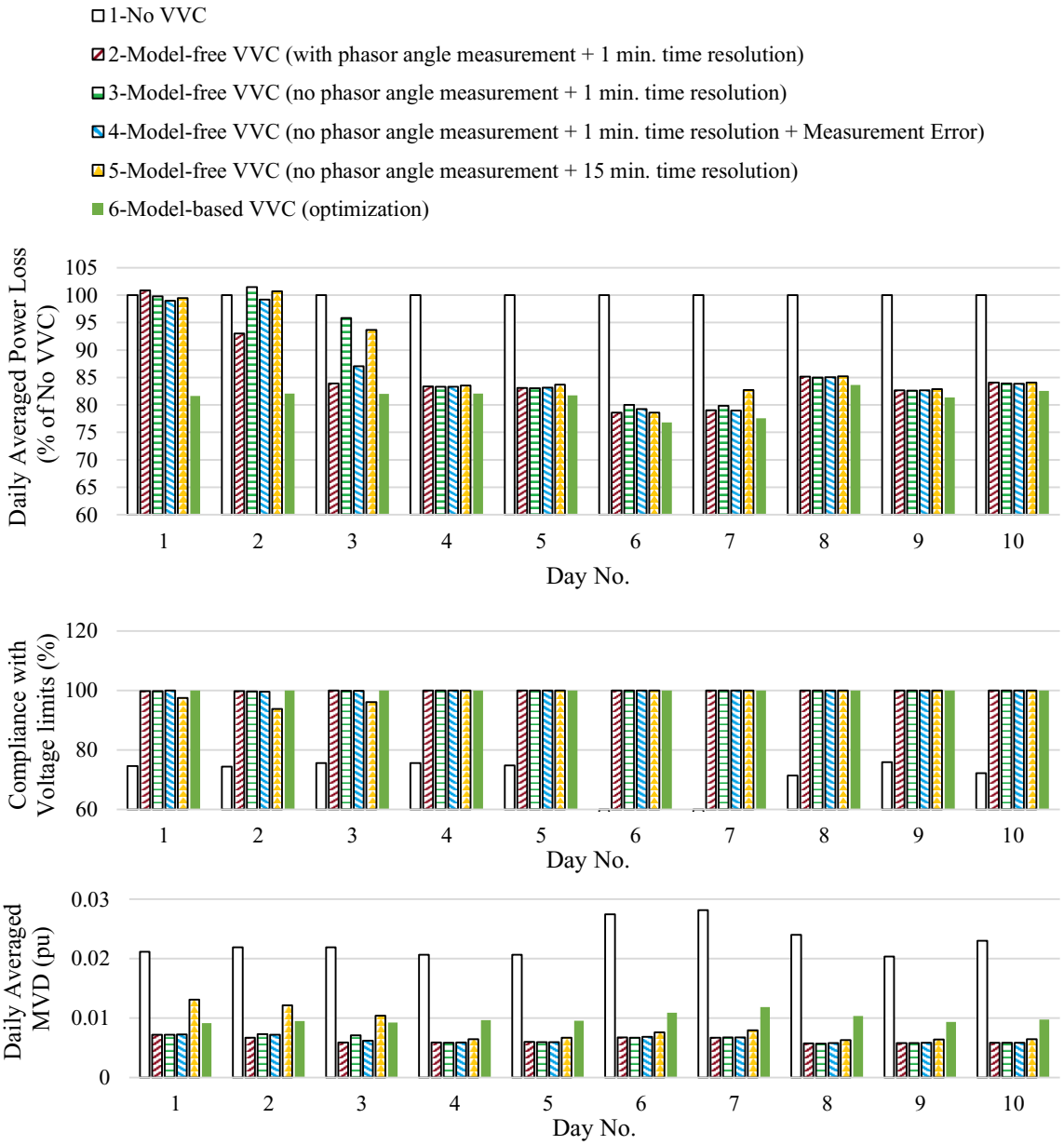


Figure 4.10 Performance of Model-free VVC on IEEE 123 Nodes system under different metering conditions

### b. Number of Capacitor Switching during Exploration

The effect of capacitor switching frequency during exploration time was studied using the base model-free VVC case (which is associated with metering without voltage angles and 1 minute time resolution). In a similar approach to studies of Elementary System, the effect of number of exploration switching times per day is assessed from two perspective: length of exploration period and VVC performance after the exploration period. As Figure 4.11 shows, the overall result is similar to that of Elementary system. Increasing number of switching events during exploration can only help to shorten the exploration period,

but it does not affect the VVC performance once the exploration period ends. Reduction in length of exploration period can never make this period shorter than one day. As the results indicate, switching the capacitor more than 70 times per day during exploration is not effective in shortening the exploration period.

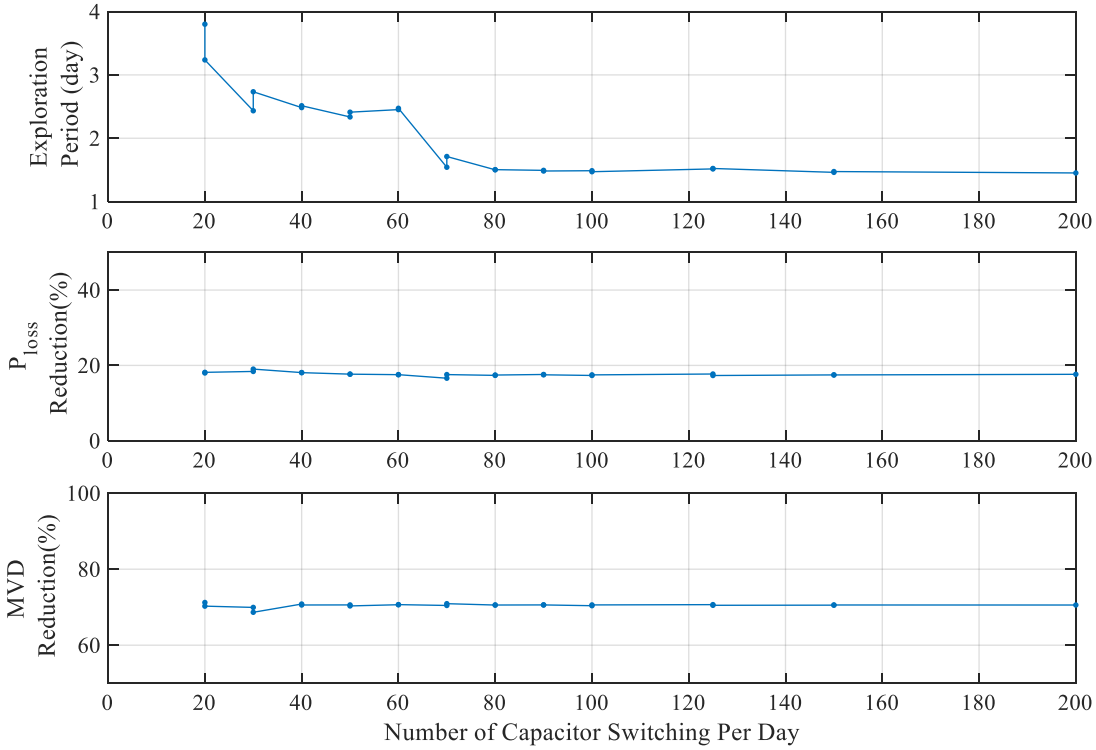


Figure 4.11 Effect of number of Capacitor switching in the exploration period on performance of model-free VVC on IEEE 123 Nodes Test System

### c. Impact of Substation Impedance and Variant Load Characteristics

Similar to sensitivity study of section 3.6.3.d in chapter 3, the effect of changing substation voltage source and variant load characteristics need to be studied on the proposed model-free VVC[38]. The base model-free VVC case is used in this study (i.e. 50 capacitor switching event per day during exploration, meters are without voltage phasor angle measurement, and AMI data time resolution is 1 minute). In one sensitivity case, an impedance of $0.1+0.1j$ Ω is included in substation source of the feeder which makes the source voltage variant by time. In other case, the voltage-dependency of loads is changed during simulation time. More details on how the load voltage-dependency is changed during simulation time is given in Appendix B. For each case the power loss and MVD results are scaled using results associated with its equivalent of running No VVC.

[38] Refer to discussion of section 3.6.3.d in chapter 3 regarding essence of such considerations.

Figure 4.12 shows the results. As the results demonstrate, neither of the two cases had a significant impact on performance of the VVC. It shows that model-free VVC is still capable to perform even if the source voltage is variant or voltage-dependency of loads change during operation.

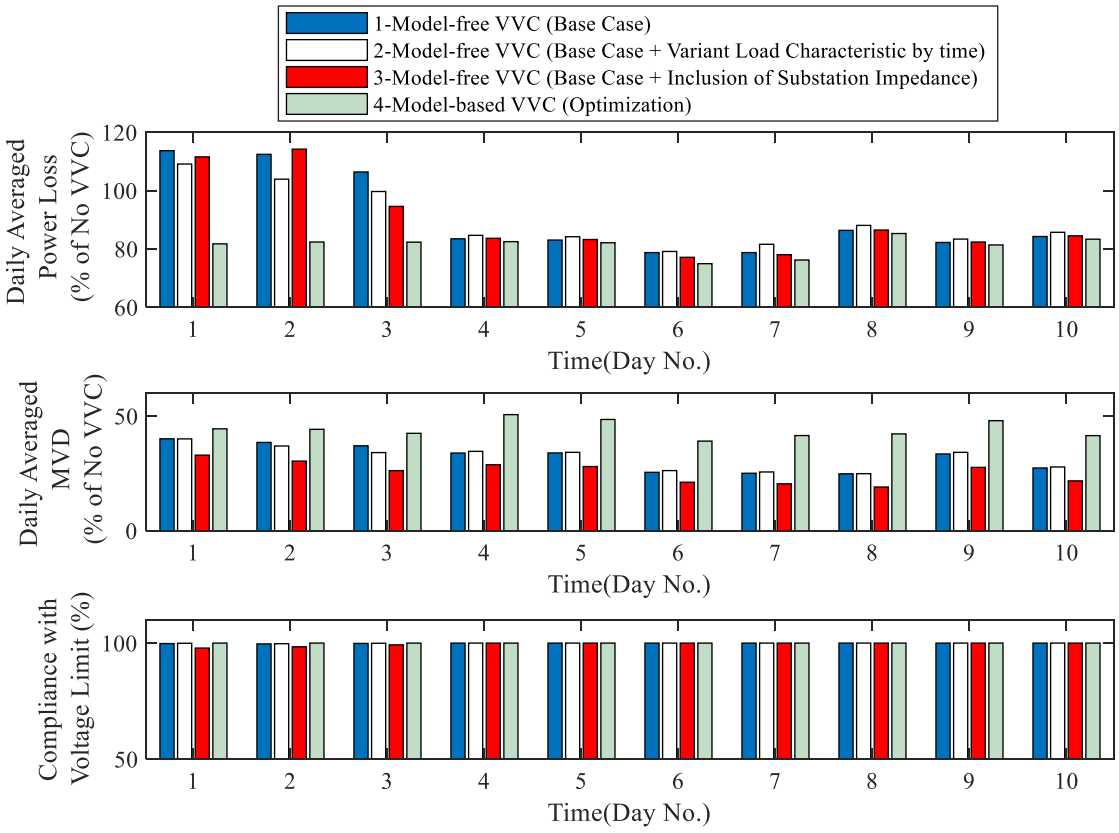


Figure 4.12 Impact of source impedance and variant load characteristic on performance of model-free VVC on IEEE 123 Nodes system

### d. Impact of Failed Smart Meters

As one real-world possibility, some of system customers (owning loads or DERs or both) may not be equipped with smart meters. Moreover, a number of smart meters might fail to send their data to the controller (the possible failure might be either due to defects in the meter device or AMI communications). As an important practical aspect of the method, these scenarios of smart meter loss should be also studied.

Missing some of smart meter data can influence both capacitor and VR controllers in the proposed model-free VVC scheme. For instance, estimated maximum/minimum voltages of each zone could become less accurate for the VR controller. However, the more significant impact will be on power loss estimations; the error will be equal to the total power of loads/DERs associated with the missed meters (see equation (3.1)), hence the error is quite considerable, and could be even larger than the calculated value for power

loss. Fortunately, the proposed scheme only uses power loss changes caused by capacitor switching events. Hence, the effective error will be summation of total changes in loads/DERs associated with the missed meters during the switching events. Such error can be considerably smaller than the initial error in estimation of original power loss. Therefore, the scheme can be still expected to tolerate losing data of some meters. Apparently, it is difficult to quantify the exact impact, since it will be highly dependent on the size and nature of loads/DERs associated with the lost meters.

Several sensitivity simulation cases were conducted to evaluate impact of missing some meters[39]. In each of these sensitivity cases, a random number of system meters were assumed inactive (i.e. the scheme could not collect data of those meter). For each case, the Smart Meter Loss Rate is defined by dividing number of inactive meters over number of all meters.

Figure 4.13 shows the three indices of interest resulting from these simulations. Each scatter point represents one of the simulated cases. In the plots, average of the index over period of last *7* simulation days is considered in order to exclude the Exploration periods. For the purpose of comparison, mean of each index associated with traditional rule-based VVC cases (discussed in section 4.6.3) is also plotted by a dashed line. Hence, the cases giving worse indices than the dashed lines can be considered unacceptable.

As expected, the power loss saving aspect of proposed VVC shows some tolerance against low meter loss rates up to almost 10%. There is a high chance of unacceptable results in case more than 20% of system meter data is lost. On the other hand, the performance of method is found very robust in the aspect of voltage control. The scheme is found capable of voltage regulation and reduction of voltage deviation under different meter missing rates. There are two possible reasons for it. First, estimation of maximum/minimum voltages are less affected by losing data of a number of meters. Second, even considering the error in estimation of maximum/minimum voltage, the voltage-centering feature of VR controller keeps voltages around center of the standard voltage range, and thus reduces probability of limit violation.

[39] The simulations were performed by 40 switching/day during exploration, assuming no voltage angle measurement and 1 minute time resolution of AMI data.

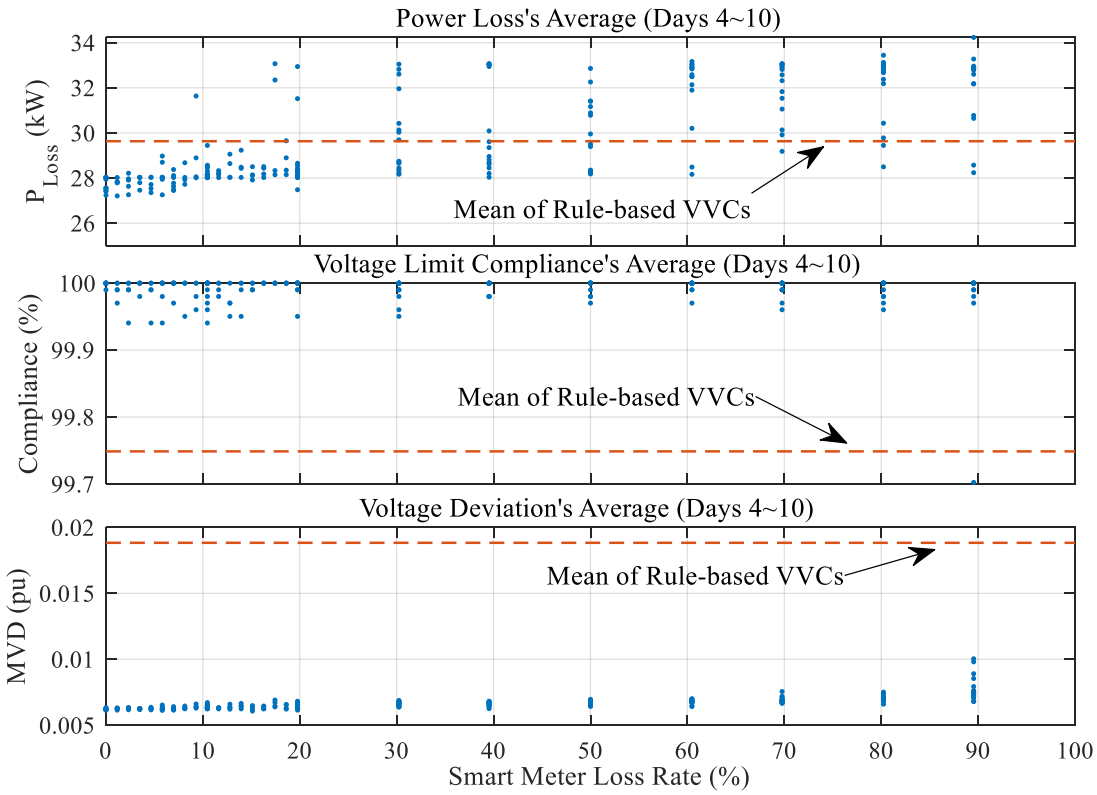


Figure 4.13 Performance of model-free VVC under different smart meter loss rates

## 4.8 Summary

A new model-free VVC scheme was introduced that is structured based on statistical analytics on the AMI data. Unlike the traditional rule-based counterparts, the proposed scheme is backboned by a rigorous statistical framework, capable to deliver better performance regarding loss minimization and voltage profile control. On the other hand, the model-free feature eliminates difficulties associated with network-model data gathering for each individual feeder. In addition, the errors due to model inaccuracies are mitigated by the proposed VVC.

The effectiveness of proposed method was demonstrated by simulation studies on one elementary system and IEEE 123 Node Test Feeder. In order to better represent the current operation challenges in modern feeders, DER units were also added to the studied system. The results showed that proposed VVC is capable to give an acceptable performance close to that of a model-based optimization technique. In addition, comparative case studies revealed the superiority of proposed method over traditional rule-based VVC schemes. The simulation studies also revealed the following information on the proposed scheme:

- Due to noise filtering nature of the employed statistical techniques (PCA and KNN), the method was found effective even with presence of measurement noise. The scheme was also found

effective with a data time resolution up to 15 minutes. In addition, simulation studies demonstrated that the method can still perform effectively without measuring phasor angles of system voltages. Thus, it is consistent with present AMI technologies which are not generally equipped for synchro-phasor measurement.

- The scheme showed robustness against meter failure. The results showed satisfactory performance even when data of up to 10% of feeder smart meters get lost.
- Increasing the capacitor switching frequency during Exploration period was observed to shorten this period, while it didn't have tangible effect on VVC performance after exploration. Nonetheless, the exploration period was never observed to become shorter than one full day even if the capacitors were switched very frequently during exploration.

# Chapter 5

# Model-free Conservation Voltage Reduction (CVR)

A model-free data-driven CVR scheme is presented in this chapter. The objective of this scheme is to reduce voltages of every system nodes as much as possible without violating the regulatory voltage limits. Since power of most loads are proportional to voltage, this strategy will automatically minimize the overall load consumption in a distribution feeder. Unlike the model-free VVC, this CVR scheme does not necessarily need a complete set of AMI data. Indeed, the proposed CVR scheme can perform without an AMI system. A number of meters are only required at VR locations and some critical buses such as end points of the feeder. This flexibility emerges from the fact that estimation of system losses is not a necessary condition for CVR. The scheme will be defined in a way to cover operation of multistep capacitor banks, as well. Similar to previous chapters, simulation studies will be presented to demonstrate the efficacy of proposed methods.

## 5.1 Literature Review

The main concept of CVR is to lower feeder voltages to achieve more energy saving and reduce the peak demand on the system [11],[45]. The earliest report of testing this idea dates back to 1973, when American Electric Power System (AEP) performed a CVR program on some of their feeders for a short period [46]. This track of testing CVR idea was continued by many other utilities such as Bonneville Power Administration [47], BC Hydro [48], and Hydro Quebec [49]. The results of these tests have shown effective reduction of load powers up to 1% for a 1% voltage reduction. Since then, CVR has remained as a key for energy saving available to utilities operating distribution networks.

Similar to VVC platforms, the methods to implement a CVR can be also divided into two classes of rule-based and model-base optimization techniques. As a traditional rule-based approach, reducing the voltage setting of SLTC at feeder's substation has been the most convenient and straight-forward method to realize a CVR [52]. Although such approach comes with no extra cost, it involves the risk of undervoltage during peak-load hours, especially for the customers located at the end of feeder. In CVR implementations such as [53]-[55], the end-of-feeder voltage was also measured or estimated to avoid such problem.

Beside the SLTC, capacitors can be also an effective element in CVR applications. Contribution of capacitors comes from their ability to flatten voltage of a feeder or power-line, so that SLTC voltage setting can be further decreased without the concern of undervoltage at some points of the feeder. CVR

implementations presented in [55]-[59] are examples of employing capacitors. Some of these schemes also involve VRs as part of the CVR. Overall, these studies show that addition of VRs and capacitors to a CVR scheme can increase its efficiency by 60% (for example, average voltage reduction due to CVR can be increased from 2.5% to 4% by including capacitors and VRs).

Several utilities such as Inland Power and Clatskanie PUD have implemented CVR programs as an integral part of their VVC schemes [62]-[63]. Referred as closed-loop CVRs, some of these schemes also benefit from feedback of measurement data such as AMI [64]-[65].

In recent years, the idea of CVR is even leveraged to the concept of voltage-led load management. In such schemes, the voltage of customers are lowered to reduce the demand from transmission network. This action also gives more flexibility to the operator of transmission system in balancing generation and demand [60]. Such advanced form of CVR has been tested in U.K. as a big project known as CLASS[40]. Running from 2014 to 2016, this project involved 60 distribution substations and realized the operation flexibility to manage the demand from feeders which were collectively supplying electricity of more than 350,000 customers [61]. The outcome of such a project demonstrates that value of CVR is not limited to energy savings, and it can also serve as a mean of flexibility for transmission operations.

All of the CVR schemes discussed above employ a rule-based technique to control SLTC, VR and capacitor equipment. In the literature, several studies have also suggested to implement CVRs by optimization algorithms using circuit model analysis. Recent works such as [50]-[51] have included CVR objective as an integral part of a sophisticated optimization VVC platform.

Although more effective, model-based CVR is troubled with the same problems similar to those of model-based VVCs as discussed in chapter 1 and 4. The presented model-free CVR in this chapter offers a middle way. It can operate independent of system models, while also benefiting from measurement and statistical estimations to achieve more optimal performance compared to the traditional rule-based techniques.

## 5.2 Proposed Data-driven CVR scheme

Figure 5.1 shows the scheme of the proposed data-driven CVR. The main difference with the model-free VVC scheme[41] introduced in chapter 4 is the meter requirement. Unlike model-free VVC, an AMI system is not required for model-free CVR. The meters are only required at VR and SLTC and other critical points of the feeder such as end-of-the-line. However, the control structure is similar to that of model-free VVC. VRs and capacitors are controlled by separate modules, and the capacitor control module consists of

[40] CLASS stands for Customer Load Active System Services.
[41] See Figure 4.1.

the Decider and Estimator units. The overall objective of the scheme is to reduce voltages of every node as much as possible without violating regulatory limits.

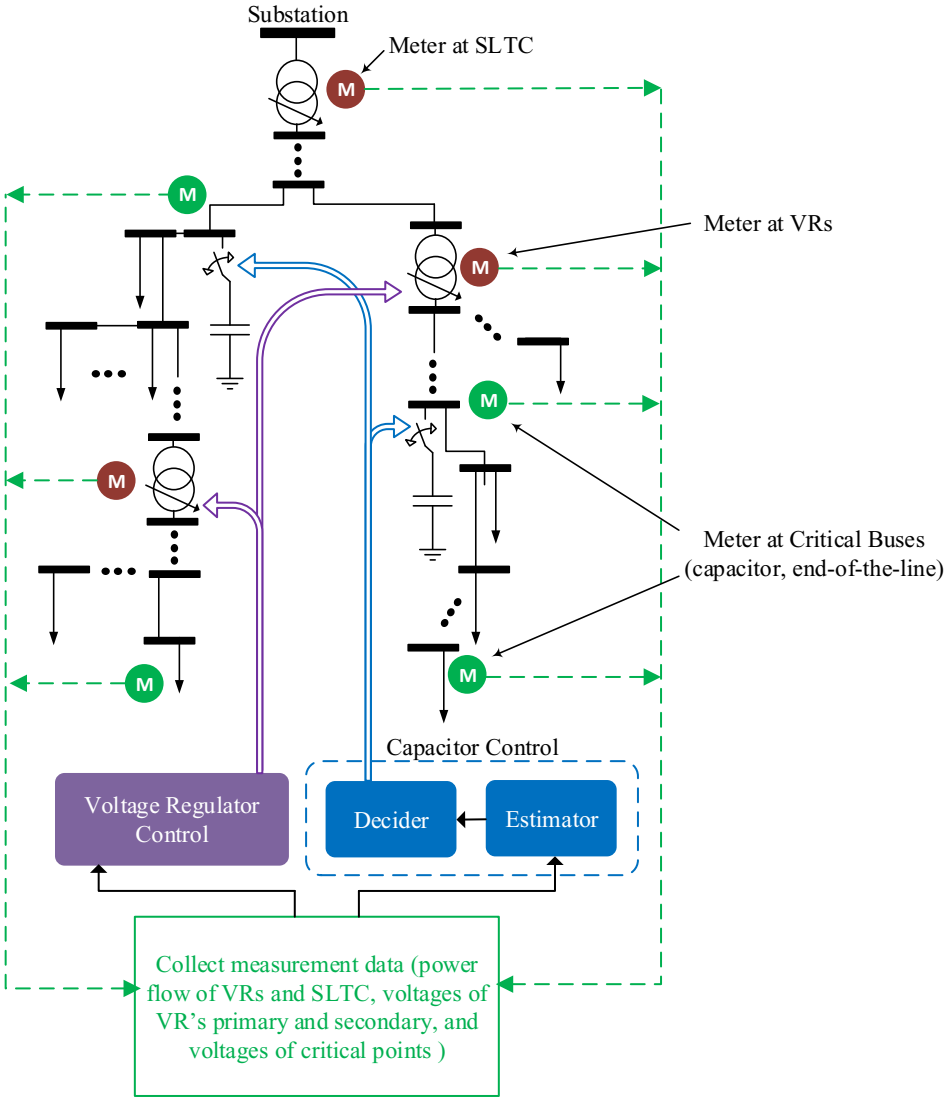


Figure 5.1 Scheme of proposed data-driven CVR

## 5.3 Voltage Regulator Control

Similar to model-free VVC, the VR controller is only tasked to manage the feeder voltages. The VR control is based on definition of VR zones offered in section 4.4 of the previous chapter. The meters inside each VR zone gives an estimate of minimum voltage in that zone ($V_{min,z}$). However, different from the VVC scheme, the VR controller has no objective of voltage centering for each zone, rather, the controller aims to keep this minimum voltage of its zone as close as possible to the minimum regulatory voltage limit ($V_{Min,Lim}$). Thus, tap position of each VR is adjusted according to estimated minimum voltage in its own zone. A CVR voltage bandwidth (denoted as $BW_{CVR}$) needs to be considered here. If minimum voltage of

the zone goes above minimum limit for a larger margin than this bandwidth (i.e. $V_{min,z} > V_{Min,Lim}+BW_{CVR}$), the tap position of VR is reduced by one step. On the other hand, the tap position is increased if the zone's minimum voltage goes below the minimum limit ($V_{min,z}<V_{Min,Lim}$). Since these two commands are in reverse directions, the CVR bandwidth ($BW_{CVR}$) should be chosen wide enough to avoid a trapping effect leading to repetitive tap operations.

## 5.4 Capacitor Control

As explained early, the main role of capacitors in a CVR is to flatten the feeder's voltage profile, or in the other words, reduction of voltage spread in the system. A flatter voltage profile allows for further reduction of VR or SLTC settings resulting in a more effective CVR. This objective already sets the task of the Estimator and Decider unit in capacitor control: achieving lowest voltage spread in the feeder. Hence, the term of voltage spread needs to be quantified. The most straightforward way is to define it as the difference between maximum and minimum voltage of the system (i.e. $V_{max}$ -$V_{min}$); the lower such index, the flatter the voltage profile is. The drawback with such simple definition is its vulnerability to estimation errors, since it is directly affected by errors in voltage estimation of two system nodes at one instant. A better option is to use standard deviation of system voltages as expressed below:

$$STD_V = \frac{1}{N-1}\sqrt{\sum_{i=1}^{N}(|V_i|-V_{mean})^2} \quad \text{where} \quad V_{mean} = \frac{1}{N}\sum_{i=1}^{N}|V_i| \tag{5.1}$$

Standard deviation is a more robust index from perspective of estimations, since voltages of every node appear in it, and there is a higher chance that individual errors of estimating each node collectively cancel each other. Therefore, the capacitor control objective will be to predict above $STD_V$ for different capacitor states, and at each time choose for the one leading to the lowest value of it. However, $STD_V$ is affected by tap ratios of VRs, too. The objective of capacitor control is better not to be affected by VR operations, since VR and capacitor controllers operate independently, and VR operations could be much more frequent than capacitors. This issue can be resolved by considering the standard deviation for each VR zone separately. We define $STD_{VZ,i}$ as standard deviation of voltages inside the VR zone supplied by $i^{th}$ tap changing equipment. Since the system is radial, one can assume that tap changes of a VR causes an almost equal change in voltages of that VR zone, thus, $STD_{VZ,i}$ is not significantly affected by the VR operations. This makes $STD_{VZ,i}$ as a suitable objective candidate for the capacitor controller. One will face a multi-objective problem here, since there are more than one VR zone, and a capacitor state might lead to a lower $STD_{VZ,i}$ for one zone, and higher $STD_{VZ,i}$ for another one. In fact, $STD_{VZ,i}$ reduction should be prioritized for the zones that contain loads which exhibit higher dependency of power over voltage. The proposed scheme can

measure such quantity since each VR records its power flow, making it possible to measure power consumption at each zone. After tap changes of each VR, the ratio of power changes to tap change can be collected for the respective VR zone and averaged for the whole operation period. We denote this index for the $i^{th}$ VR zone as $(dP/da)_i$. This index can be used as weighting coefficient to introduce a single objective for this multi-objective problem; the goal of capacitor controller becomes to minimize the following:

$$OBJ_{CVR} = \left(dP/da\right)_1 \cdot STD_{VZ,1} + \left(dP/da\right)_2 \cdot STD_{VZ,2} + \cdots + \left(dP/da\right)_{N_{VR}} \cdot STD_{VZ,N_{VR}} \tag{5.2}$$

Based on definition of modified voltage vector in chapter 2, difference of modified voltage and original voltage is equal for every node inside a single VR zone. Therefore, since the standard deviation of a group of parameters is only dependent on relative distance of those parameters, $STD_{VZ,i}$ can be directly obtained by using the modified voltage vector. Therefore, the Estimator unit can operate based on the same mechanism as for model-free VVC presented in chapter 4 to predict the modified voltage vector for different switching events. The Estimator unit, thus, can predict standard voltage deviation for each zone for all possible capacitor states. The algorithm of interaction between Decider and Estimator units will be also similar to the proposed one for model-free VVC. The overall mechanism includes Explore commands, data sample collection, and estimations similar to what was laid out in chapter 4 (see Figure 4.2). The estimation functions are, however, grouped in a similar fashion to chapter 3 rather than chapter 4. Each estimation function is devoted to individual turn OFF or turn ON event of each capacitor. For capacitor banks, the turn ON/OFF functions are equivalent of adding one capacitor bank-step in/out. The followings will be the data samples for each function (functions relating to capacitor bank operation are denoted as $H_V^{C_n:+}$ and $H_V^{C_n:-}$ respectively):

$$\begin{aligned}
&X\left[H_V^{C_n:ON}\right] = X\left[H_V^{C_n:+}\right] = \left\{\overrightarrow{V'(t_i)} \mid i \in \{1,2,\cdots,T-1\} \wedge \Phi\left[\overrightarrow{C(t_{i+1})} - \overrightarrow{C(t_i)}\right] = n\right\} \\
&Y\left[H_V^{C_n:ON}\right] = Y\left[H_V^{C_n:+}\right] = \left\{\overrightarrow{V'(t_{i+1})} - \overrightarrow{V'(t_i)} \mid i \in \{1,2,\cdots,T-1\} \wedge \Phi\left[\overrightarrow{C(t_{i+1})} - \overrightarrow{C(t_i)}\right] = n\right\} \\
&X\left[H_V^{C_n:OFF}\right] = X\left[H_V^{C_n:-}\right] = \left\{\overrightarrow{V'(t_i)} \mid i \in \{1,2,\cdots,T-1\} \wedge \Phi\left[\overrightarrow{C(t_{i+1})} - \overrightarrow{C(t_i)}\right] = -n\right\} \\
&Y\left[H_V^{C_n:OFF}\right] = Y\left[H_V^{C_n:-}\right] = \left\{\overrightarrow{V'(t_{i+1})} - \overrightarrow{V'(t_i)} \mid i \in \{1,2,\cdots,T-1\} \wedge \Phi\left[\overrightarrow{C(t_{i+1})} - \overrightarrow{C(t_i)}\right] = -n\right\}
\end{aligned} \tag{5.3}$$

Differently from chapter 3 and chapter 4, the above modified voltage vectors ($V'$) only include the critical nodes. As we will see in the simulations, this does not cause a problem in estimations since not all system voltages are required to reflect the system conditions (refer to discussions in section 2.8 of the second chapter for these types of assumptions). Figure 5.2 shows the overall algorithm of capacitor control in the CVR:

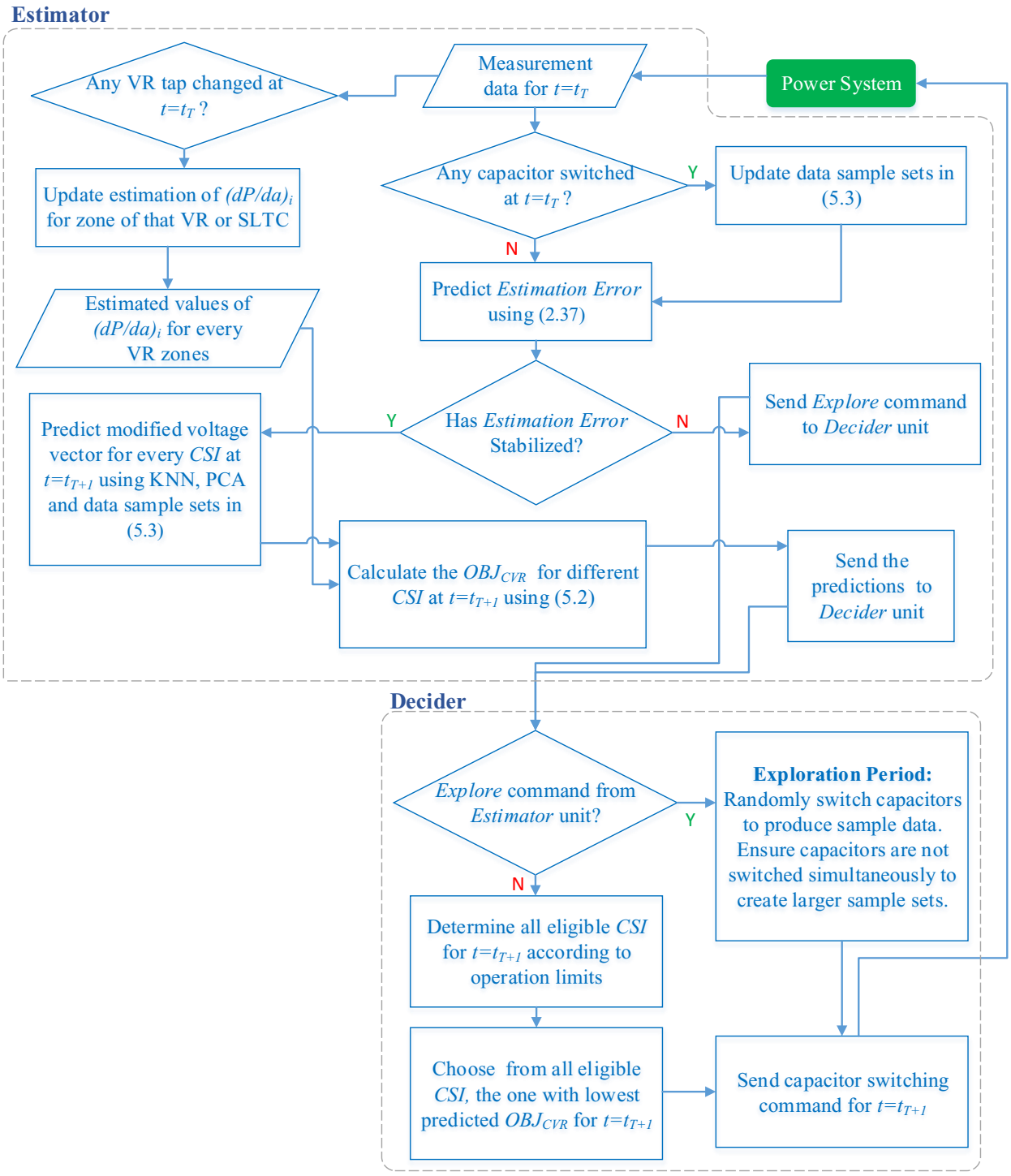


Figure 5.2 Capacitor control flowchart for proposed Model-free CVR

## 5.5 Simulation Study Setup

Simulation studies were performed to evaluate effectiveness and feasibility of the proposed model-free CVR scheme. Similar to studies of chapter 3 and 4, load flows were conducted by OpenDSS interface in Matlab. The statistical estimation process as well as the control algorithms were also implemented by Matlab codes. Both of the Elementary and IEEE 123 Nodes Test systems were used for simulation of studies of this Chapter as well.

In order to evaluate performance of the CVR scheme, the systems were also simulated under normal condition where no CVR command is in effect (i.e. every capacitors were turned OFF and every VR were left at *1pu* tap ratio for the whole simulation period). Other cases were also performed where the VR controller of proposed CVR scheme was in operation, but the capacitors were abandoned in an OFF state for the whole period. Labelled as partial CVR in the figures, these cases aid to evaluate the capacitor control module of the proposed scheme.

The main index to quantify performance of a CVR scheme is system's total power consumption which is the real power (kW) that feeder draws from transmission system at its substation. In most of the results that follows, this amount is scaled based on total nominal load (kW) served by the feeder.

## 5.6 Simulation Studies on Elementary System

The same Elementary system as described in previous chapter was used for simulations of this chapter (see section 4.6.1 of previous chapter). The only difference is the load models in the simulation were updated as given in Table 5-A. This change is intended to make the loads generally more dependent on their voltage so that impact of CVR can be better observed in the simulation results.

Table 5-A The models assigned to loads of Elementary System for CVR simulations[42]

| Load Model | Bus of the Load | | | | | | | | | |
|---|---|---|---|---|---|---|---|---|---|---|
| | 1R | 2 | 3 | 4R | 5 | 6 | 7 | 8 | 9 | 10 |
| *Constant P & Q* | | | ✓ | | | | | | | |
| *Constant Z* | | ✓ | | | ✓ | | | ✓ | ✓ | ✓ |
| *Linear P, Quadratic Q* | ✓ | | | ✓ | | | | | | |
| *Constant P, Constant I* | | | | | | ✓ | ✓ | | | |

[42] The assignment is conducted in a random manner, however, with a distribution which prioritizes more voltage-dependent type of models such as *Constant Z*

### 5.6.1 Test Description

Most of the test parameters were set similarly to those for model-free VVC in the previous chapter: scheme was simulated for a five day period with 15 capacitor switching per day for the Exploration period. The criteria chosen for stability of estimations was similar (i.e variation of estimation errors in last 12 hours becomes less than 20% of its initial value). However, only two principle components from PCA were also kept for estimations (i.e. $p=2$ in PCA process described in chapter 2). The time resolution of measurement data was assumed 1 minute, and the meters were assumed to provide voltage magnitudes only. Time delays of VR controllers were also set quite similar to model-free VVC described in section 4.6.1. A $0.01pu$ safety margin was also considered in voltage regulation. The same amount was considered as the voltage bandwidth for CVR (i.e. $BW_{CVR}=0.01pu$, see section 5.3).

### 5.6.2 Test Results

Test results are shown on Figure 5.3. For both partial and model-free CVR cases, the VR controller has successfully reduced minimum voltage of the system close to minimum regulatory limit (i.e. $0.95pu$). However, the resulted $STD_{VZ,1}$ and $STD_{VZ,2}$ are almost equal for No-CVR and Partial CVR scenarios, which demonstrates that, as expected, the VR controller alone cannot reduce voltage spread in the system. The voltage spread is only influenced by the model-free CVR case where capacitor controller is also in operation. Once the exploration period ends at the late hours of second day, both $STD_{VZ,1}$ and $STD_{VZ,2}$ are observed to decrease in the proposed CVR case. Similarly, the lowest amount of total feeder consumption is achieved by the model-free CVR after its exploration period. Nonetheless, the overall results indicate that impact of VR controller is more significant in this system. That is why total feeder consumptions under operation of partial and complete CVR cases are close to each other.

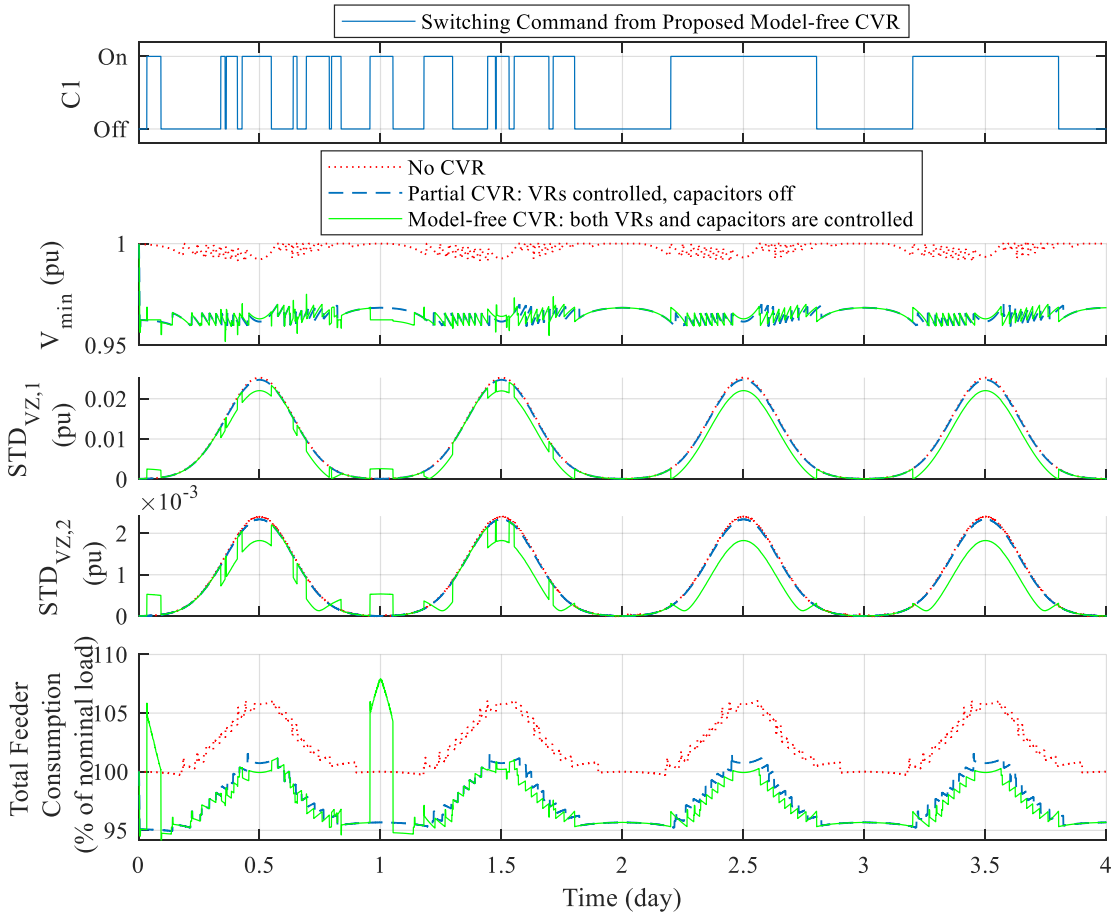


Figure 5.3 Model-free CVR performance on Elementary System (first 4 days only shown for visual quality)

## 5.7 Simulation Studies on IEEE 123 Nodes Test Feeder

The IEEE 123 Nodes Test Feeder was simulated with the load profiles described in Chapter 3 (see section 3.6). Full details such as load info and network model are given in [29]. Figure 5.4 depicts the system for simulations of this chapter. As shown on the figure, four switchable three-phase multi-step capacitor banks were added to this system for CVR simulations. Each capacitor bank consists of 8 steps of *50kvar* on each phase. Figure 5.4 also shows the location of meters which provide the data for operation of the model-free CVR scheme. Meters at critical buses are assumed to provide voltage magnitude only, while, the meters at VRs are expected to provide VR power flow and primary/secondary voltage magnitude of the VR. In order to highlight the CVR effect on the system the load models in simulations were updated to reflect more voltage-dependency on power. Table 5-B gives the assigned models for each load in the system[43].

[43] The assignment is conducted in a random manner, however, with a distribution which prioritizes more voltage-dependent type of models such as *Constant Z*

Table 5-B The models assigned to loads of IEEE 123 Nodes System for CVR simulations

| Load Model | List of Loads (labelled as *bus+phase*) |
|---|---|
| *Constant P & Q* | 7a,11a,19a,20a,28a,38b,39b,59b,63a,69a,74c,75c,77b,83c,85c,88a,90b, 100c,114a |
| *Constant Z* | 1a,2b,6c,9a,12b,16c,17c,22b,24c,30c,31c,32c,33a,34c,35a,37a,41c,42a, 43b,46a,47,48,49a,49b,49c,50c,51a,55a,58b,60a,62c,65a,66c,68a,73c,76a,79a,84 c,92c,95b,99b,107b,111a |
| *Linear P, Quadratic Q* | 4c,5c,10a,29a,45a,52a,70a,71a,76b,82a,86b,87b,94a,98a,112a,113a |
| *Constant P, Constant I* | 53a,56b,64b,65b,65c,76c,80b,96b,102c,103c,104c,106b,109a |

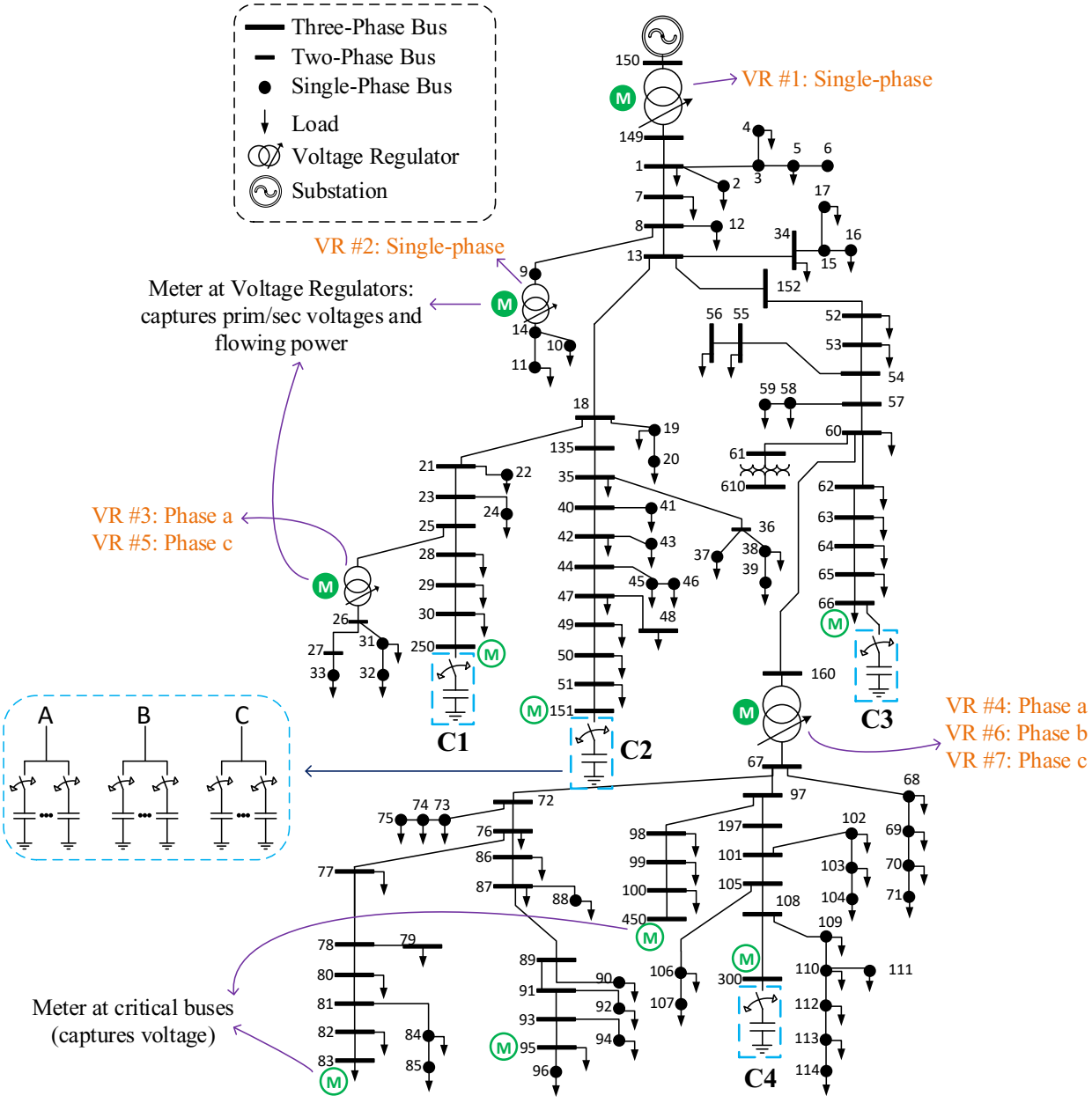


Figure 5.4 Location of capacitor banks and meters for model-free CVR test on IEEE 123 Nodes system

### 5.7.1 Base Test Description

Most of the test parameters were set similarly to those for model-free VVC in previous chapter: scheme was simulated for a ten day period with each phase of capacitor banks being switched 50 times per day for the Exploration period. The criteria chosen for stability of estimations was similar (i.e variation of estimation errors in last 12 hours becomes less than *20%* of its initial value), and four principle components from PCA were also kept for estimations (i.e. $p=4$ in PCA process described in chapter 2). The time resolution of measurement data was assumed 1 minute, and the meters were assumed to provide voltage magnitudes only. Time delays of VR controllers were also set quite similar to model-free VVC described in section 4.6.1. A *0.01pu* safety margin was similarly considered in voltage regulation. The same amount was considered as the voltage bandwidth for CVR (i.e. $BW_{CVR}=0.01pu$, see section 5.3).

### 5.7.2 Base Test Results

Figure 5.5 shows the simulation results. Only switching states of *C1* capacitor bank are shown in this figure. The length of exploration period is almost two and half days. Different number of capacitor bank steps have been switched ON for this period to collect sample data for model-free CVR. As the figure shows, the model-free CVR has successfully reduced the total feeder consumption after finishing its exploration period. In order to better illustrate the merits of proposed scheme, the true load consumption is also plotted in the figure as well. Here, the true load consumption is defined by subtraction of power loss from total feeder consumption. Hence, this index better demonstrates the performance of CVR which is mainly focusing on bringing the voltages down as much as possible. As the results show, the proposed CVR is much more effective compared to the partial CVR, especially in terms of decreasing true load consumption. The operation of model-free CVR can be further investigated by aid of Figure 5.6 and Table 5-C. Table 5-C gives the $(dP/da)_i$ coefficients calculated by the model-free CVR for this system. As explained in section 5.4, these coefficients constitute the weighting factors in overall objective of CVR's capacitor control module. Based on the this table results, the plots in Figure 5.6 makes no surprise that model-free CVR has caused the largest reduction of voltage deviations for VR zones #1 and #4 (i.e. $STD_{VZ,1}$ and $STD_{VZ,4}$). Table 5-C shows the largest $(dP/da)_i$ coefficients for these two VR zones. The model-free CVR does not necessarily need to reduce the voltage spread in every VR zone, but it certainly has to reduce it for VR zones which show the highest dependency of their load power in respect to the voltage. This is a direct outcome of the way CVR's capacitor control objective was set up in (5.2).

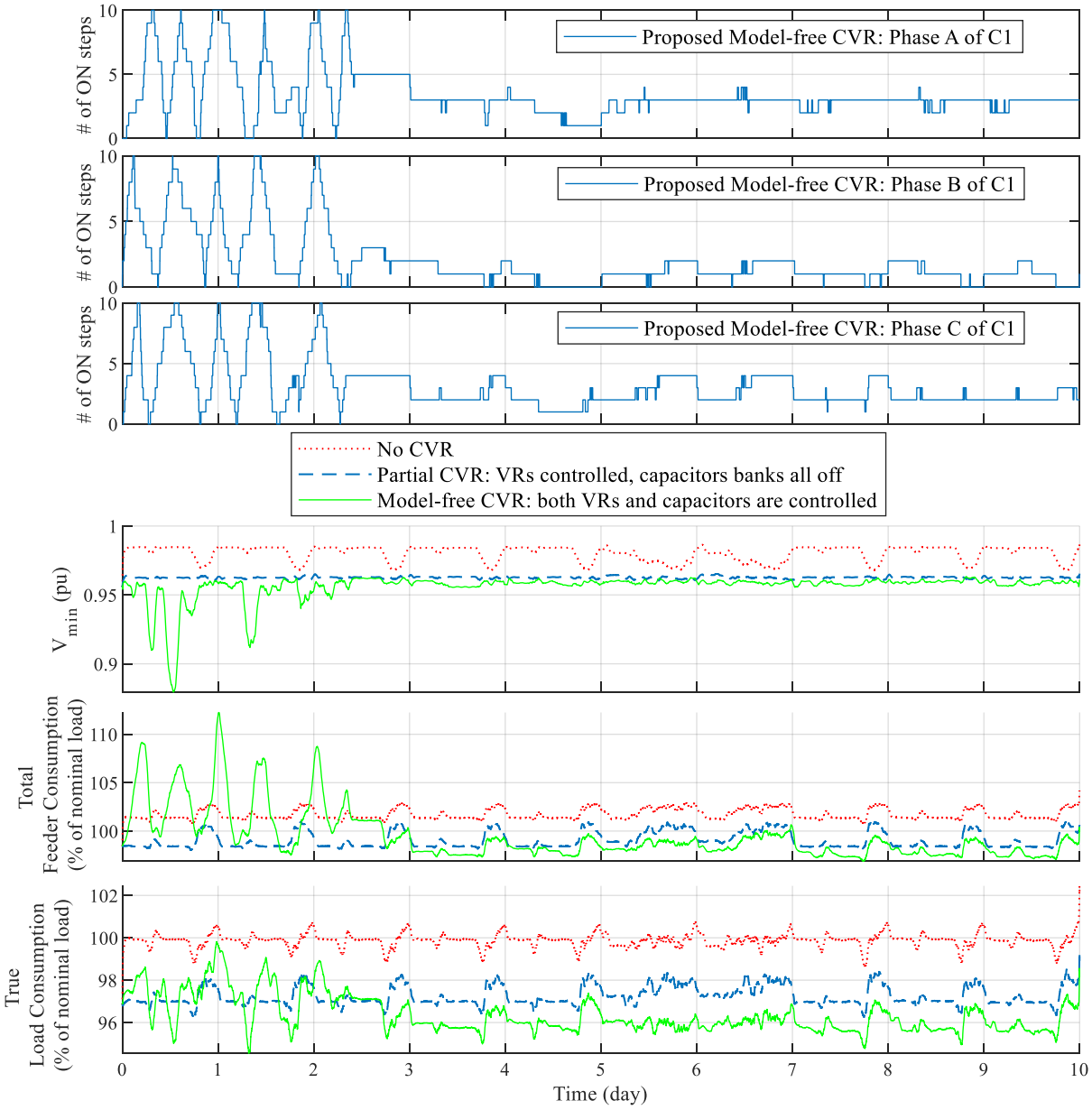


Figure 5.5 Results of model-free CVR on IEEE 123 Nodes System (plots are smoothed for better visualization)

Table 5-C *dp/da* ratio for different VR zones of IEEE 123 Nodes System obtained by model-free CVR

| VR zone No. | 1 | 2 | 3 | 4 | 5 | 6 | 7 |
|---|---|---|---|---|---|---|---|
| $\left(dP/da\right)$ | 1858.89 | 1.41 | 29.51 | 251.62 | 57.36 | 241.33 | 132.39 |

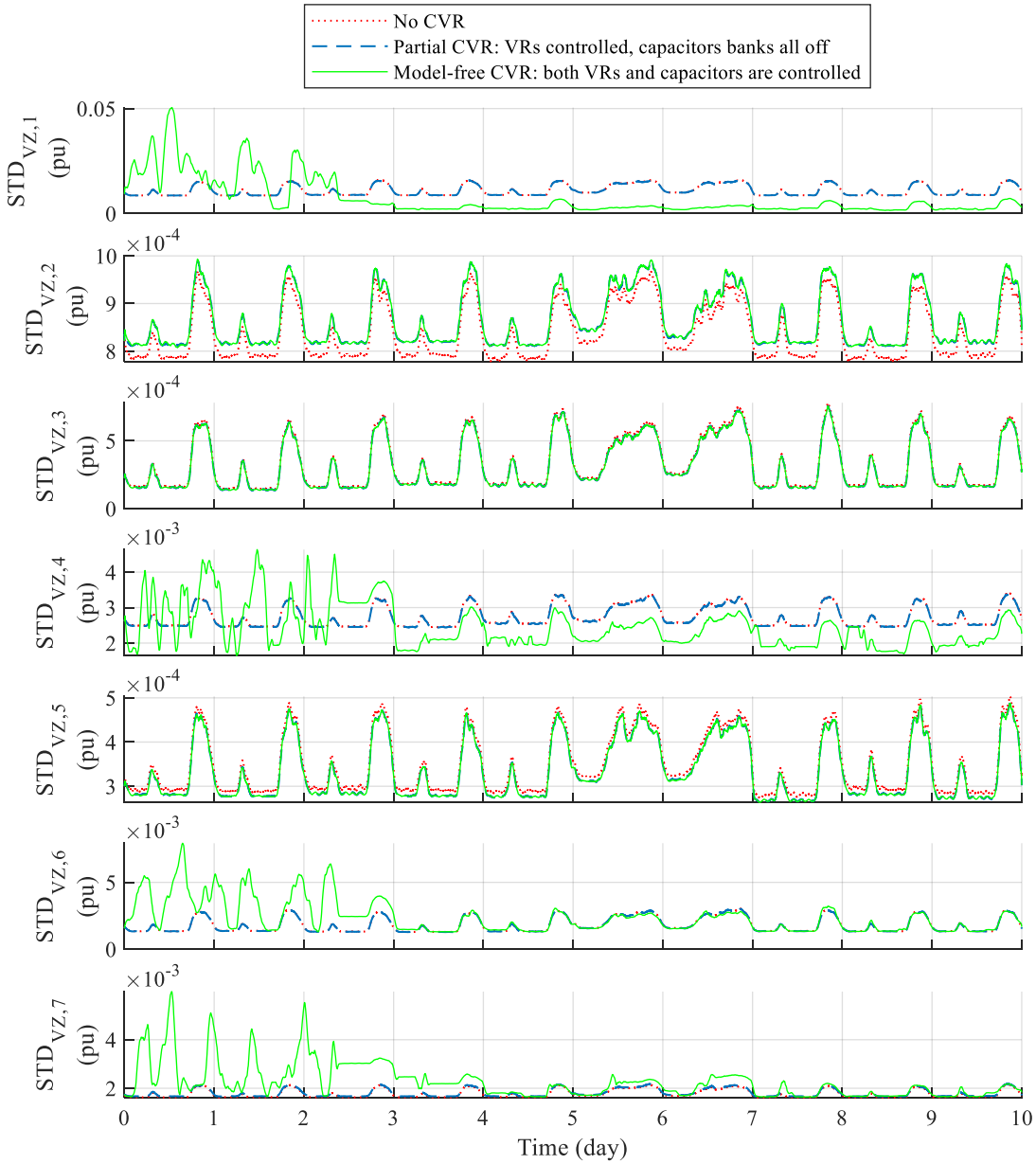


Figure 5.6 Standard deviation of voltages in VR zones of IEEE 123 Nodes System during CVR simulation

### 5.7.3 Sensitivity Studies

#### a. Presence of DERs

The base test was repeated for the IEEE system with presence of DERs. DERs were added to the system with the same characteristics described in section 3.6 of Chapter 3. DER generation profiles were also assumed to be according with Figure 3.18. The results are shown on Figure 3.18. Because of DER generations, the feeder consumption index can be no longer scaled using total nominal load. Thus, the daily average values are presented here. The chart is also replotted by scaling the results on the basis of normal condition of system (i.e. no CVR). Overall, the results demonstrate the effectiveness of proposed CVR scheme even in presence of DERs.

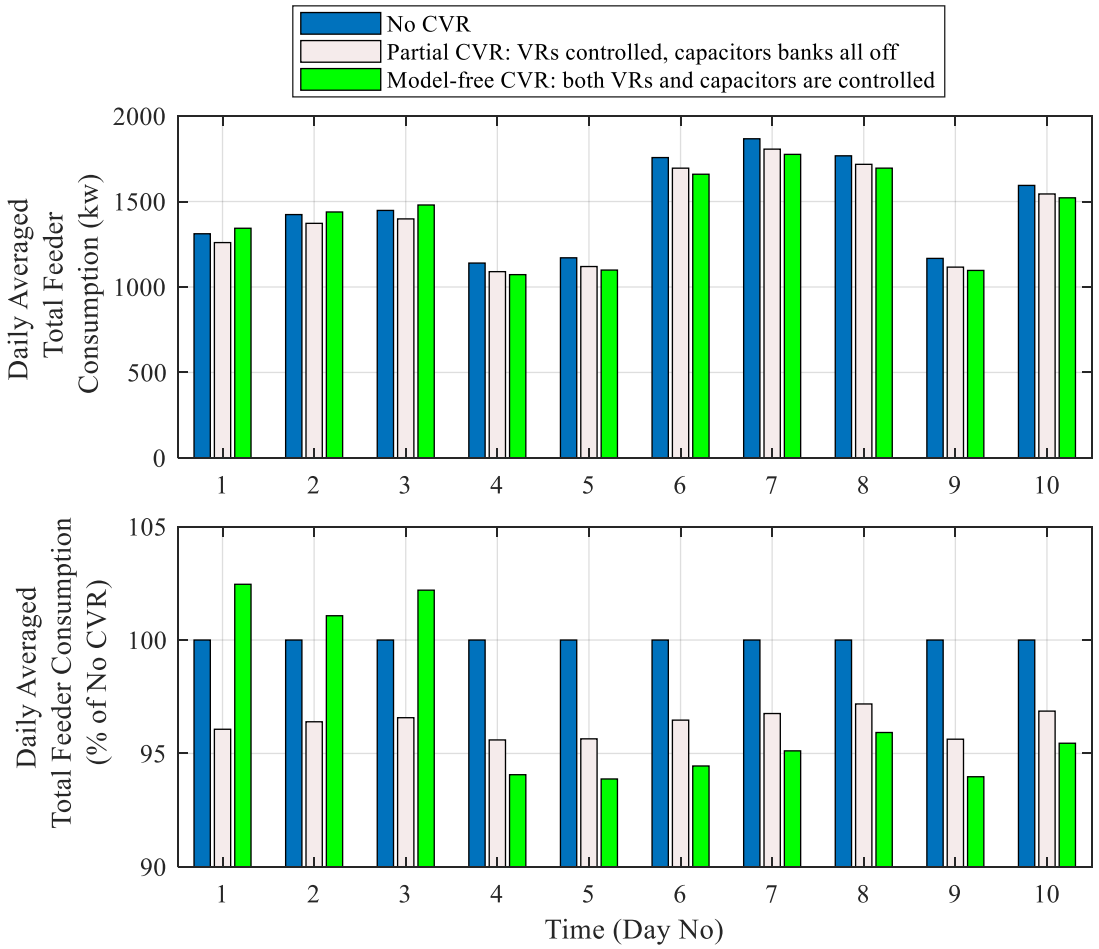


Figure 5.7 Performance of Model-free CVR on IEEE 123 Nodes Test Feeder with DERs

### b. Metering Condition

In this sensitivity study, effect of different metering conditions on performance of model-free CVR is investigated. In one sensitivity case, we assume that the scheme is supplied by AMI data, therefore, instead of only critical buses, it has access to voltages of every system nodes with the loads. The possible benefit of measuring voltage phasor angles is assessed in another simulation case. In two other cases, the effect of measurement noises is evaluated. Figure 5.8 summarizes the performance of model-free CVR under these different conditions. The results show that inclusion of AMI data has not increased the efficiency of proposed CVR scheme. Neither the case with phasor angle measurements has improved the CVR performance significantly. At least for this system, it seems that measurement of voltage magnitudes of critical nodes is sufficient for effective operation of model-free CVR. Based on the results of last two cases in the figure, the proposed CVR scheme is found robust against measurement errors up to 1%. The only observed negative effect is for case 6 in the figure, (0.5% measurement error), where the measurement error has made the exploration period longer.

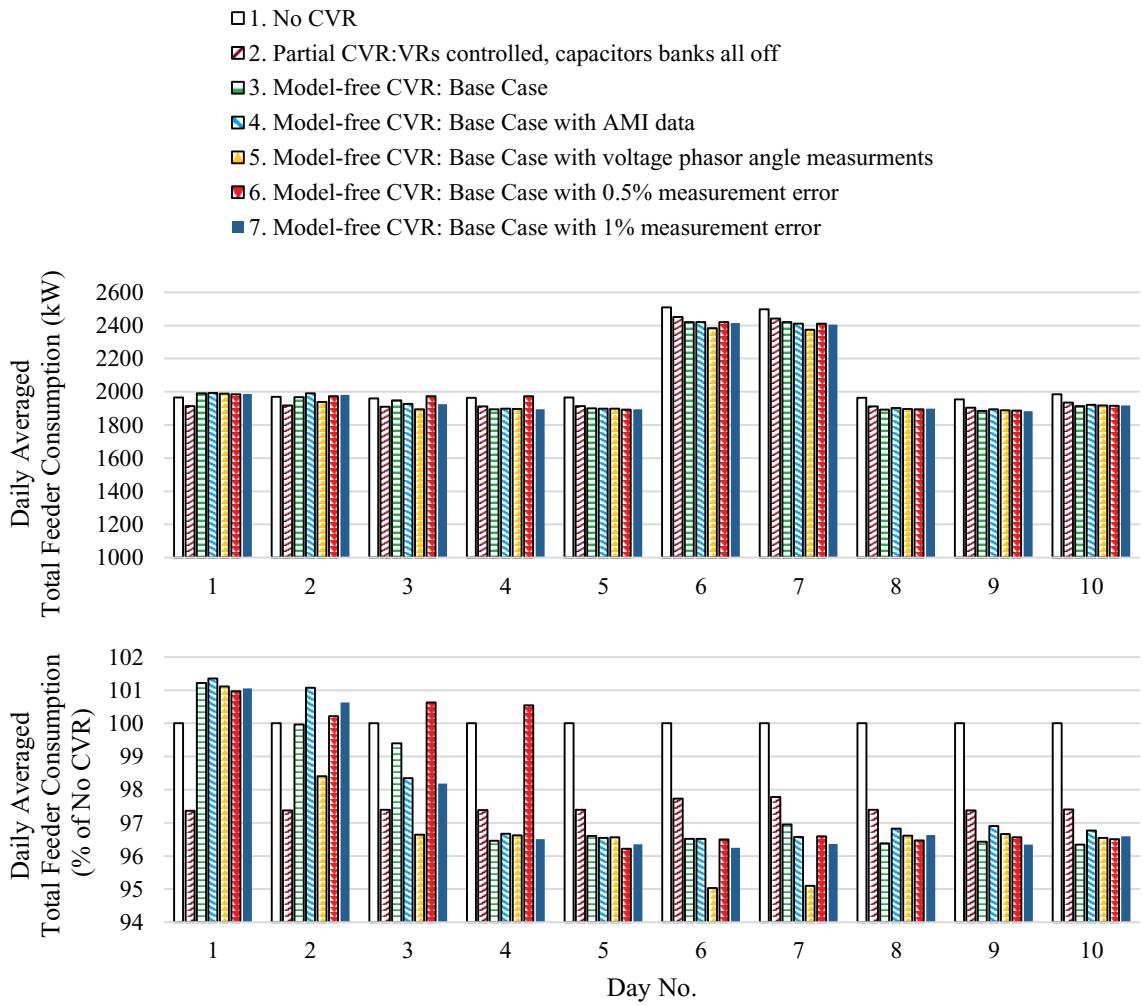


Figure 5.8 Performance of Model-free CVR under different metering scenarios

## 5.8 Summary

A model-free CVR scheme was presented in this chapter. The scheme can operate using the data from meters at substation and on VRs as wells as some critical buses such as end-of-the-line points for the system. It is also capable to control multi-step capacitor banks. Simulation studies on an Elementary system and IEEE 123 Nodes Test Feeder demonstrated the satisfactory performance of the proposed method. The proposed CVR method was also found robust against measurement noises up to 1% or lack of phasor angles in the measurement data. Interestingly, sensitivity studies showed that including AMI data for this scheme will not enhance its performance in a tangible way. Hence, the scheme can be implemented by installing a number of meters on the distribution feeders which are not equipped with AMI systems. This fact adds to the practical value of this model-free CVR scheme.

# Chapter 6

# Voltage Sag State Estimation (VSSE)

Data-driven techniques have a promising role in PQ assessment of distribution systems. VSSE is a relatively new concept for evaluating PQ condition of a system due to occurrence of voltage sag disturbances. VSSE aims to conduct this assessment on a feeder using limited number of measurement units. Most of the available VSSE methods in the literature are based on the assumption that meters only record number of the occurred sag events. In this chapter, present VSSE approach is extended by considering the fact that most of modern meters are also capable to record the voltage magnitudes of their buses during a sag event. From this perspective, a generalized formulation of VSSE is provided to cover both radial and meshed networks. This general framework can also consider the effects of an LVRT-capable DER contributing to sag profile. Available methods to solve the proposed VSSE framework are also studied. Simulation studies on the IEEE 123 nodes test feeder will be also presented to evaluate efficacy and accuracy of the proposed VSSE framework.

The studies of this chapter focus on the sag events caused by the faults inside a distribution system. The effect of VRs on sag voltage profiles is ignored. However, discussions are presented to show how the proposed formulation is capable to account for VRs or voltage sags due to transmission-system faults, motor starting or transformer energization.

## 6.1 Literature Review

Voltage sag is a short-duration reduction in a system's voltages due to short-circuit faults, overload or starting of the large motors. In technical terms, a voltage sag occurs when the RMS (Root Mean Square) of voltage is reduced below a given threshold (generally 90% of nominal voltage) from one cycle to several seconds (up to one minute) [66]-[68]. Short-circuit faults are the most common cause of voltage sags. The wide attention given to voltage sags is due to the problems they can create for operation of sensitive electrical equipment. Although they occur for a short duration, a voltage sag can happen several times a year and thus might become a source of significant financial loss [66]-[68]. According to [69], a single voltage sag event can cause manufacturer's loss from ten thousands to as high as 2 million U.S. dollars. Hence, voltage sag is widely recognized as a common and critical PQ phenomenon in a distribution system. This makes the study of severity and frequency of voltage sags as an essential part of ensuring PQ for a power distribution system. In the literature, two general approaches can be found in characterizing the

performance of a grid in terms of voltage sag occurrence. The first approach is to use stochastic methods to predict frequency and magnitude of voltage sags for a system. The predictions are usually based on circuit model and historical fault statistic data of the studied system [70]-[73]. The other approach is to directly measure voltage sag performance of the system. A common challenge to this approach is infeasibility of installing meters on every node of the grid to thoroughly measure and characterize occurrence of every voltage sag event. Such constraint is usually imposed by economic and practical considerations. The concept of Voltage Sag State Estimation (VSSE) was introduced by [74] to tackle this challenge.

The main idea of VSSE is to obtain voltage sag performance for the whole system based on the data from limited number of measurement units. The method offered by [8] is, however, limited to radial configurations. The research work in [75] employs integer linear programming to solve VSSE for meshed networks as well. In [76], genetic algorithms are applied in a similar VSSE framework. Singular-value-decomposition (SVD) was offered in [77] as a simpler and non-iterative alternative to linear programing and genetic algorithms in solving the VSSE problem. However, unlike traditional state estimations where one faces redundant number of measurements, the VSSE methods in [75]-[77] are actually dealing with an underdetermined set of equations. As the authors of [78] have noted, these techniques can be quite vulnerable to restrictive situations such as sag events due to high-impedance faults, or when observability of every faults is not guaranteed due to the number and location of installed meters. Therefore, a hybrid approach has been recently proposed by [78] and [79], which tries to combine the strength of VSSE and the stochastic methods. These works apply a Bayesian inference tool to draw the most probable conclusions on feeder sag performance using both measurements and fault statistic data. Although promising, these hybrid methods require historical data from the feeder site such as statistical fault data. And this type of requirement distinguishes them from the classic VSSE approach.

A common assumption in all of the VSSE frameworks studied in [75]-[79] is that meters only record number of occurred sag events during the monitoring period. This assumption can appear as too restrictive for modern applications, especially with the consideration of recent advances in measurement technologies available for distribution feeders. In fact, if a utility installs PQ meters for sag performance monitoring, such meters can be also expected to record the voltage magnitudes resulted for each sag event. Some modern smart meters can be also programmed to record the sag voltage magnitude beside counting the number of occurred sag events (e.g. meters by General Electrics and Aclara [80],[81]). By adopting the assumption that meters can record the sag voltages, this chapter presents a refreshed perspective on the subject of VSSE. This assumption is also consistent with the original definition of VSSE in [74]. Hence,

each sag event is individually assessed by the VSSE[44]. After collection and derivation of the voltage profile of each recorded sag event for the whole system, the average system-wide indices such as SARFI (System Average RMS Frequency Index) can be also established [68]. Compared to the original introduction of VSSE in [8], the formulation of VSSE is generalized in this chapter. Unlike [74], the proposed framework is also applicable to the meshed networks, and the impact of large DER with Low Voltage Ride-Through (LVRT) capability on the voltage sags is also taken into the account.

## 6.2 Generalized Formulation of VSSE

For a distribution grid and a specific sag event, the VSSE's task is to estimate voltage sag profile of the whole system using the measured voltages of limited number of system nodes. The circuit model of the system is also a part of the input data [74]. The exact cause of the sag event (i.e. fault type, location, etc.) is unknown. The amounts of system loads at the time of the event are generally unknown, too.

The classic state estimation formula in power system literature is as follows [84]:

$$m_i = h_i(\vec{x}) + e_i \tag{6.1}$$

The objective of state estimation is often stated as an optimization problem to find the state vector ($x$) in a manner to minimize the Sum Square of Errors ($SSE$):

$$SSE = \sum_{i=1}^{N_m} \left[ m_i - h_i(\vec{x}) \right]^2 \tag{6.2}$$

This classic formulation can be adopted for VSSE, too. The state vector will be then the system voltages during the sag event. Similarly, the measurement variables ($m_i$) will be the voltage recording of available meters during the event. The optimization problem for VSSE will be also subject to one additional equality constraint on the state vector based on the circuit equations. Since the size of state vector is larger than the number of measurements, using such framework results in an underdetermined problem which will be difficult to solve. Although the mentioned equality constraint provides some information to solve it, but it also makes the solution process more difficult at the same time. Therefore in this thesis, a new perspective is presented to simplify the VSSE problem. As a condition for this approach, we have to ignore the effect

[44] Since this definition of VSSE focuses on individual sag events, rather than total counts of the sag occurrences, one might find similarities with Fault Location Search (FLS) studies in the literature ([82],[83]). However, it remains important to recognize the distinction between VSSE and FLS methods. The primary purpose of FLS is finding the exact location (or approximate area) of a fault, while, VSSE is only concerned with voltages of the system buses during the fault event. In one view, FLS might be considered as part of solving the VSSE. Since by knowing the specification of the fault causing the sag event, one can use the system model to derive voltage of every node during the event. However, results of FLS methods generally lack full characteristics of the fault such as accurate short-circuit impedance or exact connection of phases (to each other and/or to the ground) at the fault location. Besides, a voltage sag might be caused by reasons other than faults such as motor starting. Such limitations make it hard to directly employ FLS techniques for solving the VSSE.

of loads on the VSSE problem, and the circuit is analyzed as if no loads are on it[45] . Adopting this assumption, the full specification of the fault (including its type and location), and source voltages (i.e. voltages at feeder's main substation(s)) of the feeder will be enough to fully determine voltages of every node (i.e. the state vector). Therefore, the target of VSSE is shifted from the original state vector to the full specification of the fault and the voltages at feeder source. A vector can be defined containing voltage phasors representing system voltage source(s):

$$\overrightarrow{V_S} \triangleq [V_{S,1} \quad V_{S,2} \quad \cdots \quad V_{S,N_S}]^T \tag{6.3}$$

As already stated in previous chapters, each phase of a bus is treated as a separate node in this thesis. Thus, $N_s$ in above equation represents the number of single-phase voltage sources for the system. For example, in a feeder with one three-phase substation, one should use $N_s=3$.

The process of quantifying the fault specification can itself turn as a challenging issue. Thus, a simplifying technique is used in this thesis to fully model the effect of a fault on VSSE, without the concern for detailed characteristics of the fault: any type of fault on a line is modelled as unknown current sources at sending and receiving ends of the powerline (see Figure 6.1). Although this modelling technique cannot reflect the detailed situation inside the faulted line, it is sufficient for the objective of VSSE, because it can fully represent effect of the fault on voltages of every system nodes.

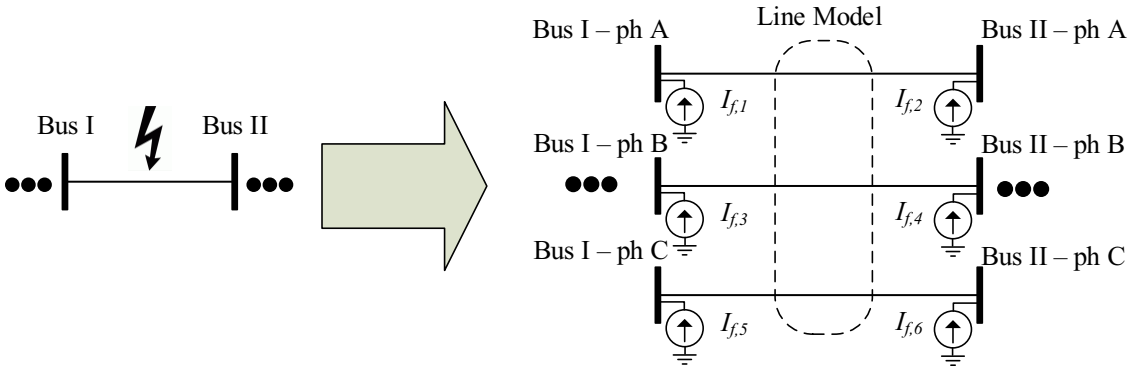


Figure 6.1 Example of modelling of (any type of) fault on a three-phase power-line with equivalent current sources

A vector can be defined to contain the unknown current phasors associated with these sources:

$$\overrightarrow{I_f} \triangleq [I_{f,1} \quad I_{f,2} \quad \cdots \quad I_{f,2\times Nph_l}]^T, \tag{6.4}$$

where $l$ is the identifier number of the line with the fault (every powerline in the system is assigned with an identifier number in our formulation). This modelling technique eliminates the difficulty of quantifying the fault type, impedance and exact location. As the next step, the relationship between sag voltages and defined vectors of $I_f$ and $V_S$ needs to be established. By circuit theory, voltages of every node can be formulated as a linear function of the voltage source vector and current injection at the other system nodes:

[45] In simulation section, the possible negative impact of this assumption will be examined.

$$\vec{V} = \mathbf{H}\vec{V_S} + \mathbf{Z}\vec{I} \tag{6.5}$$

By having the circuit information, one can obtain the above **Z** and **H** matrices by applying Kron Reduction on the bus impedance matrix ($\mathbf{Z_{bus}}$) of the system [85]. Since the loads are ignored in our formulation, a zero current injection can be assumed for every node except those belonging to the faulted line[46]. One can accordingly build the full *I* vector based on $I_f$ as shown below (all of the system nodes except the voltage source ones are assigned with an identifier number (*n)* in our formulation, and they are sorted in both *I* and *V* vectors according to their identifier numbers):

$$\vec{I}(n) = \begin{cases} \vec{I_f}(j) & \text{if } n_{l,j} = n \text{ for } j \in \{1,2,3,\cdots,2\times Nph_l\} \\ 0 & \text{else} \end{cases} \tag{6.6}$$

Overall, the state vector for generalized formulation of VSSE will consist of the voltage source vector, the equivalent current representing the effect of fault, and the identifier number of the faulted line:

$$\vec{x} = [\vec{V_S}^T \quad \vec{I_f}^T \quad l]^T \tag{6.7}$$

Based on this definition, the size of state vector can be even smaller than number of measurements. Therefore, VSSE is not necessarily an underdetermined problem anymore. In addition, the equality constraint is also eliminated, allowing a smoother solution process to VSSE.

In summary, we have defined the VSSE as an optimization problem to minimize *SSE* as defined in (6.3), where the state vector is defined in (6.7), and measurements and state variables are related as in (6.1). If the meters provide voltage phasor angles, each $m_i$ is a complex phasor value, and the definition of $h_i(x)$ will be as follows:

$$h_i(\vec{x}) = \sum_{j=1}^{2\times Nph_l} \left[ \mathbf{Z}(n_i^M, n_{l,j}) \cdot I_{f,j} \right] + \sum_{j=1}^{N_s} \left[ \mathbf{H}(n_i^M, j) \cdot V_{S,j} \right] \tag{6.8}$$

If phasor angles are not available and meters only provide voltage magnitudes, the outcome of above function should be only the magnitudes, and not a complex number. Therefore, $h_i(x)$ will change to the following form:

$$h_i(\vec{x}) = \left| \sum_{j=1}^{2\times Nph_l} \left[ \mathbf{Z}(n_i^M, n_{l,j}) \cdot I_{f,j} \right] + \sum_{j=1}^{N_s} \left[ \mathbf{H}(n_i^M, j) \cdot V_{S,j} \right] \right| \tag{6.9}$$

Once *l,* $I_f$ and $V_S$ are determined, one can use (6.5) and (6.6) to estimate voltage of every node during the sag event.

[46] The special case of nodes with DER will be discussed in next section.

## 6.3 Solutions for proposed VSSE framework

Type of the solution method for the formulated VSSE problem depends on whether the meters have the synchro-phasor capability to provide voltage phasor angles or not. Both of these conditions are considered in this section.

### 6.3.1 Measurements with voltage phasor angles

Assuming that the faulted line is specified, which means $l$ is known, then the VSSE formulas (6.1) and (6.8) can be organized into the following linear relationship presented in matrix format:

$$[V_1^M \quad V_2^M \quad \cdots \quad V_{N_m}^M]^T = [\mathbf{H} \quad \mathbf{Zm}] \begin{bmatrix} \overrightarrow{V_S} \\ \overrightarrow{I_f} \end{bmatrix} + \begin{bmatrix} e_1 \\ \vdots \\ e_{N_m} \end{bmatrix} \tag{6.10}$$

where **Zm** is a part of **Z** as defined below:

$$\mathbf{Zm}(i,j) = \mathbf{Z}(n_i^M, n_{l,j}) \quad \text{for } i: 1 \to N_m \ , j: 1 \to 2 \times Nph_l \tag{6.11}$$

By labeling the matrices and vectors of (6.10) as below,

$$\vec{y} \triangleq \begin{bmatrix} V_1^M \\ V_2^M \\ \vdots \\ V_{N_m}^M \end{bmatrix}, \mathbf{U} \triangleq [\mathbf{H} \quad \mathbf{Zm}], \vec{\beta} \triangleq \begin{bmatrix} \overrightarrow{V_S} \\ \overrightarrow{I_f} \end{bmatrix}, \vec{e} \triangleq \begin{bmatrix} e_1 \\ e_2 \\ \vdots \\ e_{N_m} \end{bmatrix} \tag{6.12}$$

The VSSE problem is transformed into a classic case of Linear Least Squares (LLS) problem [38]):

$$\vec{y} = \mathbf{U}\vec{\beta} + \vec{e} \tag{6.13}$$

The *SSE* for such LLS problem can be expressed in form of matrix multiplication:

$$SSE = (\vec{y} - \mathbf{U}\vec{\beta})^H (\vec{y} - \mathbf{U}\vec{\beta}) \tag{6.14}$$

As a typical LLS problem with complex parameters, the solution to minimization of above *SSE* will be:

$$\hat{\vec{\beta}} = (\mathbf{U}^H \mathbf{U})^{-1} \mathbf{U}^H \vec{y} \tag{6.15}$$

By using (6.12), the above estimation of $\beta$ can easily determine $V_S$ and $I_f$. However, this solution process was based on the assumption that the faulted line (i.e. $l$) is known. In order to determine this parameter ($l$), one can repeat the above procedure for all possible values of $l$ (i.e. every system line) and choose the one which leads to the lowest minimized *SSE*. As an alternative for saving computational burden/time, one can

limit this search to only more probable values of *l*. For example, the search space can be reduced to only include lines around nodes with relatively lower recorded values of voltage.

### 6.3.2 Measurements without voltage phasor angles

For this case, the *SSE* (which is the objective of optimization) will have a more complicated and nonlinear format. Based on (6.9), *SSE* can be expressed as:

$$SSE = \sum_{i=1}^{N_m} \left[ V_i^M - \left| \sum_{j=1}^{2\times Nph_l} \left[ \mathbf{Z}(n_i^M, n_{l,j}) \cdot I_{f,j} \right] + \sum_{j=1}^{N_s} \left[ \mathbf{H}(i,j) \cdot V_{S,j} \right] \right| \right]^2 \tag{6.16}$$

Differently from (6.10), the $V_i^M$ values will no longer be the complex voltage phasors, but become voltage magnitudes. In this case, minimization of *SSE* becomes a classic format of Nonlinear Least Square (NLLS) problems. Thus, one of the several algorithms available in literature for solving NLLS problems can be applied here [38]. Nature of $I_f$ and $V_S$ is different from *l;* one is discrete, and the other two consist of continuous complex numbers. Generally, it is difficult to handle both discrete and continuous variables in most of the NLLS algorithms. Therefore, a better approach is to repeat the NLLS algorithm with different *l* and choose the one leading to the lowest minimized *SSE* (similarly to our suggestion for LLS in previous section). Each complex variable is also more convenient to be implemented as two separate variables (one for real part and the other for imaginary part, or, one for magnitude and the other for angle). To help with the solution process of NLLS, one can also assume that angles of voltage sources are known (i.e. assigning angles of *0°,-120°,120°* to three-phase of the source, by assuming a balanced source at substation). Thus, only magnitudes of $V_S$ is put inside the unknown variables to be determined by the NLLS algorithm.

## 6.4 Other considerations for VSSE

So far in this chapter, the generalized formulation for VSSE in distribution systems, and the corresponding solution techniques have been presented. These discussions assumed a generic distribution feeder without any large DER unit. The next topic to consider is how the proposed VSSE framework can cover this factor in a distribution feeder.

For DERs and their impact on VSSE or voltage sags in general, one only needs to concern about the large units that have LVRT capability. Because, the other relatively smaller DER units will usually trip due to an under-voltage or over-voltage protection during sag or swell events, thus their role on voltage sag profiles (and VSSE) can be neglected. Similar to $I_f$ definition, the contribution of a DER on system voltages can be accounted for by a vector of current phasors representing DER current injection into the grid. Next, this unknown vector ($I_{DER}$) can be included in the state vector of VSSE as follows:

$$\vec{x} = [\overrightarrow{V_S}^T \quad \overrightarrow{I_{DER}}^T \quad \overrightarrow{I_f}^T \quad l]^T \tag{6.17}$$

Now, all the same procedure and algorithms described in previous sections can be still used to solve the VSSE.

The impact of feeder switches can be also recognized in the proposed VSSE framework by noting that they will change the **Z** and **H** matrices. Without loss of generality, we assume that status of feeder switches are known during the recorded sag events. If unknown (i.e. the monitoring system does not record status of feeder switches), these variables can be also included as part of VSSE problem similar to the $l$ parameter. Although VR equipment are not considered in this chapter, they can be also recognized in the VSSE formulation by similar modifications.

In the studies of this thesis, we have ignored the possibility of simultaneous faults leading to a sag event. However, the formulation can be expanded to take this possibility into account as well (e.g. more than one $I_f$ vectors can be defined inside the state vector). If the fault which is causing voltage sag is outside the main feeder (e.g. on parallel feeder or on transmission system), its effect will be still reflected on the $V_S$ vector, thus the proposed VSSE formulation can cover such scenarios, too. In addition, if the sag event is not caused by a fault, but a motor starting or transformer energization, its source can be still captured as additional elements of $I_f$ in the state vector of VSSE.

## 6.5 Simulation Studies

Simulation studies were performed to evaluate the accuracy and efficacy of proposed VSSE framework. Several sag events were simulated to study the proposed VSSE methods under different conditions such as meshed or radial feeder configuration, DER presence, and various fault locations. Both meter possibilities of whether having or not having phasor angle measurement capability were taken into account. Simulation of the sag events were conducted by OpenDSS software with the Matlab interference. The algorithm of VSSE methods were implemented by the Matlab codes.

### 6.5.1 System Description

The IEEE 123 Nodes Test Feeder was chosen for the simulations. Unlike simulations presented in previous chapters, one of the default feeder switches of this system is also included to provide the opportunity to study this system under both radial and meshed configurations. Figure 6.2 shows the schematic of this system where this feeder switch is also shown. Detailed information of this system including lines and the loads can be found in [29]. Since this system includes both balanced and unbalanced loads, three-phase and two/single-phase feeder sections, it can serve as a serious test to the proposed VSSE methods. As

aforementioned, VRs are not considered in the studies of this chapter, hence, VRs of this test system were replaced by short-circuit connections for the simulations. As shown on Figure 6.2, a relatively large DER unit with generation of 10MW is also added to bus 250 of this system (See Figure 6.2 for bus labels). This DER unit is assumed with a LVRT capability, thus it avoids disconnection during sag events, and needs to be accounted for in the VSSE process.

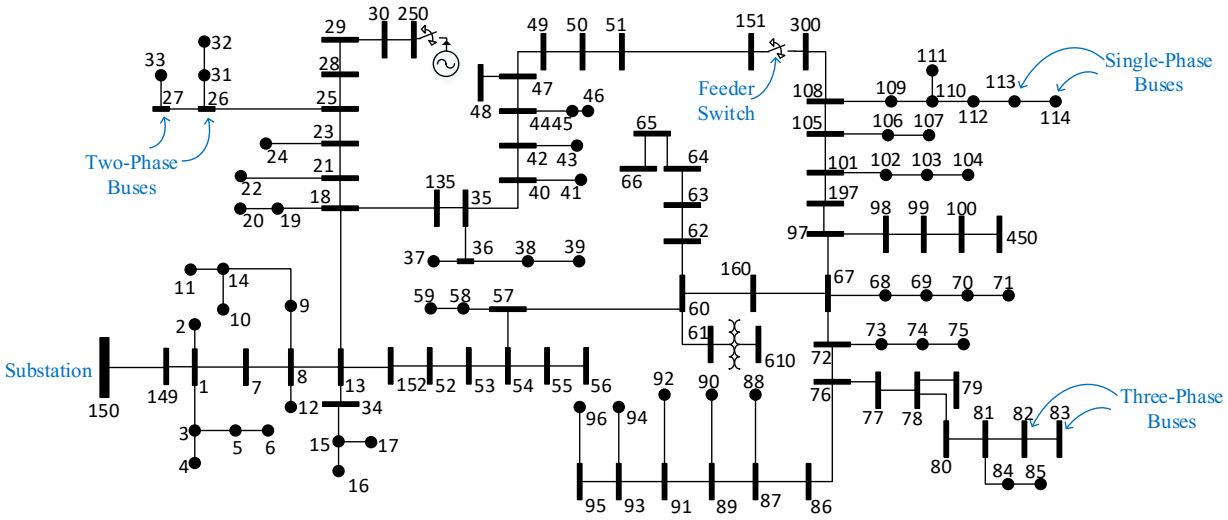


Figure 6.2 Schematic of IEEE 123 Nodes Test Feeder with the feeder switch and VRs eliminated

### 6.5.2 Scenario Description

In order to consider different measurement possibilities and system capabilities, each of the sag events were studied by the proposed VSSE framework under four scenarios:

**Scenario 1:** the sag meters are assumed with synchro-phasor measurement capability. Therefore, captured voltages include phasors.

**Scenario 3: s**ag meters are assumed without synchro-phasor measurement capability. Therefore, captured voltages only include magnitudes.

**Scenario 2** and **Scenario 4** are quite similar to scenario 1 and scenario 3, respectively, but, a 0.5% measurement error was also considered in the measurement obtained from every meters. A Gaussian function was considered for error distribution.

For each sag event, the sag meters were randomly distributed across the system. In this chapter, the percentage of system nodes equipped with meters is also referred to as ‘meter penetration’. Five different

levels of meter penetration were tested for each sag event and each scenario: 10%, 25%, 50%, 75% and 100%.

### 6.5.3 Studied Sag Events

Several sag events were simulated to test the accuracy of proposed VSSE methods. The main studied sag events were considered to occur due to a double-phase-to-ground fault (LLG) at the power line connecting buses 57 and 60 in the system. The fault was assumed to occur on 10% (of line length) distance from bus 57, with a resistive impedance of $0.1\Omega$. These main sag events were intended to cover different conditions of the system as per the descriptions that follows.

**Sag Event 1:** the event was assumed to happen in a radial configuration of the system (i.e. the feeder switch between buses 151 and 300 is open, see Figure 6.2). The DER unit was assumed OFF the circuit.
**Sag Event 2:** the event was assumed to happen in a meshed configuration of the system (i.e. the feeder switch between buses 151 and 300 is closed, see Figure 6.2). Again, the DER unit was assumed not to be on the circuit.
**Sag Event 3:** same as the first sag event, but the DER was assumed to be connected to the system and riding through the fault event.
**Sag Event 4:** similar to the second sag event (meshed configuration), but, the DER unit was also switched ON. This sag event probably presents the most complicated condition of the test system for the VSSE.
**Sag Event 5:** same as the sag event No. 4, but the system was assumed at a no-load condition during sag event. By comparing the result VSSE on this event with the fifth sag event, we can understand the impact of ignoring loads in the proposed VSSE framework.
**Sag Event 6~20:** these sag events were considered with different fault location and type characteristics. A reliable VSSE framework is expected to remain accurate for different faults causing the sag/swell in the system. The system condition assumed during these sag events was the same as the fourth sag event (i.e. meshed configuration with the DER unit switched ON). All types of single-phase-to-ground (LG), double-phase-to-ground (LLG), and three-phase-to-ground (LLLG) faults were considered as the causes for these events. Table 6-A gives the characteristics of the faults assumed to cause each of these events.

Table 6-A Specification of the faults causing the simulated sag events

| Sag Event No. | Faulted Line | | Fault Location (%)[a] | Fault Impedance(Ω) | Fault Type |
|---|---|---|---|---|---|
| | Bus I | Bus II | | | |
| 1~5 | 57 | 60 | 10 | 0.1 | LLG |
| 6~8 | 57 | 60 | 10 | 0.1 | 6:LG, 7:LLG, 8:LLLG |
| 9~11 | 7 | 8 | 90 | 5 | 9:LG, 10:LLG, 11:LLLG |
| 12~14 | 25 | 28 | 70 | 2 | 12:LG, 13:LLG, 14:LLLG |
| 15~17 | 51 | 151 | 50 | 0.01 | 15:LG, 16:LLG, 17:LLLG |
| 18~20 | 91 | 93 | 30 | 1 | 18:LG, 19:LLG, 20:LLLG |

[a] Distance from bus I of the line (in percentage of line's length)

### 6.5.4 Employed Algorithms

For scenarios 1 and 2, the problem is linear, thus, the LLS method as described in section IV.A is sufficient. As discussed in section 6.3.2, the VSSE problem for scenarios 3 and 4 turns as a nonlinear one, thus, a NLLS method is required. For simulations of this chapter, the default NLLS algorithm of Matlab Optimization Toolbox was used: Trust-region-reflective. This algorithm is within the category of trust-region methods and operates based on the interior-reflective Newton method [87],[88].

### 6.5.5 Results

Figure 6.3 shows the voltage profile for Sag Event 4. This event is expected as one of the most serious tests to the VSSE framework, since the system is in a meshed configuration, and the DER unit is also present in the system during the event. As aforementioned, an LLG fault is causing this event. Consequently, a voltage sag is observed for the two faulted phases (A & B), while, phase C shows a voltage swell. This plot shows the estimated voltages from application of the VSSE method in the fourth scenario (i.e. voltage magnitudes are available only, and the measurement error is considered too). The results are given for both metering penetrations of 10% and 25%. For the 25% case (see Figure 6.3(b)), the actual and estimated values are matching very well in voltage profiles of all the three phases. The obtained average estimation error is 0.36%. Thus, the proposed VSSE method has been successful in estimating voltages for both the voltage sag and voltage swell in this event at the 25% meter penetration. In the case of 10% meter penetration (see Figure 6.3(b)), a mismatch between the estimation and actual values are observed for some system nodes. This shows that for any system, a particular number of meters are at least required to guarantee accurate estimations.

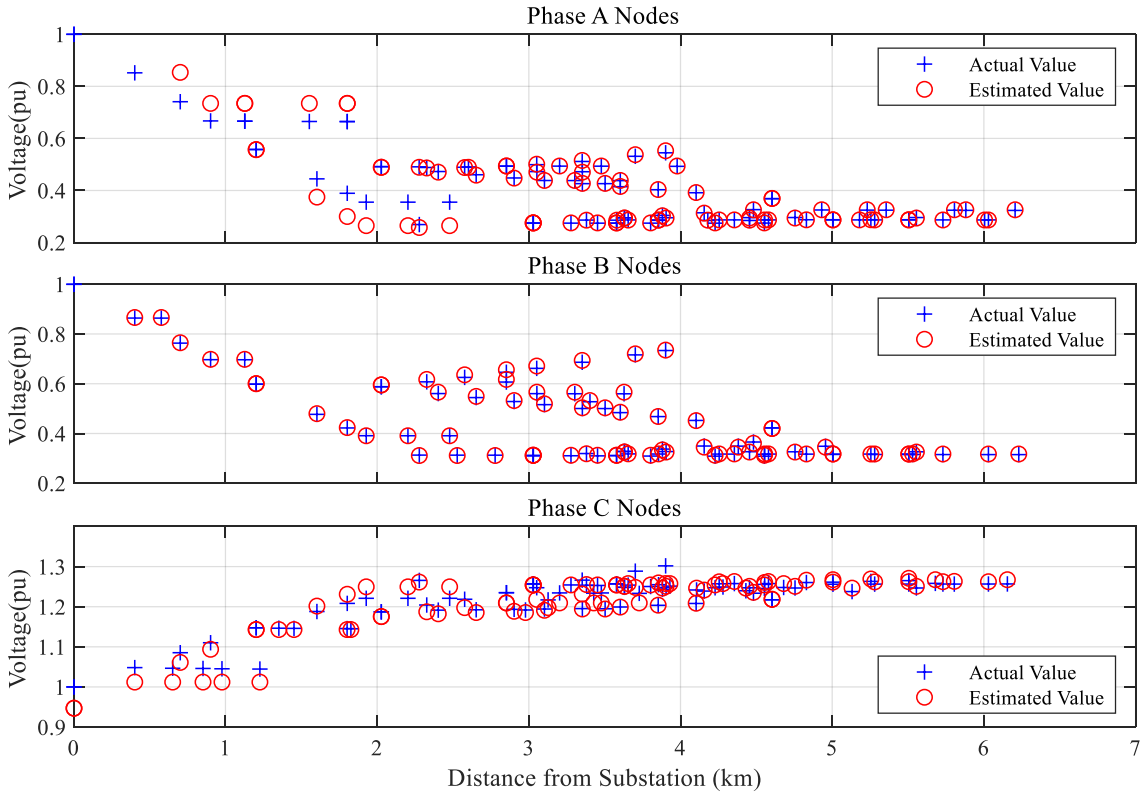


**(a)** for 10% meter penetration

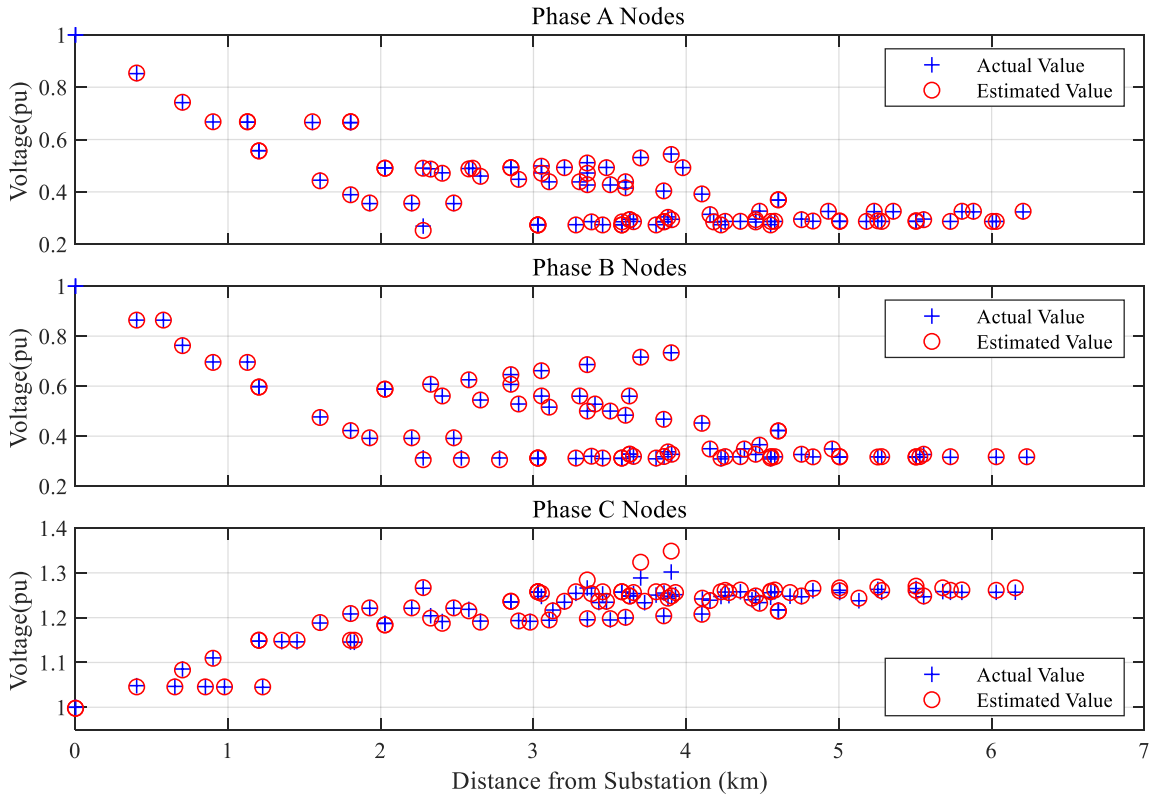


**(b)** for 25% meter penetration

Figure 6.3 Resulted voltage profile from applying proposed VSSE on sag event 4, scenario 4

As discussed in section 6.3.2, one step of the proposed VSSE process is to find the faulted line (i.e. *l* parameter in the state vector), which is done by repeating the NLLS algorithm with different lines assumed to contain the fault. The result associated with the lowest obtained minimized *SSE* will be accordingly chosen.

Figure 6.4 (a) shows some values of the lowest obtained minimized *SSE* for this case of applying VSSE. The true faulted line is from bus 57 to 60, while, the line from 54 to 57 has led to the lowest minimized *SSE*. This discrepancy is understandable due to closeness of fault location to bus 57. Indeed, the next line with the lowest value of minimized *SSE* is the true faulted line (57 to 60). Nonetheless, this type of negligible errors in detecting the faulted line can be tolerated since fault location detection is not within the purpose of proposed VSSE methods; the main objective is estimating voltages of unmonitored nodes, which is fortunately achieved by a small error. In addition, this error for detecting *l* is not always present. For instant, Figure 6.4(b) shows the obtained minimized *SSE* values in VSSE analysis of Sag Event 8 under the same scenario and meter penetration. This time, the lowest minimized *SSE* belongs to the line from bus 57 to 60 which is the true faulted line for this sag event.

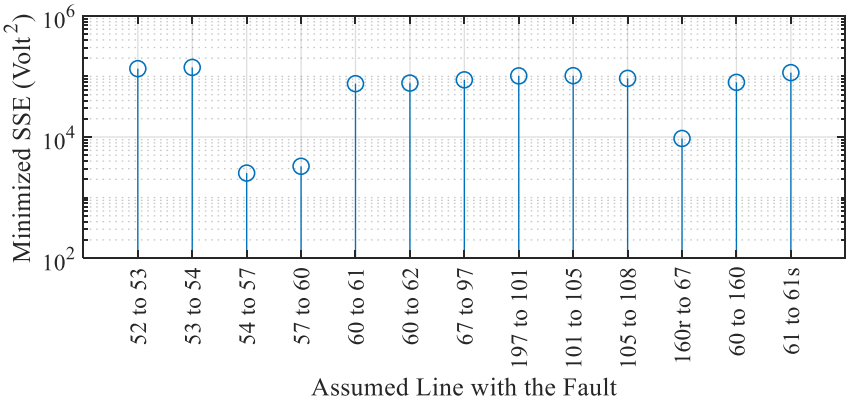


**(a)** Sag event 4, scenario 4, 25% meter penetration

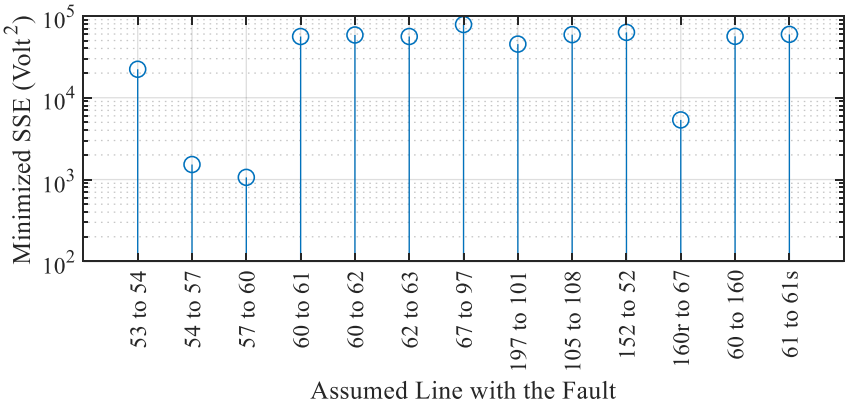


**(b)** Sag event 8, scenario 4, 25% meter penetration

Figure 6.4 Evaluating minimized SSE to detect the true faulted line

The proposed VSSE methods were tested for all the other sag events and different metering scenarios. The charts in Figure 6.5 give the average estimation error resulted from applying the VSSE methods on the cases associated with main sag events (i.e. sag event 1~5). The method has shown a very good accuracy (error of less than 1%) for all these events, especially when 25% or more of the nodes are equipped with the meters. The interesting observation is that presence of the DER unit has not adversely affected the estimation results. The error for sag events on the meshed configuration is also quite close to that of radial cases. Overall, the proposed VSSE methods are found robust against such complications in the system.

Since there is a no-load condition in Sag Event 5, it was expected to be the most compatible one and to lead to the highest accuracy with the proposed VSSE framework (which ignores the effect of system loads on the voltage sag profile). However, as Figure 6.5 shows, the error for the sag event 6 is found only slightly smaller compared to the other sag events except for scenario 1. It reveals that ignoring the effect of loads is generally harmless to the proposed VSSE framework, unless there is an ideal metering condition where voltage phasor angles are measured, and no measurement error is present.

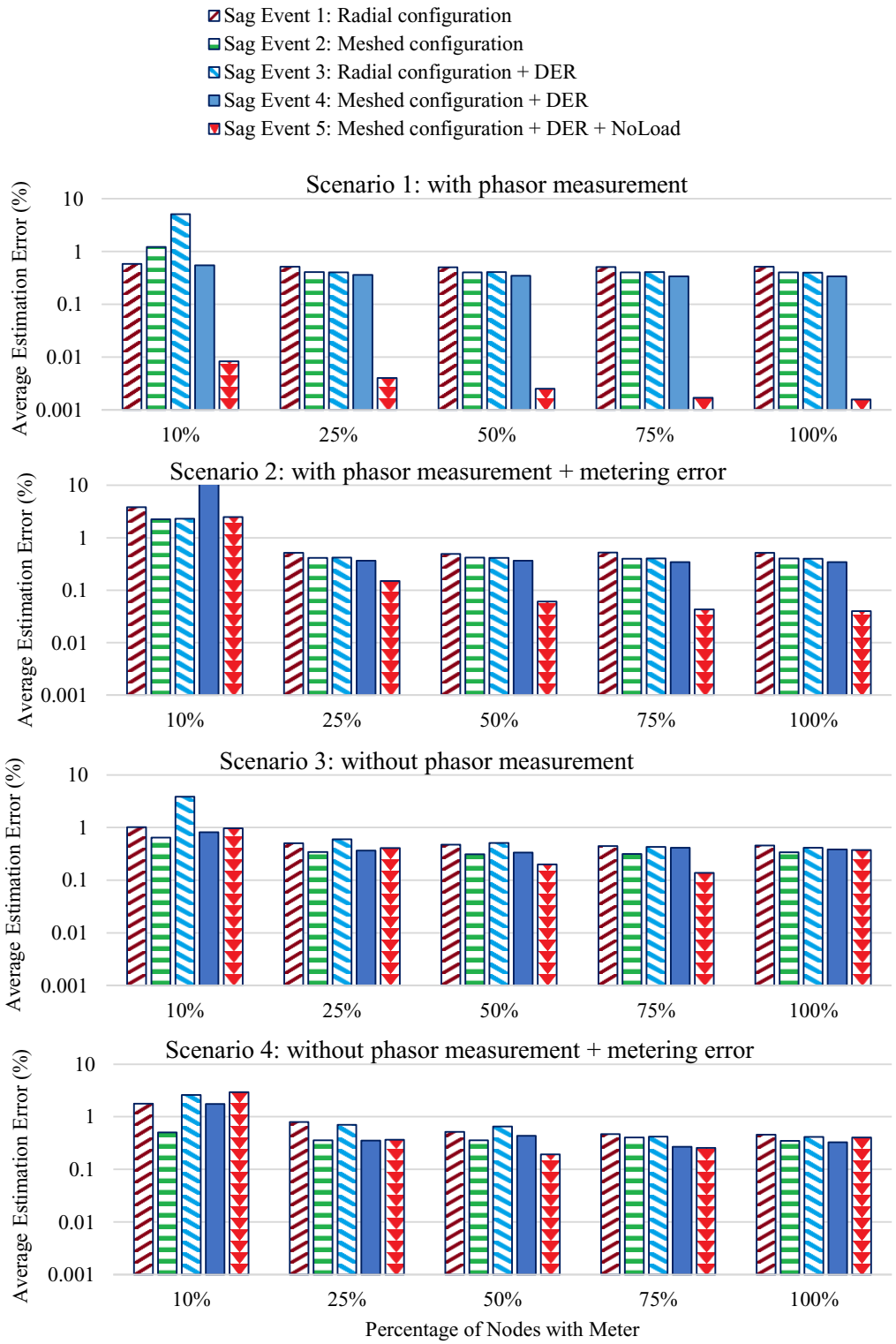


Figure 6.5 Average error of VSSE applied to sag events 1~5 at different metering scenarios

In all the studied sag events and for both scenarios of having or not having voltage phasors, a negligible effect of measurement noise on the estimation error is observed. Therefore, the proposed method seems robust against this level of measurement noise. Overall, the results of scenarios 3 & 4 are quite close to those of scenarios 1 & 2. This observation shows that lack of phasor angles in the data from sag monitoring system is not a big concern for accuracy of VSSE results. However, the advantage of having the phasor angles will certainty remains as involvement of a simpler method (i.e. LLS) in the VSSE process, leading to an overall lower computational burden.

The estimation error from applying VSSE methods on the sag events 6~20 is also presented on Figure 6.6. These results demonstrate the efficacy of proposed VSSE framework for various sag events caused by different combinations of fault types and locations. Nevertheless, some cases with 10% meter penetration have shown unacceptable errors. Thus, one can conclude that more than 10% of this system's nodes have to be equipped with meters for effective voltage sag estimation.


Figure 6.6 Average error of applying VSSE to sag events 7~21 (different fault type and locations)

In addition, results of both Figure 6.5 and Figure 6.6 show that estimation error doesn't decrease significantly for the meter penetrations more than 25%, and the 25% case gives a satisfactory result for every scenarios and sag events of this system.

## 6.6 Summary

A generalized formulation of VSSE problem was presented in this chapter. The proposed formulation can handle meshed networks and presence of DER units with LVRT characteristic contributing to voltage sags. Compared to recent advancement of VSSE in the literature, the proposed framework takes advantage of the

capability of modern meters which are not only able to capture the count of sag events, but also capable to record voltage sag magnitude. The VSSE problem was simplified to a classic form of linear-least-squares for the case that meters can capture phasor angles of the voltages. In the more common scenario where meters only record the voltage magnitudes during the sag event, the problem was shown to turn as a nonlinear-least-squares.

Simulation studies demonstrated the efficacy and accuracy of proposed VSSE frameworks. Several sag events caused by different faults (i.e. various locations, types and impedance) happening on different configurations of the feeder (e.g. meshed or radial) were considered to demonstrate versatility of the proposed VSSE methods. For the tested IEEE 123 nodes system, it was found sufficient to equip 25% of nodes with meter to guarantee accurate VSSE results. Interestingly, the studies also showed that accurate results are still achievable even if meters only record voltage magnitudes. The VSSE outcome was also found robust against a measurement noise of 0.5% on every meters.

# Chapter 7

# Conclusions and Future Work

The thesis presented a novel data-driven approach toward assessment and control of distribution systems. This data-driven approach allows for implementation of several control and assessment strategies independent of system models. Model-free feature is considerably beneficial for a system operator since it removes the challenging efforts of collecting comprehensive models for each individual distribution feeder. Moreover, the common errors and deficiencies present in the models will not affect the performance of a model-free technique. Especially, when it comes to assessment of a control scheme which is itself dependent on the system models, a model-free approach seems the only proper assessment technique.

A unified statistical framework was developed as a foundation for most model-free control and assessment techniques offered in this thesis. The theories of this framework were established by rigorous power circuit analysis. The main function of such statistical framework is to process the measurement data in order to estimate how indices such as voltages and power loss change with different capacitor switching events. Although the scheme was merely focusing on capacitor switching events, the impact of VRs were also taken into the account. It was shown how this framework can realize model-free VVC or CVR schemes which control both capacitors and VRs.

Several simulation studies were presented to evaluate the accuracy and efficacy of proposed methods. The model-free assessment method was demonstrated as effective in predicting performance of a system under different open-loop VVC algorithms. The model-free VVC and CVR schemes need a few day of initial exploration to collect enough measurement samples for their estimations. These schemes were also observed to deliver satisfactory result after their exploration period ends.

Simulation studies also confirmed that most of the stringent assumptions adopted for theories of the proposed statistical framework can be relaxed for the practical applications. Indeed, the model-free VVC remained effective by even adopting measurement characteristics consistent with existing AMI systems. For example, their performance was not severely affected by lack of synchro-phasor measurement or a 15 minute time resolution. Even loss of up to 10% of meter data didn't prove to significantly affect the performance of the proposed VVC. The proposed CVR scheme doesn't even require the installation of AMI systems. It only needs meter at the feeder's substation, VRs and on the critical buses of the system. Simulation results demonstrated the effectiveness of proposed CVR in controlling the multi-step capacitor banks as well.

As a prominent example of data-driven approach in PQ assessment, VSSE methods were also considered as a subject in this thesis. The VSSE formulation was generalized to overcome the shortcoming of the present methods in the literature. The improved formulation was shown to cover the meshed configurations as well as the radial ones. Moreover, the impact of LVRT-capable DERs were considered in the proposed framework. Simulation studies demonstrated that the proposed VSSE can accurately estimate complete sag profile of the system even when only 25% of system nodes are equipped with meters.

Overall, the studies of this thesis demonstrated feasibility of data-driven approach in assessment and control of distribution systems. This promising outcome suggests a novel application for emerging measurement and communication technologies in operation of modern grids. Nevertheless, the studies presented in this thesis only constitute the very beginning step on this novel research path. The following gives a list of the author's suggestions for continuing research on this topic:

- The proposed statistical framework was found sufficient to serve model-free VVC and CVR operation of capacitors and VRs. However, the model-free assessment method was limited to capacitor-based VVCs. If one upgrades the statistical framework to estimate power loss changes due to VR operations, more comprehensive VVCs (i.e. controlling both VR and capacitors) can be covered by the model-free assessment method. The presented definition of modified voltage vectors might be also extended to include the meshed feeder configurations as well.
- Extending the VVC assessment method to cover closed-loop VVCs which use an online feedback from system measurements
- The possible benefit of employing more advanced regression and dimension reduction techniques can be investigated. There is also the possibility of optimizing the parameters of the regression analysis (such as $k$ in KNN) during the system operation. One can also study the potential benefit of using Feature Selection techniques to realize parametric regression in the proposed statistical framework.
- A time-based weighting factor can be introduced in the proposed statistical framework in order to equip it for operation of systems which undergo feeder reconfiguration or time-variant characteristics such as power-line impedances affected by ambient conditions.
- For large-scale application of proposed data-driven methods, the statistical estimations (including regression and dimension reduction methods) can be implemented by recursive programming in order to save on the computation burden.
- A basic VVC scheme was under consideration of this thesis. In future, the model-free methods can also consider the control of multi-step capacitor banks, and possible combination of VVC and CVR objectives into a unified scheme. An extra algorithm can be also embedded inside the VR controller

to automatically detect the nodes inside each VR zone based on the measurement data. Such algorithm can continue to update this information in case of feeder reconfiguration during operation.

- The methods can be further developed and tested on more comprehensive simulation platforms. The modelling details can be extended down to the level of each electric appliance time of use and power-voltage dependency. The effect of ambient conditions can be considered too. Electric Vehicles and Storage Energy systems can be included as part of the simulations as well. A Mont-Carlo simulation platform can give account to the impact of all these probabilistic factors in a real-world system.
- In the simulation studies of this thesis, the possible effect of DER on proposed data-driven methods was examined. In future, the possible interaction of local volt/var controls of each DER[47] on these data-driven methods can be investigated too.
- The proposed VSSE framework is capable to handle the effect of LVRT-capable DERs. This framework can be expanded in future to take the VR equipment into account as well. The efficiency of this VSSE framework can be also assessed in studying the sag events that originate from transmission systems or parallel distribution feeders.

[47] See [89],[90] for more information regarding distributed or local volt/var control methods for DERs.

# References


[1] A. Ipakchi and F. Albuyeh, "Grid of the future," in *IEEE Power and Energy Magazine*, vol. 7, no. 2, pp. 52-62, March-April 2009.

[2] X. Fang, S. Misra, G. Xue and D. Yang, "Smart Grid — The New and Improved Power Grid: A Survey," in *IEEE Communications Surveys & Tutorials*, vol. 14, no. 4, pp. 944-980, Fourth Quarter 2012.

[3] H. Farhangi, "The path of the smart grid," *IEEE Power and Energy Magazine*, vol. 8, no. 1, pp. 18-28, January-February 2010.

[4] S. T. Mak, *New Technologies for Smart Grid Operation*, IOP Publishing Ltd, 2015.

[5] M. Thesing, "Integrating Electric Meter Data with Distribution Automation Applications," in *PES T&D 2012*, Orlando, FL, 2012, pp. 1-6.

[6] S. Galli, A. Scaglione and Z. Wang, "For the Grid and Through the Grid: The Role of Power Line Communications in the Smart Grid," *Proceedings of the IEEE*, vol. 99, no. 6, pp. 998-1027, June 2011.

[7] Mohassel, R.R., Fung, A., Mohammadi, F., and Raahemifar, K. "A Survey on Advanced Metering Infrastructure," *International Journal of Electrical Power & Energy Systems*, *63*, pp.473-484, 2014.

[8] T. A. Short, "Advanced Metering for Phase Identification, Transformer Identification, and Secondary Modeling," *IEEE Trans. Smart Grid*, vol. 4, no. 2, pp. 651-658, June 2013.

[9] J. Peppanen, M. J. Reno, M. Thakkar, S. Grijalva and R. G. Harley, "Leveraging AMI Data for Distribution System Model Calibration and Situational Awareness," *IEEE Transactions on Smart Grid*, vol. 6, no. 4, pp. 2050-2059, July 2015.

[10] E. T. Jauch, "Volt/var management? An essential "SMART" function," *Power Systems Conference and Exposition, 2009. PSCE '09. IEEE/PES*, Seattle, WA, 2009, pp. 1-7

[11] Z. Wang, and J. Wang, "Review on Implementation and Assessment of Conservation Voltage Reduction," *IEEE Trans. Power Systems*, vol. 29, no. 3, pp. 1306-1315, May 2014.

[12] Moein Manbachi, Hassan Farhangi, Ali Palizban, Siamak Arzanpour, "Smart grid Adaptive Volt-VAR optimization: Challenges for Sustainable Future Grids", *Sustainable Cities and Society*, vol. 28, 2017, pp. 242-255.

[13] P. Bagheri, and W. Xu, "Assessing Benefits of Volt-Var Control Schemes Using AMI Data Analytics," *IEEE Trans. Smart Grid*, vol. 8, no. 3, pp. 1295-1304, May 2017.

[14] A. Bokhari *et al*., "Experimental Determination of the ZIP Coefficients for Modern Residential, Commercial, and Industrial Loads," *IEEE Trans. Power Delivery*, vol. 29, no. 3, pp. 1372-1381, June 2014.

[15] T. Hastie, R. Tibshirani, and J. Friedman , *The Elements of Statistical Learning, Springer*, second edition, 2008, pp. 11-40.

[16] R. O. Duda, P. E. Hart, D. G. Stork, *Pattern Classification*, Wiley, second edition, 2001

[17] I. Jolliffe, *Principal Component Analysis*, Wiley StatsRef: Statistics Reference Online, 2014.

[18] L. Györfi, M. Kohler, A. Krzyzak , H. Walk, *A Distribution-Free Theory of Nonparametric Regression*, Springer, 2002, pp. 86-97.

[19] N. Markushevich, A. Berman and R. Nielsen, "Methodologies for assessment of actual field results of distribution Voltage and Var Optimization," In *IEEE PES Transmission and Distribution Conference and Exposition (T&D)*, Orlando, FL, 2012, pp. 1-5.

[20] D. T. Chessmore, W. J. Lee, W. E. Muston, T. L. Anthony, F. Daniel, and L. Kohrmann, "Voltage-Profile Estimation and Control of a Distribution Feeder," *IEEE Trans. Industry Applications*, vol. 45, no. 4, pp. 1467-1474, July-aug. 2009.

[21] Y. Shi and M. E. Baran, "Assessment of Volt/Var Control Schemes at Power Distribution Level," *North American Power Symposium (NAPS)*, Charlotte, NC, 2015, pp. 1-5.

[22] F. Shariatzadeh, S. Chanda, A. K. Srivastava, and A. Bose, "Real-time Benefit Analysis and Industrial Implementation for Distribution System Automation and Control," *IEEE Trans. Industry Applications*, vol. 52, no. 1, pp. 444-454, Jan.-Feb. 2016.

[23] S. Chanda, F. Shariatzadeh, A. Srivastava, E. Lee, W. Stone, and J. Ham, "Implementation of Non-Intrusive Energy Saving Estimation for Volt/Var Control of Smart Distribution System," *Electric Power Systems Research*, vol. *120*, pp.39-46, 2015.

[24] I. Roytelman, B. K. Wee, "Pilot Project to Estimate the Centralized Volt/Var Control Effectiveness," *IEEE Trans. Power Systems,* vol. 13, no. 3, pp. 864-869, Aug 1998.

[25] K. P. Schneider, and T. F. Weaver, "A Method for Evaluating Volt-VAR Optimization Field Demonstrations," in *IEEE Trans. Smart Grid*, vol. 5, no. 4, pp. 1696-1703, July 2014.

[26] "Measurement and Verification of Distribution Voltage Optimization Results for the IEEE Power & Energy Society," In *IEEE Power and Energy Society General Meeting*, Minneapolis, MN, 2010, pp. 1-9

[27] M. Khurmy, and B. Alshahrani, "Measurement & Verifications of Voltage Optimization for Conserving Energy," In *10th International Conference on Environment and Electrical Engineering (EEEIC)*, *2011,* pp. 1-5.

[28] K.P. Schneider, and T.F. Weaver, "Volt-Var Optimization on American Eelectric Power Feeders in Northeast Columbus," In *IEEE PES Transmission and Distribution Conference and Exposition (T&D), 2012,* pp. 1-8).

[29] W. H. Kersting, "Radial Distribution Test Feeders," *IEEE Trans. Power Systems*, vol. 6, no. 3, pp. 975-985, Aug. 1991.

[30] R. Torquato, Q. Shi, W. Xu, and W. Freitas, "A Monte Carlo Simulation Platform for Studying Low Voltage Residential Networks," *IEEE Trans. Smart Grid*, vol. 5, no. 6, pp. 2766-2776, Nov. 2014.

[31] P. Bagheri, and W. Xu, "Model-free Volt-Var Control Based on Measurement Data Analytics," *IEEE Transactions on Power Systems,* Accepted for publication in Oct. 2018, DOI: 10.1109/TPWRS.2018.2874543.

[32] R. A. Jabr, and I. Džafić, "Sensitivity-Based Discrete Coordinate-Descent for Volt/VAr Control in Distribution Networks," *IEEE Trans. Power Systems*, vol. 31, no. 6, pp. 4670-4678, Nov. 2016.

[33] B. A. de Souza, and A. M. F. de Almeida, "Multiobjective Optimization and Fuzzy Logic Applied to Planning of the Volt/Var Problem in Distributions Systems," *IEEE Trans. Power Systems*, vol. 25, no. 3, pp. 1274-1281, Aug. 2010

[34] X. Zhang, A. J. Flueck, and C. P. Nguyen, "Agent-Based Distributed Volt/Var Control With Distributed Power Flow Solver in Smart Grid," *IEEE Trans. Smart Grid*, vol. 7, no. 2, pp. 600-607, March 2016.

[35] M. Manbachi *et al*., "Real-Time Co-Simulation Platform for Smart Grid Volt-VAR Optimization Using IEC 61850," *IEEE Trans. Industrial Informatics*, vol. 12, no. 4, pp. 1392-1402, Aug. 2016.

[36] S. T. Mak, "Dynamic modeling of the distribution feeder using Smart Meters data to support feeder VOLT-VAR control," in *IEEE PES Transmission and Distribution Conference and Exposition (T&D)*, Orlando, FL, 2012, pp. 1-3.

[37] D. Atanackovic, and V. Dabic, "Deployment of real-time state estimator and load flow in BC Hydro DMS - challenges and opportunities," in *2013 IEEE Power & Energy Society General Meeting*, Vancouver, BC, 2013.

[38] T. A. Short, *Electric Power Distribution Handbook*, CRC Press, 2003.

[39] M. E. Baran and Ming-Yung Hsu, "Volt/VAr control at distribution substations," in *IEEE Trans. Power Systems*, vol. 14, no. 1, pp. 312-318, Feb 1999.

[40] V. Borozan, M. E. Baran, and D. Novosel, "Integrated volt/VAr control in distribution systems," in *2001 IEEE Power Eng. Soc. Winter Meeting*, 2001, vol. 3, pp. 1485–1490.

[41] B. R. Williams, "Distribution capacitor automation provides integrated control of customer voltage levels and distribution reactive power flow," *IEEE Power Industry Computer Application Conference*, Salt Lake City, UT, 1995, pp. 215-220.

[42] P. Brady, C. Dai, and Y. Baghzouz, "Need to revise switched capacitor controls on feeders with distributed generation," in *IEEE PES Transmission and Distribution Conference and Exposition*, 2003, pp. 590-594 vol.2.

[43] R. A. Walling, R. Saint, R. C. Dugan, J. Burke, and L. A. Kojovic, "Summary of Distributed Resources Impact on Power Delivery Systems," *IEEE Trans. Power Delivery*, vol. 23, no. 3, pp. 1636-1644, July 2008.

[44] Y. P. Agalgaonkar, B. C. Pal, and R. A. Jabr, "Distribution Voltage Control Considering the Impact of PV Generation on Tap Changers and Autonomous Regulators," *IEEE Trans. Power Systems*, vol. 29, no. 1, pp. 182-192, Jan. 2014.

[45] M. Diaz-Aguiló *et al*., "Field-Validated Load Model for the Analysis of CVR in Distribution Secondary Networks: Energy Conservation," *IEEE Trans. on Power Delivery*, vol. 28, no. 4, pp. 2428-2436, Oct. 2013.

[46] R. F. Preiss and V. J. Warnock, "Impact of Voltage Reduction on Energy and Demand," *IEEE Trans. Power Apparatus and Systems*, vol. PAS-97, no. 5, pp. 1665-1671, Sept. 1978.

[47] J. De Steese, *Assessment of Conservation Voltage Reduction Applicable in the BPA Service Region*, 1987.

[48] A. Dwyer, R. E. Nielsen, J. Stangl and N. S. Markushevich, "Load to voltage dependency tests at B.C. Hydro," in *IEEE Transactions on Power Systems*, vol. 10, no. 2, pp. 709-715, May 1995.

[49] S. Lefebvre *et al*., "Measuring the efficiency of voltage reduction at Hydro-Québec distribution," *2008 IEEE Power and Energy Society General Meeting - Conversion and Delivery of Electrical Energy in the 21st Century*, Pittsburgh, PA, 2008, pp. 1-7.

[50] M. Manbachi *et al*., "Real-Time Adaptive VVO/CVR Topology Using Multi-Agent System and IEC 61850-Based Communication Protocol," *IEEE Trans. Sustainable Energy*, vol. 5, no. 2, pp. 587-597, April 2014.

[51] T. Niknam, M. Zare, and J. Aghaei, "Scenario-Based Multiobjective Volt/Var Control in Distribution Networks Including Renewable Energy Sources," *IEEE Trans. Power Delivery*, vol. 27, no. 4, pp. 2004-2019, Oct. 2012.

[52] D. Kirshner, "Implementation of conservation voltage reduction at Commonwealth Edison," in *IEEE Trans. Power Systems*, vol. 5, no. 4, pp. 1178-1182, Nov. 1990.

[53] T. A. Short and R. W. Mee, "Voltage reduction field trials on distributions circuits," *PES T&D 2012*, Orlando, FL, 2012, pp. 1-6.

[54] W. Ellens, A. Berry and S. West, "A quantification of the energy savings by Conservation Voltage Reduction," *2012 IEEE International Conference on Power System Technology (POWERCON)*, Auckland, 2012, pp. 1-6.

[55] J. C. Erickson and S. R. Gilligan, "The Effects of Voltage Reduction on Distribution Circuit Loads," *IEEE Trans. Power Apparatus and Systems*, vol. PAS-101, no. 7, pp. 2014-2018, July 1982.

[56] D. M. Lauria, "Conservation Voltage Reduction (CVR) at Northeast Utilities," in *IEEE Power Engineering Review*, vol. PER-7, no. 10, pp. 58-59, Oct. 1987.

[57] B. W. Kennedy and R. H. Fletcher, "Conservation voltage reduction (CVR) at Snohomish County PUD," *IEEE Trans. Power Systems*, vol. 6, no. 3, pp. 986-998, Aug. 1991.

[58] J. G. De Steese, S. B. Merrick and B. W. Kennedy, "Estimating methodology for a large regional application of conservation voltage reduction," *IEEE Trans. Power Systems*, vol. 5, no. 3, pp. 862-870, Aug. 1990.

[59] C. A. McCarthy and J. Josken, "Applying capacitors to maximize benefits of conservation voltage reduction," *Rural Electric Power Conference,* 2003, pp. C4-1-C4-5.

[60] A. Ballanti and L. F. Ochoa, "Voltage-Led Load Management in Whole Distribution Networks," *IEEE Trans. Power Systems*, vol. 33, no. 2, pp. 1544-1554, March 2018.

[61] A. Ballanti, L. N. Ochoa, K. Bailey and S. Cox, "Unlocking New Sources of Flexibility: CLASS: The World's Largest Voltage-Led Load-Management Project," *IEEE Power and Energy Magazine*, vol. 15, no. 3, pp. 52-63, May-June 2017.

[62] T. L. Wilson and D. G. Bell, "Energy conservation and demand control using distribution automation technologies," *Rural Electric Power Conference, 2004*, 2004, pp. C4-1-12.
[63] L. Global Energy Partners, *Distribution Efficiency Initiative*, 2005 [Online]. Available: https://neea.org/img/uploads/distribution-efficiency-initiative-e05-139.pdf
[64] M. A. Peskin, P. W. Powell and E. J. Hall, "Conservation Voltage Reduction with feedback from Advanced Metering Infrastructure," *PES T&D 2012*, Orlando, FL, 2012, pp. 1-8.
[65] R. Neal, "The use of AMI meters and solar PV inverters in an advanced Volt/VAr control system on a distribution circuit," *IEEE PES T&D 2010*, New Orleans, LA, USA, 2010, pp. 1-4.
[66] IEEE Guide for Identifying and Improving Voltage Quality in Power Systems, IEEE Standard 1250, March 2011.
[67] IEEE Recommended Practice for Voltage Sag and Short Interruption Ride-Through Testing for End-Use Electrical Equipment Rated Less than 1000 V, IEEE Standard 1668, 2017.
[68] IEEE Guide for Voltage Sag Indices, IEEE Standard 1564, June 2014.
[69] C. Rinn, Cleavelin, "Power Quality Perspectives in the Semiconductor Industry," *EPRI Signature—A Power Quality Newsletter*, vol. 7, no. 4, Fall 1997
[70] J. A. Martinez, and J. Martin-Arnedo, "Voltage sag stochastic prediction using an electromagnetic transients program," *IEEE Trans. Power Delivery*, vol. 19, no. 4, pp. 1975-1982, Oct. 2004.
[71] M. N. Moschakis, and N. D. Hatziargyriou, "Analytical calculation and stochastic assessment of voltage sags," *IEEE Trans. Power Delivery*, vol. 21, no. 3, pp. 1727-1734, July 2006.
[72] C. H. Park, and G. Jang, "Stochastic Estimation of Voltage Sags in a Large Meshed Network," *IEEE Trans. Power Delivery*, vol. 22, no. 3, pp. 1655-1664, July 2007.
[73] E. E. Juarez, and A. Hernandez, "An analytical approach for stochastic assessment of balanced and unbalanced voltage sags in large systems," *IEEE Trans. Power Delivery*, vol. 21, no. 3, pp. 1493-1500, July 2006.
[74] B. Wang, W. Xu, and Z. Pan, "Voltage sag state estimation for power distribution systems," *IEEE Trans. Power Systems*, vol. 20, no. 2, pp. 806-812, May 2005.
[75] E. Espinosa-Juarez, and A. Hernandez, "A Method for Voltage Sag State Estimation in Power Systems," *IEEE Trans. Power Delivery*, vol. 22, no. 4, pp. 2517-2526, Oct. 2007.
[76] J. Lucio, E. Espinosa-Juarez, and A. Hernandez, "Voltage sag state estimation in power systems by applying genetic algorithms," *IET Generation, Transmission & Distribution*, vol. 5, no. 2, pp. 223-230, February 2011.
[77] A. Hernandez, E. Espinosa-Juarez, R. M. de Castro, and M. Izzeddine, "SVD Applied to Voltage Sag State Estimation," *IEEE Trans. Power Delivery*, vol. 28, no. 2, pp. 866-874, April 2013.
[78] X. Zambrano, A. Hernández, M. Izzeddine, and R. M. de Castro, "Estimation of Voltage Sags From a Limited Set of Monitors in Power Systems," *IEEE Trans. Power Delivery*, vol. 32, no. 2, pp. 656-665, April 2017.
[79] G. Ye, Y. Xiang, M. Nijhuis, V. Cuk, and J. F. G. Cobben, "Bayesian-Inference-Based Voltage Dip State Estimation," *IEEE Trans. Instrumentation and Measurement*, vol. 66, no. 11, pp. 2977-2987, Nov. 2017.
[80] *Aclara Residential Electrical Meter I-210+c*, Aclara Technologies LLC, 2017, [Online]. Available: http://www.aclara.com
[81] *GE Residential Electrical Meter I-210+c*, General Electric, 2013, [Online]. Available: http://www.gegridsolutions.com
[82] M. Majidi, M. Etezadi-Amoli, and M. Sami Fadali, "A Novel Method for Single and Simultaneous Fault Location in Distribution Networks," *IEEE Trans. Power Systems*, vol. 30, no. 6, pp. 3368-3376, Nov. 2015.
[83] F. C. L. Trindade, W. Freitas, and J. C. M. Vieira, "Fault Location in Distribution Systems Based on Smart Feeder Meters," *IEEE Trans. Power Delivery*, vol. 29, no. 1, pp. 251-260, Feb. 2014.
[84] A. Monticelli, "Electric power system state estimation," *Proceedings of the IEEE*, vol. 88, no. 2, pp. 262-282, Feb. 2000.
[85] J. J. Grainger and W. D. Stevenson, *Power System Analysis*, New York: McGraw-Hill, 1994.

[86] H. P. Christian, *Least squares data fitting with applications*, Johns Hopkins University Press, 2013.
[87] T.F. Coleman, and Y. Li., "An Interior, Trust Region Approach for Nonlinear Minimization Subject to Bounds," *SIAM Journal on Optimization*, vol. 6, pp. 418–445, 1996.
[88] T.F. Coleman, and Y. Li., "On the Convergence of Reflective Newton Methods for Large-Scale Nonlinear Minimization Subject to Bounds," *Mathematical Programming*, vol. 67, no. 2, pp. 189–224, 1994.
[89] P. Jahangiri, and D. C. Aliprantis, "Distributed Volt/VAr Control by PV Inverters," *IEEE Trans. Power Systems*, vol. 28, no. 3, pp. 3429-3439, Aug. 2013.
[90] H. Zhu and H. J. Liu, "Fast Local Voltage Control Under Limited Reactive Power: Optimality and Stability Analysis," *IEEE Trans. Power Systems*, vol. 31, no. 5, pp. 3794-3803, Sept. 2016.

# Appendices

## Appendix A Proof of Theorem 2.2 for Modified Voltage Vectors

For the proof of theorem, we need to show how the vector of tap ratios ($a$) and original voltage vector ($V$) are derivable by sole means of modified voltage vector ($V'$). In the first step, we demonstrate how $V'$ can give the $a$ vector. Figure A.1 shows the nodes around one VR or SLTC as part of a generic radial feeder. *Assumption 2.8* assures that no load, DER or capacitor is connected to primary or secondary nodes of the tap-changing equipment. Moreover, it guarantees presence of the '$u$' node upstream of tap-changing device even if it is an SLTC.

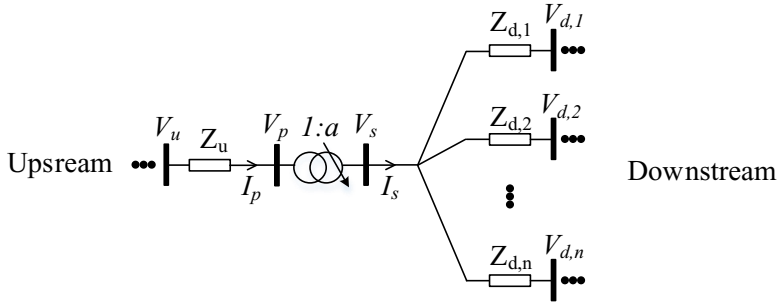


Figure A.1 Voltages around a tap-changing equipment.

Based on $V'$ definition in (2.23), difference of voltage between any two nodes which are on the same phase, and not connected through a tap-changing equipment is equal to their difference in terms of modified voltage vector. Thus, for example, in Figure A.1, we have: $V_u$-$V_p$=$V'_u$-$V'_p$ .

The above fact aids us to calculate the current at primary and secondary of the tap-changer (which are respectively denoted as $I_p$ and $I_s$ in Figure A.1):

$$\begin{aligned} I_p &= \frac{V_u - V_p}{Z_u} = \frac{V'_u - V'_p}{Z_u} \\ I_s &= \sum_{i=1}^{n} \frac{V_s - V_{d,i}}{Z_{d,i}} = \sum_{i=1}^{n} \frac{V'_s - V'_{d,i}}{Z_{d,i}} \end{aligned} \tag{A.1}$$

Then, the tap-ratio can be determined by division of these two currents:

$$a = I_p \Big/ I_s = \frac{\dfrac{V'_u - V'_p}{Z_u}}{\displaystyle\sum_{i=1}^{n} \frac{V'_s - V'_{d,i}}{Z_{d,i}}} \tag{A.2}$$

The above calculation is for a single-phase system, however, it can be simply expanded for a three-phase scenario by converting division operation of voltage by each impedance into an algebraic format (involving vector of three-phase voltage and matrix of three-phase impedance).

The whole procedure can be repeated for each tap-changing equipment in the system to establish the complete *a* vector using the modified voltage values. Next, one can inverse (2.23) to determine original voltages:

$$V_n = V'_n + V_{S,phase(n)} \times \prod_{i \in R_n} a_i \quad \text{for } n = 1 \to N \tag{A.3}$$

Overall, it is demonstrated that knowledge of modified voltage vector and substation voltage ($V_s$) is sufficient to reconstruct the tap-ratio vector and original voltage vector of the system, which serves as the proof for *Theorem 2.2* in chapter 2 of the thesis.

■

## Appendix B Details of a Sensitivity Case: Variant Load Characteristic

This appendix presents the details of load modelling for simulation of the sensitivity case in section 3.6.D (Case X). Three possible models were considered to describe how the load power change with its voltage as listed in Table B.1. In the base case, each of the loads in IEEE 123 Nodes system are assigned with one of these models for the whole simulation time. In Case X, however, model of each load is randomly updated each 5 minute. For example, Figure B.1 shows how the model assigned to the load on phase A of Bus 1 is changing during first day of simulation period:

Table B.1 Load Models

| Model No. | Voltage-Dependency Characteristic |
|---|---|
| 1 | *Constant power (P), Constant reactive power (Q)* |
| 2 | *Constant power (P), Constant current (I)* |
| 3 | *Constant impedance (Z)* |

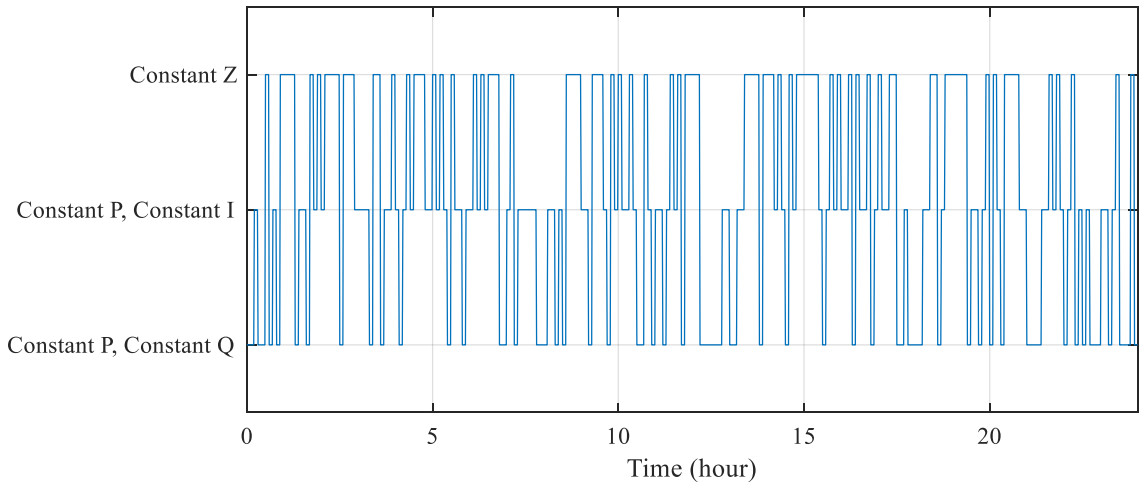


Figure B.1 Load models assigned to phase A of bus 1 for the Case X simulation of IEEE 123 Nodes Test Feeder (data is shown for first day only)

## Appendix C Model-based Optimization VVC

The model-based optimization VVCs were simulated to serve as a reference to evaluate results of different VVC schemes simulated throughout Chapter 3. Simulated Annealing was used as the main optimization algorithm preceded with an initial random search to improve the starting point for optimization algorithm. All the settings of optimization algorithm were tuned to enhance the results (through a try-and-error procedure by repeating the whole simulation period with different settings). Similar VVC operation limits as in the Case 1 were considered here. The objective function of optimization process was set as below to aim for both flat voltage profile and loss reduction:

$$\begin{aligned} &Minimize \;\; Obj = P_{loss} + w.MVD \quad , w = 50 \\ &\text{subject to } \forall i : |V_i| \geq \mathrm{V_{Min,Lim}} \wedge |V_i| \leq \mathrm{V_{Max,Lim}} \end{aligned} \tag{A.4}$$

Choosing the above weighting coefficient ($w$) equal to 50 means that the algorithm was willing to compromise almost *0.5kW* in losses for a *0.01pu* reduction in mean of voltage deviation. Although the optimization method employed for this case is relatively basic compared to advanced techniques found in recent literature, this case can still serve as an informative reference to observe how model-free VVC cases perform compared to a model-based counterpart.